UNITED STATES DEPARTMENT OF THE INTERIOR

GEOLOGICAL SURVEY

Late Cenozoic Stratigraphy and Tectonics of Fish Lake Valley, Nevada and California: Road Log and Contributions to the Field Trip Guidebook, 1991 Pacific Cell, Friends of the Pleistocene

Contributing authors:

Marith C. Reheis[1], Andrei M. Sarna-Wojcicki[2], Charles E. Meyer[2], Edwin H. McKee[2], Janet L. Slate[3], Douglas M. Burbank[4], Thomas L. Sawyer[5], and Elise G. Pendall[2]

Open-File Report 91-290

[1] Lakewood, Colorado
[2] Menlo Park, California
[3] University of Colorado
[4] University of Southern California
[5] Woodward-Clyde and Associates

CONTENTS

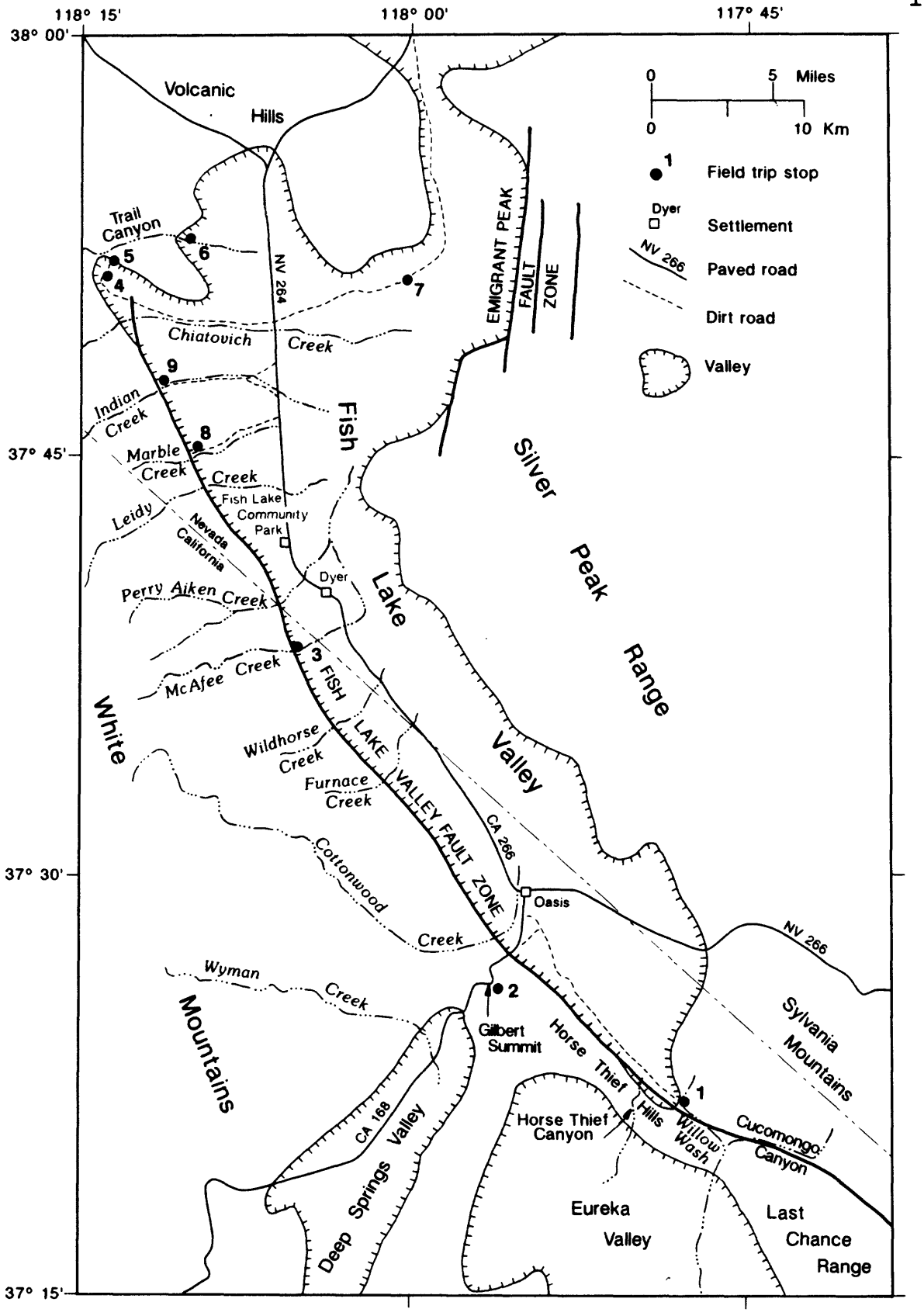

Figure 1. Sketch map of physiography, principal drainages, and locations of stops for 1991 field trip of the Pacific Cell, Friends of the Pleistocene.

ROAD LOG FOR FIELD TRIP IN FISH LAKE VALLEY, CALIFORNIA-NEVADA

Friends of the Pleistocene, Pacific Cell, May 31-June 2, 1991

by Marith C. Reheis, Thomas L. Sawyer, Janet L. Slate, and Elise G. Pendall

<Driving directions are underlined. For correlations and ages of Quaternary alluvial-fan units mentioned in this log, see table 1. For detailed dating information, see Slate (this volume). Surfaces underlain by alluvium of a given age are here informally named for that alluvium: for example, the Indian surface is underlain by alluvium of Indian Creek. Geographic locations are shown on fig. 1.>

Mileage		
Cum.	Int.	

DAY ONE

0.0	0.0	Turn south on paved road from campground at Fish Lake Valley Community Park. At 1:00, spectacular view of fault scarps up to 80 m high on fans of formerly glaciated Perry Aiken Creek. Main faulted surface is believed to be the Indian (100-200 ka?). Older deposit forming ridge 20 m higher than the Indian surface is correlated to alluvium of McAfee Creek (<740 ka). Formerly glaciated White Mountains form high range to west. Fish Lake Valley fault zone (FLVFZ), which forms northern end of Death Valley-Furnace Creek fault system, generally separates White Mountains from Fish Lake Valley (FLV), although many fault strands locally cross valley floor, and, to south, main active strand lies on valley floor. The eastern White Mountains consist largely of Mesozoic granitic rocks; north of McAfee Creek, Precambrian metasedimentary rocks crop out. Upper Miocene basalt and rhyolite cap erosion surfaces in range. Unglaciated Silver Peak Range lies to east; range consists mainly of Paleozoic sedimentary and Mesozoic intrusive rocks capped by a thick pile of late Tertiary volcanic rocks on north end.
2.6	2.6	Metropolis of Dyer, Nevada: Esmeralda Store where you can buy gas and beer, and Boonies Restaurant where you can buy food and beer in glasses. This section of FLVFZ along range front west of Dyer has biggest scarps and fastest rate of uplift in FLV (Reheis and McKee, this volume). This fault segment is the most nearly north-striking segment along range front. In the modern regime of nearly east-west least principal stress, this segment experiences mostly normal rather than strike-slip motion (Sawyer, this volume). At this latitude, not coincidentally, is White Mountain Peak, at elevation 4341 m the highest point in range.
5.8	3.2	Entrance to community dump site, where a Mono Craters tephra (about 1.15 ka) was collected from trench. From here south, range front strikes southeast, and FLVFZ is primarily strike-slip. Passing Iron and Wildhorse Creeks. Prominent fault scarps on these fans offset Indian surface. Surfaces behind main scarps are crisscrossed with a very complex fault pattern.
10.2	4.4	Passing mouth of Furnace Creek. Partway up fan is a large manmade hole exposing 3 tephra layers. At 1 m depth is a 1.15-ka Mono Craters tephra; at 4 m depth is 6.6-ka Mazama tephra; just below it is redeposited 740-ka Bishop tephra. Long linear ridge south of creek is a pressure ridge with a half-graben behind it. In fine-grained fill behind ridge are two tephras: upper one is redeposited Bishop, lower is Mazama. These Mazama ash sites are the farthest south yet found (Slate, this volume).

Table 1.--Mapping criteria and age controls for alluvial-fan deposits in Fish Lake Valley

Unit name (map symbol)	Surface form	Desert varnish	Soil development	Age
Late alluvium of Marble Creek (Qfcl).	Unmodified bar-and-swale topography; well-preserved debris flows; sparse vegetation.	None.	From none to a few weak filaments of $CaCO_3$ on clast bottoms.	Late Holocene (modern to <0.7 ka)
Middle alluvium of Marble Creek (Qfcm).	Somewhat subdued bar-and-swale and debris-flow topography; moderately vegetated--cholla common.	A few clasts with small spots in protected sites.	Sandy vesicular A horizon, 2-3 cm thick; sometimes a weak Bw horizon; stage I $CaCO_3$--common weak filaments and spots on clast bottoms.	Late Holocene (>1 ka, <1.6 ka)
Early alluvium of Marble Creek (Qfce).	Subdued bar-and-swale and debris-flow topography; incipient small areas of pavement--stones not interlocking; moderately vegetated--cholla common.	Common, thin spots on many clasts.	Vesicular A horixon, 3-5 cm thick--finer grained with moderate structure downwind of playas; Bw horizon; stage I-II $CaCO_3$--stronger in calcareous alluvium.	Middle Holocene (>2 ka, <6 ka)
Alluvium of Leidy Creek (Qfl).	No depositional topography preserved; smooth areas of pavement surrounded by rougher pavement; smooth pavement has interlocking but unsorted clasts.	Thin but continuous on most clasts; shiny and iridescent in protected sites.	Continuous, loamy vesicular A horizon, 5-7 cm thick; Bw or weak argillic B horizon--common thin clay films; stage II $CaCO_3$--stronger in calcareous alluvium.	Early Holocene late Pleistocene (>6 ka, <13 ka)
Alluvium of Indian Creek (Qfi).	Commonly deeply dissected; well packed and sorted clasts in continuous pavement; prominent solifluction treads and risers.	Continuous, thick varnish on most clasts--often shiny and iridescent.	Continuous, silty vesicular A horizon, 5-10 cm thick; moderate argillic B horizon--abundant thin to moderately thick clay films; stage II-III $CaCO_3$--stronger in calcareous alluvium.	Early late to late middle Pleistocene (>50 ka, <740 ka)
Alluvium of Trail Canyon (Qft).	Commonly deeply dissected; well packed and sorted clasts, commonly including fragments of pedogenic $CaCO_3$, in continuous pavement where preserved; prominent solifluction treads and risers where preserved.	Where preserved, continuous, thick varnish on most clasts--shiny and iridescent.	Continuous, silty A horizon, vesicular at lower elevation; strong argillic horizon--abundant thin to thick clay films; stage III $CaCO_3$, 1 m or more thick.	Middle Pleistocene (<740 ka)
Alluvium of McAfee Creek (Qfm).	Very deeply dissected; relict surface generally not preserved; ridge-crests usually concordant; more stable site have moderately well packed and sorted pavements with abundant carbonate rubble.	Where preserved, locally continuous and thick.	Where preserved, thick silty vesicular A horizon; strong argillic B horizon; Bkm horizon--stage IV laminar $CaCO_3$.	Early middle Pleistocene (≤740 ka)
Alluvium of Perry Aiken Creek (Qfp).	Extremely dissected; relict surface not preserved; ridge-crests may be concordant.	Thick where preserved.	Relict soils are stripped.	Early Pleistocene (>740 ka)

10.7 0.5 Nevada-California state line. A northeast-striking (left-lateral?) fault just north of state line splays off FLVFZ toward valley axis.

12.2 1.5 Windmill at 3:00. From Furnace Creek south, FLVFZ divides into two major strands, parallel and about 1 km apart (Sawyer, 1990). The western strand, inactive here, is against bedrock; eastern strand forms prominent fault scarps on Indian surface. Farther south, most recent Holocene faulting is on western strand, although scarps are larger on eastern strand. Near Oasis (large grove of cottonwoods ahead) is an area of southwest-striking left-lateral faults within range. Due west of Oasis, a left (east) step in both major strands and a large pressure ridge coincide with intersection of one of these left-lateral faults (Sawyer, 1990). Just south of Oasis, the FLVFZ breaks into many small strands on valley floor near another left-lateral fault intersection.

18.1 5.9 Approaching stop sign at intersection with CA 168. Before reaching sign, bend right and go west on CA 168. Straight ahead are trees along Cottonwood Creek. Note position of this creek (fig. 1); stop 2 will show the former drainage of Cottonwood Creek at 740 ka.

19.7 1.6 Inyo-Mono County line. Turn east on dirt road.

20.2 0.5 Turn right (southeast) on N. Eureka Valley road, marked by street sign. From here south, road is mainly on late Holocene fill.

20.4 0.2 Intersection of Eureka Valley road with Oasis road (street sign). Cross over Oasis road and under power line, heading southeast and then south toward irrigated fields.

20.9 0.5 Rounding a fence corner that marks the end of irrigated fields on left side of road. Here, road lies between two main strands of FLVFZ. A relatively inactive strand forms scarps on west along bedrock-alluvium contact, with little Holocene offset. Eastern strand on valley floor is virtually invisible on the ground but stands out on air photos as prominent lineaments and cracks. Two trenches excavated by Sawyer (1990) across these cracks demonstrate recent offset of fine-grained fill, but with no visible surface scarps. Small bare area east of road at south end of irrigated fields is site of one of these trenches.

24.2 3.3 Approaching windmill. On west is intrusive contact of Jurassic plutons to north with Precambrian and Cambrian sedimentary rocks. At 9:00 is site of second trench on eastern fault strand, with about 15 cm vertical offset along clay-lined fractures interpreted to be strike-slip faults (Sawyer, 1990).

25.2 1.0 Intersection with dirt road on west. South of that road are remnants of ~5-Ma basalt flows capping hills. Flows overlie angular, upper Miocene to Pliocene alluvial-fan gravel. This alluvial-fan gravel was probably shed to southwest from a fault-controlled range front, probably the FLVFZ, of Precambrian and Cambrian rocks that presently are found in the Grapevine Mountains in northern Death Valley, 50 km southeast. The fan gravel grades southwest into stream gravel deposited by drainages flowing south from the southern White Mountains (Reheis and McKee, this volume).

26.1 0.9 Eastern strand of FLVFZ jumps east and forms prominent scarps with strike-slip offset on Indian surface. Entering zone of Joshua trees; this is northernmost extent of this vegetation type. A few kilometers south at lower elevation is northernmost extent of creosote bush. Packrat middens in this area indicate the presence of juniper-shadscale woodland at 14,700 and 10,700 B.P. A shadscale-desertscrub community existed from 6,800 to 3,900 B.P., and modern vegetation did not develop until about 2,500 B.P. (Spaulding, 1980).

27.3 1.2 Intersection with road southwest to Horse Thief Canyon. This canyon represents a stream capture from Eureka Valley into alluvium of southern Fish Lake Valley. Western strand of FLVFZ dies out here under valley fill. Along eastern strand, scarp increases in height to south and is cut on Pliocene and lower Pleistocene deposits.

27.9 0.6 View southwest down Horse Thief Canyon into Eureka Valley, with Inyo Mountains and Sierra Nevada in background. At mouth of Horse Thief Canyon are upper Tertiary fluvial deposits containing numerous tephra layers that overlie several interbedded rhyolite and basalt flows; one basalt is dated at ~6.3 Ma. This sequence superficially resembles that in Willow Wash (next stop; McKee, 1968), but contains clasts of different lithologies than those in Willow Wash and were deposited by streams flowing south from southern White Mountains (Reheis and McKee, this volume).

29.5 1.6 Approaching intersection point of four fault strands. Eastern and western strands of FLVFZ merge and extend south into Willow Wash. WSW-striking fault from 12:00 to 2:00 is a range-front fault with late Quaternary offset that extends across Horse Thief Hills to Eureka Valley (Reheis, in press b).

29.9 0.4 Passing through narrow ravine in sheared Precambrian and Cambrian rocks. This ravine is upper end of another stream capture of Eureka Valley into Fish Lake Valley sediments. Valley opens up ahead into Wonderland, so named because when first mapping here, we had to believe several impossible things before breakfast. The complexity is caused by presence of several inactive faults and a compressional bend where FLVFZ strikes almost due E-W; the western strand is squeezed like toothpaste into a thrust fault dipping about 25^{o}. There is no evidence of Holocene faulting in this compressional area.

29.3 0.4 **STOP ONE.** Parking is difficult but you must leave the road open for traffic. We will be walking up the wash all morning. You can either pack a lunch up the wash or eat when you return, but be prepared to leave here at 1:00. We will walk to a viewpoint, discuss the stratigraphic and structural relations, then spend the morning examining stratigraphy, faults, and tephra (in no particular order).

WILLOW WASH SECTION

Upper Willow Wash exposes about 750 m of sedimentary strata containing numerous tephra layers. Over 50 tephra have been sampled for analyses of glass chemistry, and some for K-Ar laser-fusion dating. Paleomagnetic analyses were done on many of the finer-grained layers. The sedimentology and structure of the section and current tephrochronologic and paleomagnetic data are discussed in Reheis, Sarna-Wojcicki, Burbank, and Meyer (this volume; see fig. 1 for detailed map), and the tectonic implications are assessed in Reheis and McKee (this volume).

The sediments were deposited by streams flowing north from the Sylvania Mountains; they overlie ~11-Ma rhyolite and basalt flows, which in turn overlie quartz monzonite. The volcanic and intrusive rocks are extensively faulted by right-lateral and normal faults of the FLVFZ. Some of these faults also offset the basal sediments but die out upward. The basal one-half of the sediments (east of Willow Wash) consists mainly of fluvial gravel, sand, and silt; one part of the basal section has beds of lithic tuff and basalt probably emplaced as landslides from the older volcanic rocks. The middle part of the

section (green beds west of Willow Wash) consists of gypsiferous silt and clay interpreted to be playa or alkaline lake deposits; the base of these deposits is marked by two tephra layers correlated with the 3.2-Ma Putah and Nomlaki ash beds of the Sonoma volcanic field and the southern Cascade Mountains, respectively. The playa deposits grade upward into poorly consolidated sand and gravel, probably deposited as alluvial fans. This upper part of the section contains numerous tephra layers, derived from the Long Valley area, that range in age from about 1 to 2 Ma.

Return to vehicles; turn around and drive northwest. Entering FLV, view to northwest of two erosion surfaces on White Mountains. The higher one, below White Mountain Peak near upper treeline, is capped by ~11-Ma basalt flows with rhyolite locally exposed underneath. The flows are about the same age and may be the same as those at base of sedimentary section in Willow Wash. The lower erosion surface to north is capped by 3-4-Ma basalt flows (Reheis and McKee, this volume).

32.3 2.0 Area of Horse Thief Canyon. Tall rounded brown hill at 11:00 is Chocolate Mountain, capped by ~11-Ma basalt flows. Chocolate Mountain is part of range of hills that divides Deep Springs Valley from northern Eureka Valley (fig. 2). This divide, and hence Deep Springs Valley, probably did not form until the early Quaternary (Reheis and McKee, this volume).

37.7 5.4 At 9:30, slanting roadcut in upper part of valley in middle distance. Highest part of roadcut is cut in colluvium with beds that slope southwest, overlying probable Bishop tephra that is part of the Cottonwood Creek paleovalley (next stop; Reheis, in press b). Colluvium has a well-developed surface soil with strong argillic horizon and is offset by a left-lateral strike-slip fault that also cuts through Chocolate Mountain (fig. 2).

40.3 2.6 Intersection of N. Eureka Valley Road and Oasis Road; turn left (west) on Oasis Road toward White Mountains.

40.4 0.1 Pass under power line and bear right.

41.2 0.8 Intersection with CA 168; bear left (southwest) on paved road and ascend small unnamed drainage. This drainage approximately follows southwest-striking left-lateral fault with some post-Bishop-tephra offset; this is one of the faults that disrupt FLVFZ near Oasis. This road is narrow, twisting, and dangerous; watch for downhill traffic and confine geologic rubbernecking to passengers.

43.2 2.0 Entering Cottonwood paleovalley UNDERNEATH former stream bed. The stream came across low ridge on right. Small patch of light-colored material on ridge slope is Bishop ash overlying gravel of Cottonwood Creek.

43.6 0.4 Ascending past another remnant of Bishop tephra overlying Cottonwood Creek gravel (stop 2, fig. 2). West of here, valley has been buried by alluvial fan deposits from former valley sideslopes.

44.1 0.5 **STOP TWO.** Top of Gilbert Summit. Park in large flat area on southeast side of road. We will discuss what can be seen from here, then walk back down the paved road to look at the Bishop tephra overlying stream gravel. PLEASE STAY OFF THE ROAD TO THE RIGHT WHILE WALKING! THE ROAD IS NARROW AND DRIVING VISIBILITY LIMITED!

GILBERT SUMMIT

The view to the west is across Deep Springs Valley, mostly hidden, and the southern end of the White Mountains to the Sierra Nevada crest. To the south is Chocolate Mountain, which is Jurassic hornblende monzonite capped by ~11-Ma basalt (fig. 2). We are ABOVE the Cottonwood paleovalley, which now forms the topographic divide between Fish Lake and Deep Springs Valleys. At the time of the Bishop Tuff eruption (0.74 Ma), the low granitic hills to the south were the topographic divide between the Cottonwood Creek paleovalley and the Wyman Creek paleovalley. Wyman Creek now puddles in Deep Springs Valley, but at 0.74 Ma flowed across the present site of Deep Springs Valley and through a wind gap on the south side of Chocolate Mountain into northern Eureka Valley, where Wyman Creek probably merged with Cottonwood Creek. Soldier Pass is a similar wind gap south of the Wyman Creek wind gap that contains perched stream gravel of unknown age from the White Mountains. Hence, Deep Springs Valley did not have its present form at 740 ka (Reheis and McKee, this volume).

COTTONWOOD CREEK PALEOVALLEY (TEPHRA SITE FLV-4-WP)

The Bishop tephra site near Gilbert Summit (fig. 2) was first reported as a pumice mine (Chesterman, 1956); the ash is included in "older alluvium" as mapped by McKee and Nelson (1967). The outcrop is narrow and elongate to the northwest. The tephra is at least several meters thick but poorly exposed; it overlies weathered, well-rounded stream gravel exposed in a shallow ravine north of the mined area. The deposit is confined within bedrock walls on both sides. The eastern valley wall consists of Cambrian rocks; the western valley wall consists of Jurassic hornblende monzonite. At the northern end of the deposit is an outcrop of distinctive, Jurassic olivine-augite monzonite.

To the northwest of this tephra site is a low bedrock ridge capped by a light-gray patch, which is Bishop tephra overlying well-rounded stream gravel. Smaller patches of tephra and rounded gravel also crop out to the northwest along the valley behind the low ridge. This northwest-trending valley ends in a high ridge with patches of tephra and gravel; this ridge is the south side of the canyon of modern Cottonwood Creek, and lies near the point where the southeasterly course of Cottonwood Creek turns abruptly east toward Fish Lake Valley (fig. 2). The stream gravel to the northwest contains lithologies typical of the rocks in the headwaters and upper course of Cottonwood Creek. The stream gravel near Gilbert Summit is similar, with one exception; it contains clasts of olivine-augite monzonite not found in the other gravel deposits.

Based on the location and composition of the gravel and tephra outcrops, Cottonwood Creek must have flowed southeast along the present topographic divide between Fish Lake and Deep Springs Valleys during or just before the Bishop eruption. To the southeast, remnants of Bishop tephra and stream gravel are scattered along the walls of the modern valley that heads at Gilbert Summit and extends into Eureka Valley (fig. 2). These remnants are inferred to represent the lower course of Cottonwood Creek when it flowed into Eureka Valley (Reheis, in press b).

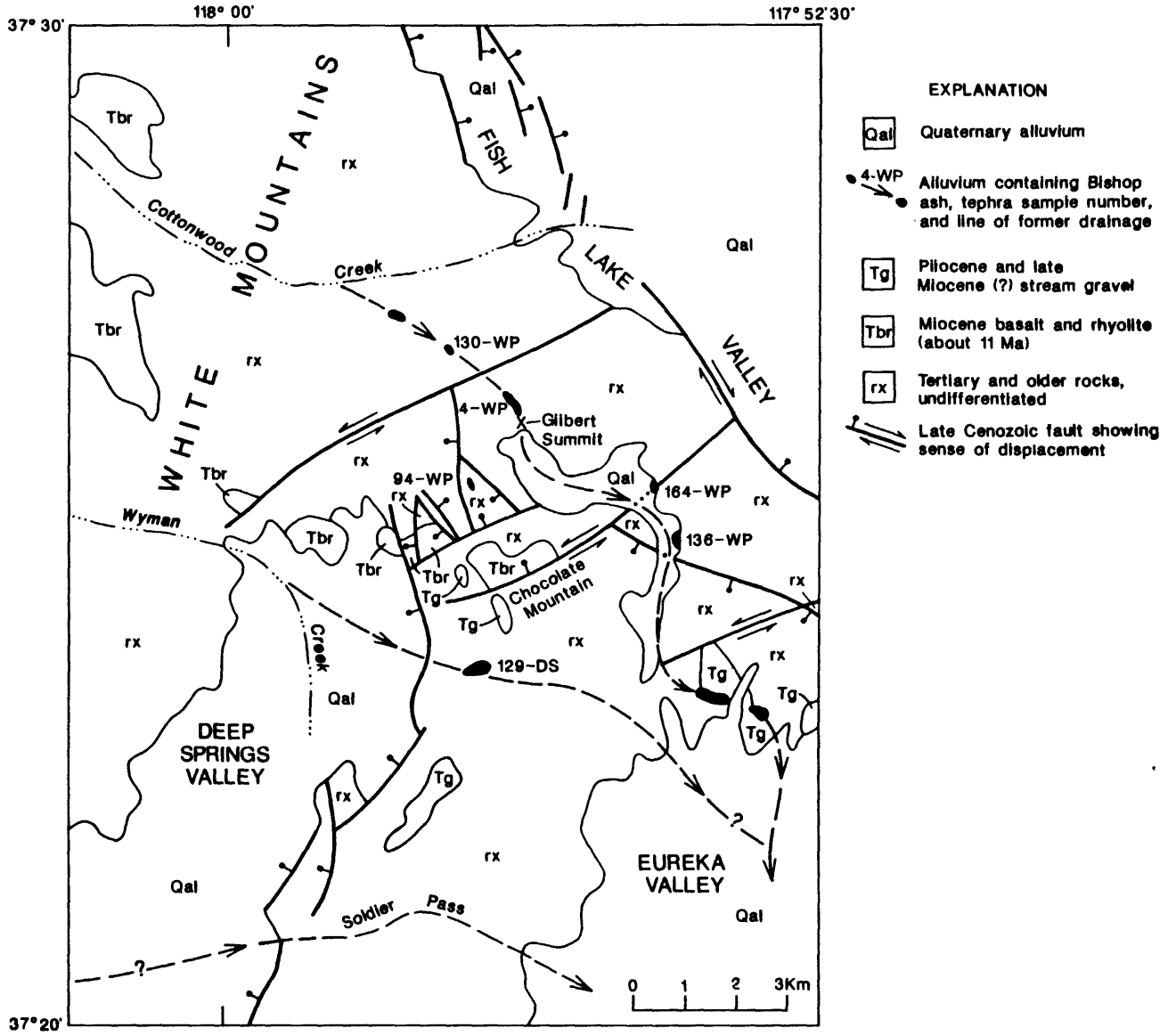

Figure 2. Generalized geologic map of the area around Gilbert Summit (stop 2 of field trip) and northern Deep Springs Valley, California and Nevada.

Turn around and proceed east on CA 168.

48.3 4.2 Entering FLV, dark hills to east just above valley floor are capped by volcanics that may be correlative to those at base of Willow Wash section and on high erosion surface in White Mountains visible at 10:00. Near 12:00 are Mt. Montgomery and Boundary Peak, at 4008 m the highest peak in Nevada.

49.2 0.9 Turn left on CA 266 and proceed north toward Dyer.

61.3 12.1 At 10:00 is mouth of McAfee Creek, stop 3. White sediments against bedrock at range front are Bishop tephra, overlain by a thick fan gravel (alluvium of McAfee Creek). North of McAfee Creek is dark-colored older gravel, the alluvium of Perry Aiken Creek.

62.7 1.4 At Esmeralda County mile marker 6, turn left (west) on unmarked dirt road that passes between irrigated fields.

63.4 0.7 Bend right around west side of irrigated field.

63.5 0.1 Turn left through old fenceline with no gate and turn sharp left again to head south along old fenceline. Pass through gate; last car be careful to close it.

63.6 0.1 Turn right (west) on dirt road that goes up McAfee Creek fan. At fork, bear right. McAfee Creek is one of five perennial creeks of FLV, mostly diverted for irrigation. On south side of McAfee Creek is Indian surface (fig. 3). On north side is alluvium of McAfee Creek overlying Bishop ash. At eastern base of McAfee remnant is a probable Leidy surface, partly eroded and partly buried by fault-scarp colluvium.

65.1 1.5 **STOP THREE**. Park here and proceed on foot to examine exposures.

MCAFEE CREEK (TEPHRA SITES FLV-65-MA AND FLV-66-MA)

About 71 m of gravel and tephra, identified as the Bishop tephra based on glass chemistry, thickness, and coarse grain size, are exposed on the north side of McAfee Creek (fig. 3). This deposit and its inferred origin are described in detail in Reheis, Slate, Sarna-Wojcicki, and Meyer (this volume). The tephra deposit was first described, but not identified, by Elliott-Fisk (1987) as underlying "glacial outwash and till" believed to be correlative with the Sherwin Till. In contrast, we infer that the tephra was deposited as a delta of McAfee Creek at the margin of a pluvial lake. The deltaic deposits are interbedded with and overlain by alluvial-fan deposits, clearly of post-Bishop and therefore of post-Sherwin age. The tephra and gravel are in fault contact on the west with bedrock along an inactive strike-slip strand of the FLVFZ. A second inactive fault cuts the bottom half of the deposit but dies out above; hence, this fault was active during deposition. A third fault, the presently active strand, bounds the deposit on the east.

Retrace route to paved road.

67.5 2.4 Intersection with paved road; turn north toward Dyer. At this time of day there is usually wonderful low-sun-angle light on fault scarps around Dyer. Feel free to stop and snap away.

72.2 4.7 Turnoff to Fish Lake Valley Community Park.

END DAY ONE

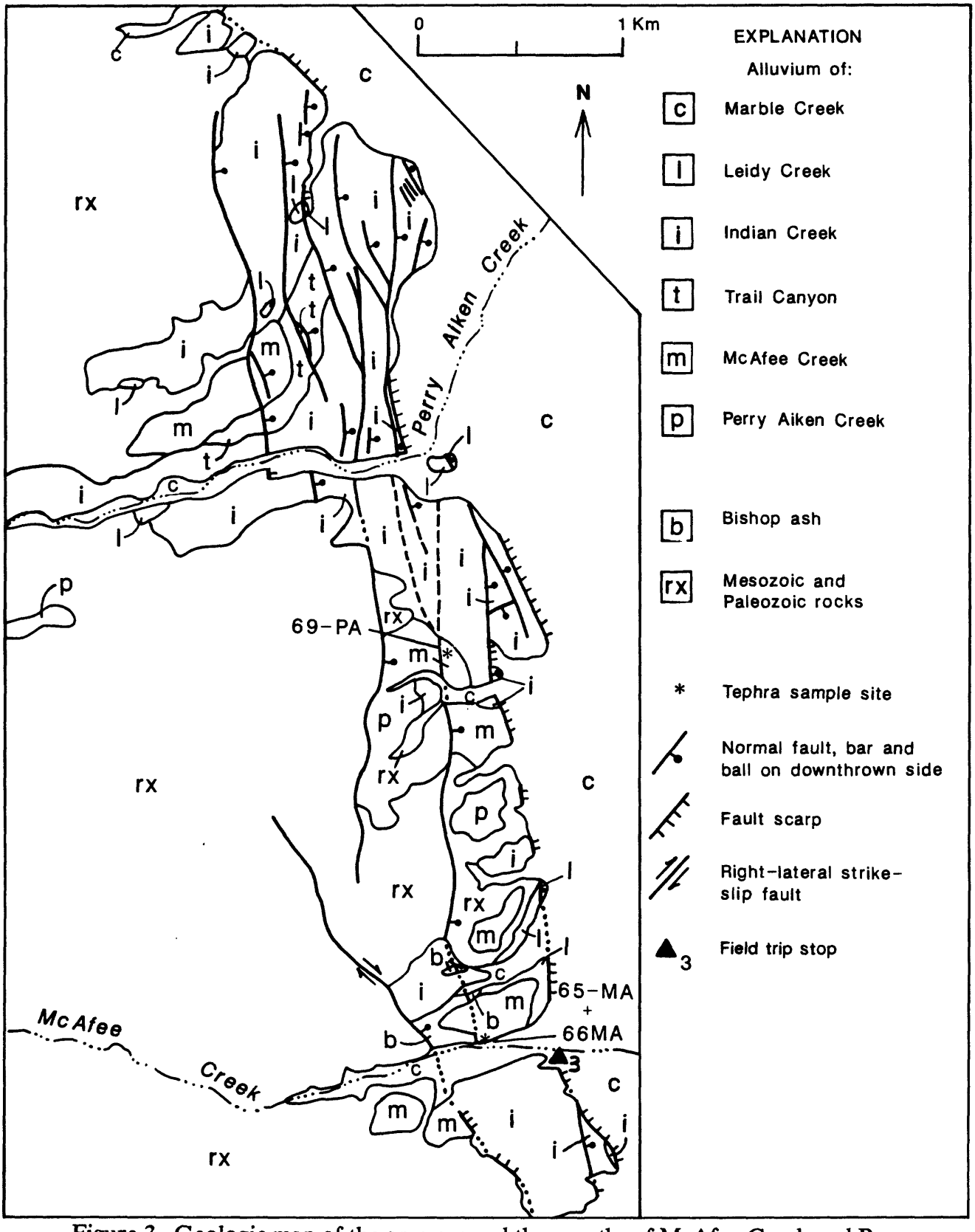

Figure 3. Geologic map of the area around the mouths of McAfee Creek and Perry Aiken Creek in west-central Fish Lake Valley, California and Nevada (stop 3 of field trip). Faults are dashed where inferred, dotted where concealed.

DAY TWO

0.0 0.0 Turn left (north) on paved road from community park. On west side of road is Busher Creek, draining unglaciated part of White Mountains. Holocene faulting is not obvious south of Busher Creek along north-striking Dyer subzone (Sawyer, 1990), but may be obscured by large, steep fault scarps.

0.5 0.5 On right, Fish Lake Community School (grades K-8). Older children may choose to attend class either in Bishop, Calif., or Tonopah, Nev., and board with volunteer families during the school week.

1.0 0.5 Intersection with road east to cemetery. On west is large perennial drainage of formerly glaciated Leidy Creek. The black hills at 12:00 are capped by ~5-Ma basalts, the youngest of the Silver Peak volcanic rocks. Volcanism started about 23 Ma (Robinson and others, 1968). Younger andesites on White Mountain side and north of FLV in Volcanic Hills are probably from a different source; the two sets of volcanic rocks have different trace-element chemistry (R.A. Thompson, written commun., 1991).

1.8 0.8 Fault scarp to left on Leidy surface marks beginning of horsetail splay that forms northern end of FLVFZ. Strike-slip motion ends to north and fault zone steps east across valley floor in a series of en echelon normal faults to Emigrant Peak fault zone (Sawyer, this volume), visible at about 2:00 on left side of prominent dark hill composed of Cambrian rocks. Tertiary volcanic rocks have slid off this hill to the east along a low-angle normal fault (Reheis, in press a). J.S. Stewart and others (oral commun., 1989) have mapped detachment faults between Paleozoic and Tertiary rocks farther to northeast in Silver Peak Range.

On valley floor to east there are few lineaments in Holocene fill (they are more abundant farther north). Adjacent to Silver Peak Range are small faults buried by Holocene deposits of Fish Lake marsh (Macke and others, 1990).

3.5 1.7 At 10:00 are prominent east-facing scarps of west side of complex graben on "shattered fan" of Indian Creek (Sawyer, 1990, this volume), part of horsetail splay at north end of FLVFZ.

4.3 0.8 Passing transformer station on left. Most areas along road consist of fine-grained sediments, but some clasts are visible along paved road. Farther east, sediments are very fine-grained; one trench exposes 3-4 m of silt and clay with a few sand layers. Commonly, coppice dunes and locally, barchan dunes overlie fine-grained valley fill.

5.6 1.3 Passing barchan dune field. Curving dune crests indicate winds from south. Other lineations on air photos are straight lines of bushes rooted in low ridges (< 10 cm high) of sand. These lineations trend northeast at angle to dune crests; some lead into fault scarps. Lineations may reflect tectonic cracking with little or no vertical displacement. Cracking may concentrate water and allow bushes to root and grow more readily; bushes then trap sand blowing across valley floor.

9.1 3.5 Approaching this mileage, pass large wooden sign for Chiatovich Creek Ranch and house set in grove of trees on left, next to creek. Turn left (west) on dirt road with stop sign just past Chiatovich Creek. Road lies on alluvium deposited by the combined flows of three large, formerly glaciated drainages (Chiatovich, Davis, and Middle Creeks) that merge to form Chiatovich Creek. This fan is much larger than any other in valley, due to large drainage area and little faulting.

Straight ahead is Davis Mountain, capped by 3-4-Ma andesites of the Volcanic Hills; andesites also crop out on next ridge to north between Chiatovich and Middle Creeks (Robinson and Crowder, 1973). These andesites locally overlie or are interbedded with alluvium. They have been elevated about 100-300 m above the modern valley floor by faulting along the FLVFZ and tilted to the east by more rapid uplift of the White Mountains along the White Mountain fault zone (dePolo, this volume).

11.3 2.2 Passing fancy log cabin on south. From 1:00 to 3:00 is long low basalt ridge mapped as same age as that capping Davis Mountain.

12.6 1.3 From 1:00-3:00 is large curving fault scarp, cut on alluvium of Indian Creek, striking northeast across fan toward basalt ridge and then east parallel to ridge. This change in fault strike is seen along many other fault strands at the northern end of the FLVFZ.

16.4 3.8 Intersection of Middle Creek road and Trail Canyon road. Turn right (north) on Trail Canyon road. On south side of Middle Creek, due south of intersection, are rounded hills formed on old alluvial-fan deposits, probably of two different ages. The lower, younger deposit (unit Qft, fig. 4) may correlate either with alluvium of Trail Canyon (most likely) or with alluvium of McAfee Creek. The older, higher deposit (unit Qg, fig. 4) can be discontinuously traced upstream to an exposure of fluvial deposits capped by debris flows; the fluvial deposits contain two tephra layers (no glass chemistry as yet). The upper tephra, based on large pumice size, may correlate to the Bishop ash; the lower may be an older Glass Mountain tephra. The two are separated by a buried soil.

16.6 0.2 At 9:00 is light-colored gravel of unit Qg poking out from ridge that bounds north side of Middle Creek (fig. 4).

16.9 0.3 Pass turnoff to unnamed creek.

17.2 0.3 **STOP FOUR.** Turn left up Dry Creek in order to use a triangular intersection to park for this stop. At 0.15 miles, turn sharp right on road leading back to main road; park anywhere along these two short road segments. Dry Creek is a mining area for cinnabar in a thrust (?) fault in Paleozoic rocks. Ridge on north divides Dry Creek from Trail Canyon and Rock Creek. Ridge is mostly 3-4-Ma basalt overlying rhyolite, but at 9:00 is thick fill of old gravel (unit Qg, fig. 4).

OLD GRAVEL AT DRY CREEK (TEPHRA SITES FLV-6-TC AND FLV-7-TC)

The old Quaternary deposits at Dry Creek crop out in a hill that stands above the level of the relatively smooth bajadas to the north and south. South of the hill, the bajada is underlain mostly by Holocene alluvium; north of the hill, the bajada is underlain by the middle Pleistocene alluvium of Trail Canyon (unit Qft, fig. 4). Unit Qft as yet has no independent age control. We believe, however, that it represents aggradation onto topography incised into an older fill (Gillespie, this volume), which is now represented only by erosional remnants such as this hill and a few other exposures west of here and in Middle Creek. Hence, the tephra in the hill at Dry Creek (and those yet to be identified at Middle Creek) provide a maximum age for the episodes of aggradation and incision of unit Qft (stop 5).

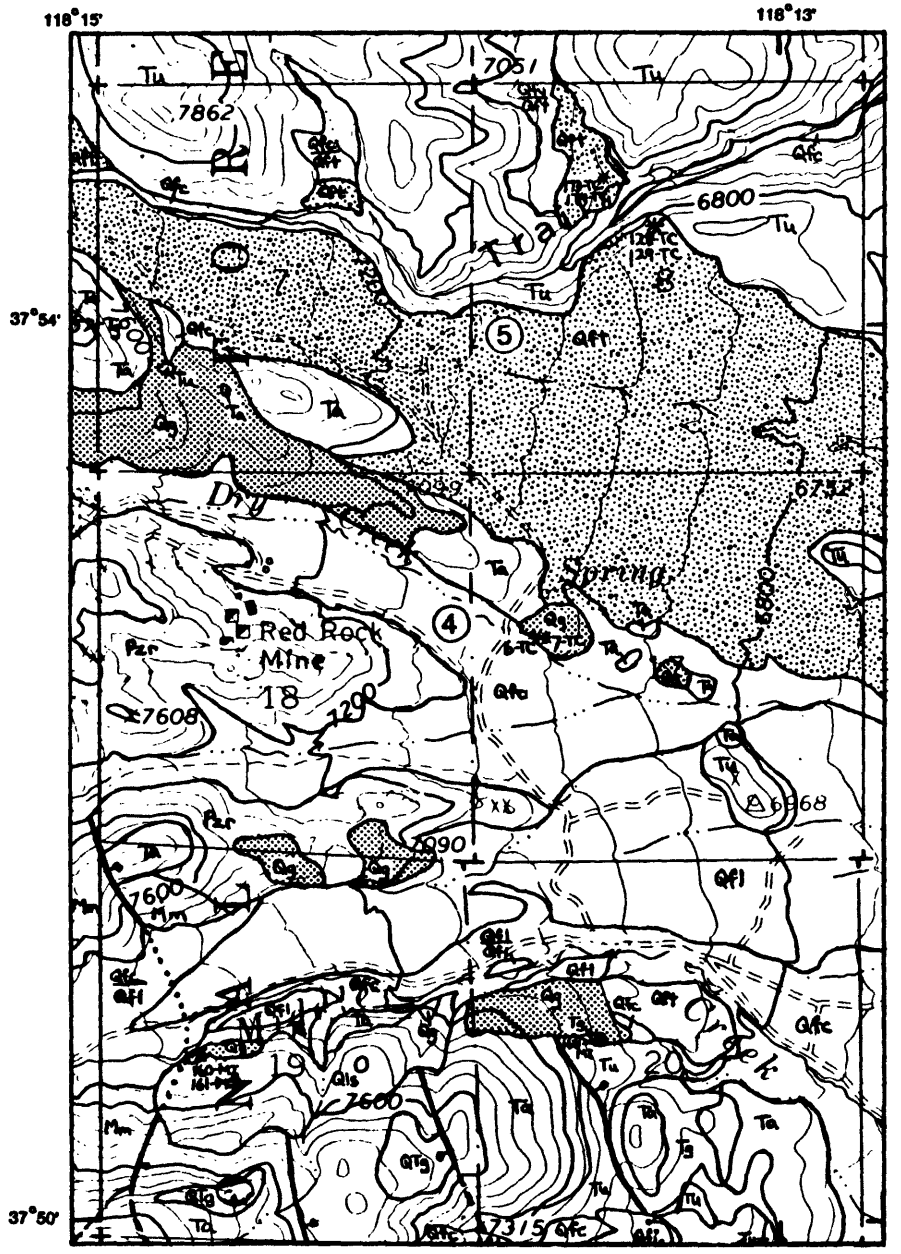

EXPLANATION

Alluvial-fan units

Alluvium of:

- Qfc — Marble Canyon
- Qfl — Leidy Creek
- Qfi — Indian Creek
- Qfc — Trail Canyon

Fluvial units

- Qfg — early Quaternary gravel
- QTg — Quaternary-Tertiary gravel
- Tg — Tertiary gravel

Bedrock units

- Ta — Tertiary andesite
- Tu — Tertiary volcanic and sedimentary rocks, undivided
- Mm — Mesozoic intrusive rocks
- Pzr — Paleozoic and Precambrian rocks

Fault, bar and ball on downthrown side

160-MT — Tephra site

④ — Field trip stop

0 — 1 Mile

0 — 1 Kilometer

Figure 4. Geologic map of the area between the mouths of Middle Creek and Rock Creek in northwestern Fish Lake Valley, Nevada (stops 4 and 5 of field trip). Fractional map symbols (Qfc/Qft) are used when a thin veneer of a younger unit overlies an older unit. Unit Qft here is the older part of alluvium of Trail Canyon (unit Qfto in text).

About 17 m of Quaternary deposits are exposed in a streamcut north of the mouth of Dry Creek and east of the dirt road (fig. 4). These deposits overlie weathered rhyolite at the east end of the cut. The general stratigraphy at this site is similar to that described above for an outcrop of unit Qg in Middle Creek. The deposits at Dry Creek consist chiefly of about 15 m of pebbly sand overlain by about 2 m of very coarse, poorly sorted gravel with subangular boulders as much as 2 m in diameter; the contact is marked by a flat bench. The pebbly sand contains two tephra layers, each about 0.75 m thick. FLV-106-TC, near the base, consists of coarse pumiceous sand, light-gray and well-sorted, with local lenses of finer sand. This tephra is continuous along the outcrop for at least 20 m. FLV-107-TC, near the top, is very similar but contains more lithic grains, is more heavily burrowed, and is less extensive along the outcrop. The upper tephra overlies a bouldery layer that may contain a buried soil.

Glass in both tephra layers have major-oxide chemistry that is a close match (A.M. Sarna-Wojcicki, written commun., 1988) for both the 0.74-Ma Bishop ash (normal polarity) and the ~1-Ma Glass Mountain ashes (reversed polarity). Paleomagnetic analyses are currently in progress on the basal tephra. Based on the lack of coarse pumice clasts, we currently think that these two tephra layers correlate with the older Glass Mountain ashes.

17.8 0.3 Continue northwest on Trail Canyon Road. Hill at 9:00 is composed of unit Qg. Now driving on pre-capture surface of Rock Creek (Gillespie, this volume), underlain by alluvium of Trail Canyon (fig. 4).

18.1 0.3 Fork right (north) on dirt track toward stone cabin.

18.4 0.3 **STOP FIVE.** Park in area around stone cabin. We will walk a short distance downfan to look at stratigraphy of the alluvium of Trail Canyon exposed in roadcut, and at soil exposed in backhoe pits, then return to cars for lunch.

UPPER TRAIL CANYON (PRE-CAPTURE SURFACE, UPSTAIRS)

The bajada in the area of stop 5 is underlain by a fill, well exposed in upper Trail Canyon in roadcuts and streamcuts (older alluvium of Trail Canyon, unit Qft, fig. 4), that ranges in thickness from about 15 m to about 65 m. The section exposed on the south side of Trail Canyon consists of 15-20 m of volcanic alluvium derived from a south-trending paleovalley (fig. 4) deposited on volcanic bedrock. The volcanic alluvium is overlain by about 25 m of granitic alluvium derived from Rock Creek. The granitic alluvium contains lenses of pebbly to silty material, as much as 13 m thick on the north side of the canyon, that was apparently deposited at the interface between the two fans aggrading to the south and to the east. This finer material contains tephra beds that have not yet been identified. The surface of unit Qft is certainly younger than about 1 Ma and possibly younger than 0.74 Ma based on the inset relationship of this surface to deposits of unit Qg containing Glass Mountain and Bishop (?) tephra (stop 4).

The variable thickness and irregular subjacent bedrock topography suggest that the alluvium of Trail Canyon represents aggradation onto an erosional landscape that may have been incised after deposition of unit Qg (stop 4; fig. 4). Rock Creek is incised as much as 80 m into unit Qft in the area of stop 5. This deep incision apparently occurred when the aggradation of ancestral Rock Creek overtopped passes in low volcanic hills. Rock Creek was then diverted down lower Trail Canyon and two other unnamed drainages,

and subsequently deposited the younger alluvium of Trail Canyon (unit Qfty, fig. 5). The capture history of Rock Creek/Trail Canyon is described in Gillespie (this volume).

Soils in the "Upstairs" surface (unit Qft) are developed on granitic alluvium near the present lower treeline. Soils studied on the lower Trail Canyon fan (stop 6), in contrast, formed on parent materials with proportions of rhyolite and basalt inversely related to age (Gillespie, this volume) in a more arid climate about 430 m lower in elevation.

Soil profile 1a has a thick A horizon underlain by argillic B horizons with well developed structure and clay loam or sandy clay loam textures. Dithionite-extractable iron (Fed) in the argillic B horizons may be derived either from in-situ weathering or from eolian dust. Thick Bk horizons extend from 45 to at least 250 cm in depth. ^{14}C dating of $CaCO_3$ at about 120 cm gave a mean age of 11,500 yr B.P., whereas occluded organic carbon extracted from $CaCO_3$ at the same depth was 3600 yr B.P.; hence, not only is the pedogenic $CaCO_3$ significantly younger than the surface on which the soil has formed, but also organic matter has infiltrated the older pedogenic $CaCO_3$. Stable C and O isotopes show the influence of a cooler, moister climate at this higher elevation with respect to soils on the lower Trail Canyon fan, but when corrected for elevation are still lighter than the isotopic composition of younger soils. This suggests greater soil respiration and less evaporation (or cooler precipitation) in soils of this age than in Holocene soils. Harden and others (this volume) discuss pedogenic processes in the Trail Canyon soils, and Pendall and others (this volume) discuss the isotopic data.

		Return down Chiatovich Creek to paved road.
27.5	9.1	Turn north (left) on paved road.
29.8	2.3	Passing Combined Metals Corporation on east side of road--one of two places in the valley where a flat tire can be fixed if you provide the tube.
30.5	0.7	Turn left on dirt road at 45° to main road and proceed northwest. Sign says "Caution, minimum maintenance only." Driving on upper Holocene alluvium in intersection area of Chiatovich Creek and lower Trail Canyon fans.
32.2	1.7	On lower Trail Canyon fan. 3-4-Ma basalt flows on left (Robinson and Crowder, 1973). Cross nearly invisible channel of Rock Creek.
33.1	0.9	Turn left and proceed southwest on dirt road, driving on upper Holocene alluvium of lower Trail Canyon.
34.3	1.2	Pass close against basalt on right. On left, channel of Rock Creek is incised into late alluvium of Marble Creek (unit Qfcl, fig. 5). Charcoal from 2 m below surface (composite sample) is about 1 ka.
34.4	0.1	Soil profile 7b at stream bank consists of a series of stratified debris flows and fluvial deposits, and has no vesicular A horizon (Harden and others, this volume).
34.6	0.2	**STOP SIX.** Park in open area OFF THE ROAD. View is up lower Trail Canyon to Boundary Peak and Mt. Montgomery. We will spend most or all afternoon examining soils, surficial characteristics, and datable materials in this area. Up hill on north side of road is fault scarp of unknown age; offsets basalt and trends west as strong lineament with springs along it. See Harden and others (this volume) and Pendall and others (this volume) for soil descriptions, data, and interpretations. THOSE WHO WISH TO SEE OPTIONAL STOP 7, RETURN TO VEHICLES EARLY AND WE WILL LEAVE BY 3:30 PM.

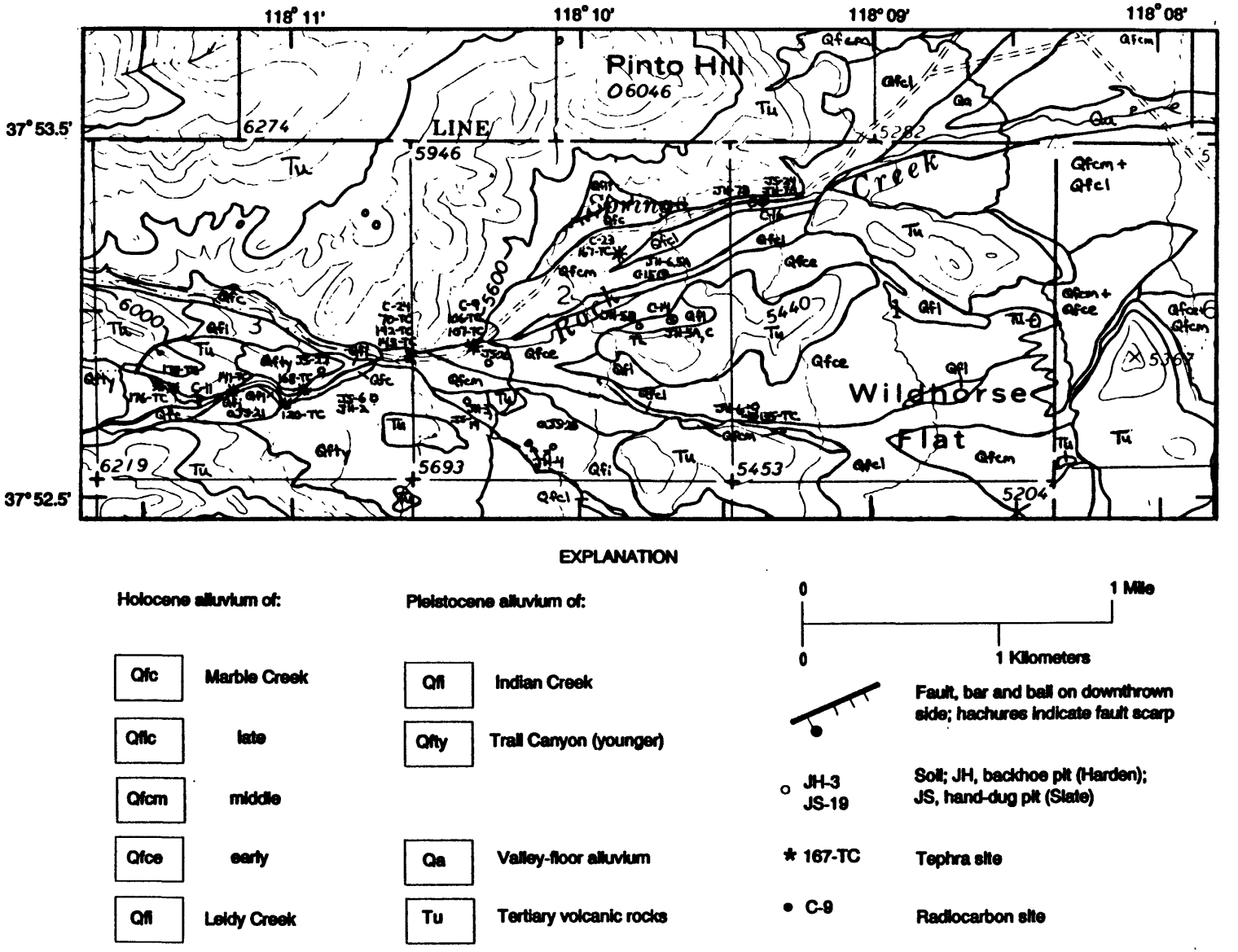

Figure 5. Generalized geologic map of the Trail Canyon alluvial-fan deposits in northwestern Fish Lake Valley, Nevada. Combined map symbols (Qfcm + Qfcl) are used where two map units are closely interspersed. Stop 6A is at soil profile JH-5A,C; stop 6B is at soil profile JH-6; stop 6C is at soil profile JH-4.

LOWER TRAIL CANYON FAN (DOWNSTAIRS)

Walk south across fan to a small remnant of the Leidy surface tucked against north end of low basalt ridge (fig. 5). En route, note complex of modern channels and older debris flows and debris-flow lobes. Approaching Leidy surface, age of surficial deposits increases as reflected by increasing development of surface pavement and desert varnish on clasts.

Stop 6A, soil pit on the Leidy surface (profile 5c). Detrital charcoal from about 1 m depth was dated at about 6300 yr B.P., and two thermoluminescence ages on buried A horizons in profile 5b are 7500 and 11,000 yr B.P. (table 1). The soil has a discontinuous "juvenile" Bt horizon and stage I $CaCO_3$ in the Bk horizon to about 1 m depth; pedogenic gypsum occurs at greater depth. Carbonate from clast coats at 40-50 cm depth in profile 5b has a mean ^{14}C age of 2700 yr B.P., whereas occluded organic carbon has a mean age of 1640 yr B.P. Stable C and O isotope data suggest greater evaporation, lower soil respiration rates, and possibly more C4 plants during development of Holocene soils (profiles 5b and 6a) than during development of Pleistocene soils (profiles 1a and 4c).

Walk south over saddle in basalt ridge and east about 1 km downfan to next stop. PLEASE AVOID GAS SAMPLING TUBES AROUND SOIL PIT!

Stop 6B, soil pit on early Marble Creek surface (profile 6a). Tephra FLV-135-TC crops out in this pit at about 90 cm depth; elsewhere on the lower Trail Canyon fan, a correlative tephra bed is directly underlain by charcoal dated at 3800 yr B.P. Thin clay films occur in this soil at about 20-30 cm depth, and stage I $CaCO_3$ occurs as clast coatings between 30 and 50 cm depth. Horizonation in this soil is mainly controlled by stratified debris flows. Stable C isotopes in pedogenic $CaCO_3$ and occluded organic carbon are in equilibrium with modern soil CO_2 measured in May, suggesting that carbonate may be precipitating in late spring to early summer.

Walk west up fan surfaces of increasing age to next stop.

Stop 6C, soil pit on Indian surface (profile 4c). This eroded surface is believed to be early late Pleistocene to late middle Pleistocene in age, but the only age control at present is by correlation to a buried vesicular A horizon below the Indian surface at Furnace Creek with a thermoluminescence age of >50 ka. The Av horizon is silty and thick; it is capped by a well varnished desert pavement. B horizons display pedogenic accumulations of clay, opaline silica, carbonate, and manganese; a duripan has formed between about 25 and 50 cm depth, and calcic horizons are at greater depth. Small remnants of a buried Av horizon occur locally at 80 cm depth; PLEASE DO NOT DESTROY THE EVIDENCE BY POKING AT IT! Buried Bk horizons continue to a depth of 160 cm. Another soil pit directly upfan on this surface shows a thick Bk horizon cut by a Holocene channel; however, little or no difference can be seen in surface morphology or desert varnish on the two deposits. Any ideas? These profiles illustrate the great degree of variability in age that may exist on what appears to be a uniform surface in aerial photographs.

Soil carbonate from profile 4c at 37-63 cm depth gave a mean age of 2200 yr B.P.; organic carbon gave an age of 4200 yr B.P. This may indicate that both inorganic and organic carbon have low mean residence times in this semiarid climate, and (or) that some pedogenic materials in this soil are of fairly recent origin.

Walk northwest about 0.5 km back to the road. Cuts in Holocene sediments at two stream crossings expose several tephra and charcoal layers (fig. 5). The eastern cut reveals inverse stratigraphic relations in the form of a young burned root and an even younger long-necked Budweiser bottle that appear to be stratigraphically beneath much older tephra layers; the bottle is within sediments that were plastered onto an undercut bank.

Return to paved road.

38.7 4.1 Intersection with paved road; turn right (south).

41.7 3.0 Intersection with Chiatovich Creek road. To go back to camp, continue straight ahead. **To go to optional stop 7, turn left (east).**

44.5 2.8 Passing through belt of sand dunes built on top of upper Holocene alluvium. Tephra collected from middle alluvium of Marble Creek (?) beneath dune in roadcut on south side of road as yet unidentified.

45.8 1.3 To right, alluvium of Chiatovich Creek is very saline due to high groundwater level; white areas to right are sand flats crusted with salt. Across valley to east is Emigrant Peak fault zone. Prominent fault scarps from 12:00 to 1:00 are on dissected middle to early Quaternary gravels; from 1:00 south, scarps are on early Marble, Leidy, and Indian Creek surfaces. Dissected older gravel is as old as 2 Ma (ashes correlative to Tuff of Taylor Canyon, Reheis, in press a), and as young as 0.74 Ma (interbedded beach deposit of Bishop ash). Older gravel probably contains at least one unconformity.

47.0 1.2 Passing old homestead in trees on right; active springs there are along a low fault scarp, which we intersect at next stop.

47.5 0.5 **STOP SEVEN** (OPTIONAL)

SINTER MOUND (TEPHRA SITE FLV-148-CS AND FLV-148A-CS)

This low mound of rocks north and south of the road consists mainly of pumiceous, glassy sand and silt cemented by opaline silica, and is described in detail in Reheis, Slate, Sarna-Wojcicki, and Meyer (this volume). Near the top of the mound, the glass in one sample (FLV-148A-CS) is chemically correlative to the Bishop ash. Based on the similarity of pumice and glass and the character of the opal cement throughout the outcrop, the rocks are inferred to represent a deposit of Bishop ash cemented by siliceous hot-spring waters. In one location south of the road, the sinter mound is underlain by marl and micrite oolite. The sedimentology and bedding of the rocks suggests that they were deposited as a sinter mound in shallow water at the edge of the same pluvial lake indicated by the deltaic sediments at McAfee Creek (stop 3, day 1). Because vertical faulting has been minor in this area, the elevation of the top of the sinter-mound rocks is inferred to represent the shoreline elevation (1410 m) of the pluvial lake at 740 ka.

Turn around and drive west back to paved road.

53.3 5.8 Turn left (south) on paved road.

65.4 12.1 Turn right into campground.

END DAY TWO

DAY THREE

0.0 0.0 From campground, turn left (north) on paved road. Repeat road log of second day.

4.3 4.3 Intersection with Sage Hen Road, marked on west by green mailbox for Evergreen Mine and transformer station. Turn left (west), passing transformer on south, and proceed up Marble Creek fan. Road is mostly on late alluvium of Marble Creek. Leidy Creek at 11:00, marked by cottonwood trees, has prominent fault scarps at range front. Road points to mouth of Marble Creek, an unglaciated small drainage sandwiched between large fans of Leidy Creek on south and Indian Creek on north. Indian Creek marked by cluster of trees at old homestead at 2:00. To right, not easily seen, are east-facing faults (light-colored streaks) of a huge graben complex breaking Indian surface ("shattered fan" of Sawyer, this volume).

4.8 0.5 Pointed at hill formed by 3-4-Ma basalt flow at range front. Basalt is downfaulted from same flow at top of ridge above hill. Relatively little strike-slip motion occurred on this inactive strand, because both basalt outcrops overlie stream gravel with Indian Creek composition, and apparent horizontal separation between the outcrops is no more than about 0.3 km. If fault had been moving for 3 million years at present local rate of 0.6-0.8 mm/yr (Sawyer, this volume), separation of the two basalt outcrops should be 1.2-1.6 km. At about 3 Ma, Indian Creek must have flowed a little south of present course and perhaps was diverted to its present course when valley was dammed by basalt.

Main active fault ("master fault" of Sawyer, this volume) visible to right of basalt hill at increase in fan gradient. Abrupt east-facing scarp, 30-50 m high, offsets Indian surface and is part of graben on south side of Indian Creek fan. West-facing fault of graben reverses throw to north near Indian Creek (fig. 7). North of Indian Creek is Davis Mountain, capped by 3-4-Ma andesite flows up to 250 m thick (Robinson and Crowder, 1973). Top of Davis Mountain illustrates east-tilted nature of White Mountains caused by more uplift on west side (dePolo, this volume).

6.5 1.7 Pointed at fanhead trench with light-colored, bouldery alluvium spilling out. Bedrock at mouth of Marble Creek is dominantly quartz monzonite but large areas of marble-bearing Precambrian Wyman Formation crop out upstream (Krauskopf, 1971); hence, alluvium is calcareous.

7.1 0.6 At 2:30, good view of basalt hill faulted against granite to west.

7.4 0.3 Driving on very young bouldery debris flows with little or no soil development (unit Qfcl, fig. 6). Prominent fault scarp south of Marble Creek cuts Indian surface on Leidy Creek fan with as much as 92 m of right-lateral offset (stop 8D; Sawyer, this volume).

7.6 0.2 At 11:00, where onfan drainage emerges from fault scarp, is fault trench (stop 8C, fig. 6). Marble Creek is remarkable for wood fragments in debris flows; age control is primarily from ^{14}C dates on wood.

8.4 0.8 **STOP EIGHT.** Park across from house-sized boulder north of road. We will spend all morning viewing faults, age control, and soils on the Marble Creek and Leidy Creek fans (fig. 6). The boulder lies on the Leidy surface, whereas the road is on the slightly lower early Marble Creek surface. The southern half of the Marble Creek fanhead is comprised of an uplifted remnant of alluvium of Indian Creek which is locally buried by younger deposits.

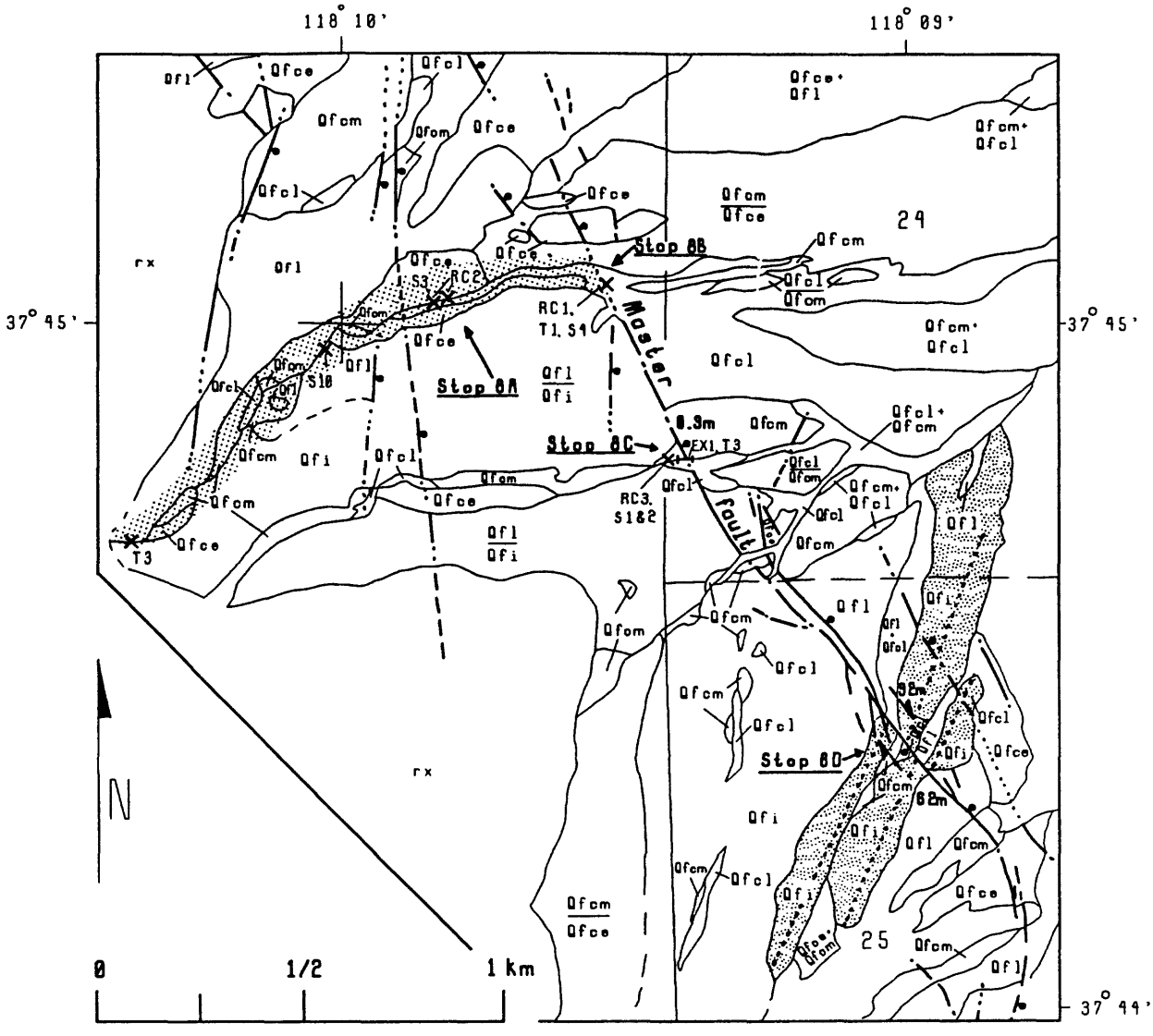

EXPLANATION

Alluvium of:

- Qfcl — late
- Qfcm — middle
- Qfce — early
- Qfl — Leidy Creek
- Qfi — Indian Creek; levee w/ crest projections (dotted line)
- rx — bedrock

Fault, bar and ball on downthrown side, arrows show sense of displacement; displacement in meters where known; dashed where inferred, dotted where concealed

Sample site: S, soil; RC, radiocarbon; T, tephra

EX1 — Trench site

Area of fanhead trench

Figure 6. Geologic map of alluvial-fan deposits and faults near the mouth of Marble Creek and the northern edge of the Leidy Creek fan, northwestern Fish Lake Valley (stop 8 of field trip). Combined map symbols (Qfcm + Qfcl) are used where two map units are closely interspersed. Fractional map symbols (Qfl/Qfi) are used when a thin veneer of a younger unit overlies an older unit.

MARBLE CREEK

Stop 8A, fanhead trench at parking area. In the north wall of the fanhead trench is a bristlecone pine log 2.2 m below the surface. The ^{14}C age of this log is 2155 yr B.P., calibrated by dendrochronology (cal B.P.). The early alluvium of Marble Creek (unit Qfce) is separated from the alluvium of Indian Creek (unit Qfi) by a buttress unconformity about 0.8 m below the log. A second log, 20 m downstream and 5 m below the surface, also in unit Qfce, has a ^{14}C age of 2340 cal B.P. In the south wall, a calcic paleosol on the Indian surface is buried under 2-3 m of early alluvium of Marble Creek (fig. 5 in Sawyer, this volume).

Walk east down the fanhead trench.

Stop 8B, fanhead trench at intersection of master fault. Here the fanhead trench is crossed and apparently truncated by the master fault (fig. 6). East of the fault, Marble Creek is actively depositing a fan composed mainly of late alluvium of Marble Creek (unit Qfcl), which contains abundant wood fragments and one tephra layer. Three ^{14}C ages on wood from unit Qfcl range from 120 cal. B.P. at 5 to 26 cm below the surface to 680 cal. B.P. from wood within a tephra layer about 2 m below the surface. The chemistry of the glass and the relation of the tephra to the dated wood suggests that the tephra correlates with an ash erupted at about 640 yr B.P. from Panum Crater in the Mono Craters area (A.M. Sarna-Wojcicki, 1989, written commun.).

Walk south along the master fault about 0.5 km.

Stop 8C, fault trench at minor drainage crossing master fault. On the north side of this drainage, sediments offset by the master fault are exposed in the streamcut and in a hand-excavated trench. On the downthrown side of the fault, the drainage forms an inset fanlette composed of middle and late alluvium of Marble Creek (units Qfcm and Qfcl, fig. 6). The middle Marble surface has been offset about 0.3 m across the fault. Relations within the exposed and offset sediments, including a Mono Craters tephra (3400-4100 yr B.P.?) and a fragment of wood dated at 1555 cal. B.P., indicate two paleoseismic events in the last 3400 to 4100 years, with the last event occurring since about 1500 yr B.P. (Sawyer, this volume).

Walk south along the master fault 0.5 km.

Stop 8D, offset debris-flow levees of unit Qfi on the northern Leidy Creek fan. At this site (fig. 6), the northeast levee forms a shutter ridge that diverts a minor interfluve northwest along the fault. An EDM-theodolite survey indicates about 92 m of right-lateral displacement across the master fault, with little vertical displacement. Age and displacement estimates for the levees suggest a late Pleistocene slip rate of 0.8 mm/yr (Sawyer, this volume).

The northwest flank of the northeast levee has well developed micro-relief steps arranged in flights. These patterned-ground features probably formed by mass wasting of a veneer of desert loess (Av horizon) by solifluction (Sawyer, this volume, and 1990). The less permeable argillic horizons and partially cemented Bk horizons of the Indian-aged soils apparently facilitate this unique mode of solifluction.

Turn around and return east on Marble Creek road. At 10:00 are west-facing scarps of graben complex on shattered fan of Indian Creek; center of graben at about 9:00. Total width of graben is more than 3 km.

12.5 4.1 Intersection with paved road; turn left (north).

14.8 2.3 Just north of mile marker 17, turn left (northwest) on unmarked dirt road; sign 50 m up road reads "Caution, minimum maintenance only". This road is southern access to Indian Creek fan. Entire expanse of fan surface south of road, from point where fan gradient steepens to range front with prominent east-facing fault scarp, is Indian surface.

16.1 1.3 At 10:00 is northeast-striking scarp facing south on Indian surface. This scarp marks the northeast corner of the large graben complex.

16.5 0.4 Merge with dirt road (northern access) coming in from northeast. Sign says "Gate locked 7 1/2 miles ahead." Continue west up fan past old homestead and trees. Driving on Holocene alluvium of various ages.

19.2 2.7 Crossing poorly expressed fault; youngest surface faulted is of early Marble age. West of strand, road is on Leidy surface as far as main fault scarp. At 3:00 is big fault scarp; several other scarps visible to the west. These scarps spread out in broad distributed pattern on Chiatovich Creek fan and represent northern end of the FLVFZ. Faults step east from this area across valley to Emigrant Peak fault zone bounding northeast side of FLV.

19.7 0.5 Crossing main fault scarp (fig. 7). Laterally offset debris-flow channel on Leidy surface is south of road. In stream channel north of road, middle Marble surface is offset.

20.0 0.3 **STOP NINE.** Crossing another fault strand; park off road to permit passage of through traffic. We will spend the afternoon here looking at faults, age control, and soil development.

INDIAN CREEK

A large graben offsets the Indian and younger surfaces south of the road (fig. 7). To the west, south of the creek, an older inactive fault offsets both the Indian surface and an old landslide that forms the range front south of Indian Creek. North of the creek, a low hill of 3-4-Ma andesite is downfaulted from the flows that cap Davis Mountain. Trace-element chemistry on samples from these flows (R.A. Thompson, written commun., 1991) suggest little or no strike-slip displacement on this inactive fault.

Quaternary deposits at the mouth of Indian Creek are well preserved as inset terraces (fig. 7). The lowest extensive surface north of the creek is Leidy in age. Two charcoal samples were collected from debris-flow deposits underlying this surface; one sample, at about 3.5 m below the surface, was dated at 6.5 ka. The next higher surface north of the creek is Indian in age. Due west, the highest deposits are correlated to the alluvium of McAfee Creek based on surface and soil morphology. Inset within the Leidy surface is a complex of middle to late Holocene deposits correlated with early, middle, and late alluvium of Marble Creek. The two older of these Holocene units have been dated here using several charcoal deposits (Slate, this volume); the ages are in fairly good agreement with the wood-dated units at Marble Creek. We will examine these dating sites and soil development on the Holocene deposits.

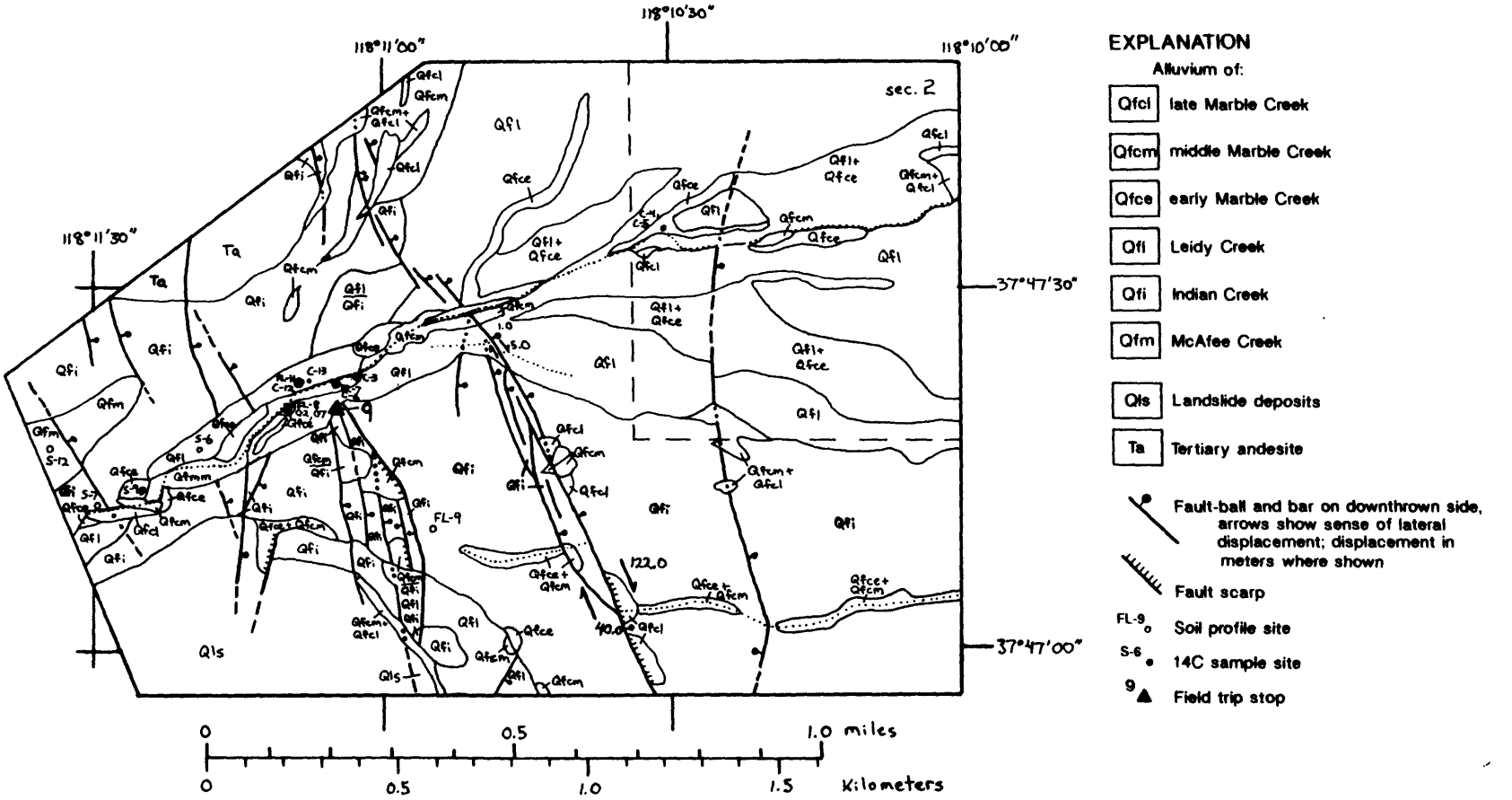

Figure 7. Geologic map of alluvial-fan deposits and faults at the mouth of Indian Creek, northwestern Fish Lake Valley (stop 9 of field trip). Combined map symbols (Qfcm + Qfcl) are used where two map units are closely interspersed. Fractional map symbols (Qfcm/Qfi) are used when a thin veneer of a younger unit overlies an older unit. Faults are dashed where inferred, dotted where concealed. Lines of small dots represent stream or debris-flow channels.

END OF FIELD TRIP

Those travelling north should take the left fork at the Y intersection downfan; those travelling south, the right fork.

References

Chesterman, C.W., 1956, Pumice, pumicite, and volcanic cinders in California: California Division of Mines, Bulletin 174, 97 p.

dePolo, C.M., 1991, Uplift history of the White Mountains, California and Nevada: Guidebook, Pacific Cell, Friends of the Pleistocene, this volume.

Elliott-Fisk, D.L., 1987, Glacial geomorphology of the White Mountains, California and Nevada: Establishment of a glacial chronology: Physical Geography, v. 8, p. 299-323.

Gillespie, A.M., 1991, Trail Canyon fans: Capture history of Rock Creek, in Guidebook for field trip to Fish Lake Valley, California-Nevada: Pacific Cell, Friends of the Pleistocene, p. 178-184.

Harden, J.W., Lamothe, Paul, Chadwick, O.A., Pendall, E.G., and Gillespie, A.M., 1991, Soil formation on the Trail Canyon alluvial fan: U.S. Geological Survey Open-file Report 91-291, and in Guidebook for field trip to Fish Lake Valley, California-Nevada: Pacific Cell, Friends of the Pleistocene, p. 139-160.

Krauskopf, K.B., 1971, Geologic map of the Mt. Barcroft quadrangle, California-Nevada: U.S. Geological Survey Geologic Quadrangle Map GQ-960, scale 1:62,500.

Macke, D.L., Schumann, R.R., and Otton, J.K, 1990, Uranium distribution and geology in the Fish Lake surficial uranium deposit: U.S. Geological Survey Bulletin 1910, 22 p.

McKee, E.H., 1968, Age and rate of movement of the northern part of the Death Valley-Furnace Creek fault zone, California: Geological Society of America Bulletin, v. 79, p. 509-512.

McKee, E.H., and Nelson, C.A., 1967, Geologic map of the Soldier Pass quadrangle, California and Nevada: U.S. Geological Survey Geologic Quadrangle Map GQ-654, scale 1:62,500.

Pendall, E.G., Harden, J.W., and Trumbour, Sue, 1991, Pedogenic isotopic indicators of climate and carbon cycling in Fish Lake Valley, Nevada: U.S. Geological Survey Open-file Report 91-296, and in Guidebook for field trip to Fish Lake Valley, California-Nevada: Pacific Cell, Friends of the Pleistocene, p. 161-177.

Reheis, M.C., in press a, Geologic map of late Cenozoic deposits and faults in the western part of the Rhyolite Ridge 15' quadrangle, Esmeralda County, Nevada: U.S. Geological Survey Miscellaneous Investigations Map I-2183, scale 1:24,000.

Reheis, M.C., in press b, Geologic map of late Cenozoic deposits and faults in parts of the Soldier Pass and Magruder Mountain 15' quadrangles, Inyo and Mono Counties, California, and Esmeralda County, Nevada: U.S. Geological Survey Miscellaneous Investigations Map I-2268, scale 1:24,000.

Reheis, M.C., and McKee, 1991, Late Cenozoic history of slip on the Fish Lake Valley fault zone, Nevada and California: U.S. Geological Survey Open-file Report 91-290, this volume.

Reheis, M.C., Sarna-Wojcicki, A.M., Burbank, D.M., and Meyer, C.E., 1991, The late Cenozoic section at Willow Wash, east-central California: A tephrochronologic rosetta stone: U.S. Geological Survey Open-file Report 91-290, this volume.

Reheis, M.C., Slate, J.L., Sarna-Wojcicki, A.M., and Meyer, C.E., 1991, An early Pleistocene pluvial lake in Fish Lake Valley, Nevada-California: Ringside resort for the eruption of the Bishop Tuff: U.S. Geological Survey Open-file Report 91-290, this volume.

Robinson, P.T., and Crowder, D.F., 1973, Geologic map of the Davis Mountain quadrangle, Esmeralda and Mineral Counties, Nevada, and Mono County, California: U.S. Geological Survey Geologic Quadrangle Map GQ-1078, scale 1:62,500.

Robinson, P.T., McKee, E.H., and Moiola, R.J., 1968, Cenozoic volcanism and sedimentation, Silver Peak region, western Nevada and adjacent California, *in* Coats, R.R., Hay, R.L, and Anderson, C.A., Studies in Volcanology: Geological Society of America Memoir 116, p. 577-611.

Robinson, P.T., Stewart, J.H., Moiola, R.J., and Albers, J.P., 1976, Geologic map of the Rhyolite Ridge quadrangle, Esmeralda County, Nevada: U.S. Geological Survey Geologic Quadrangle Map GQ-1325, scale 1:62,500.

Sawyer, T.L., 1990, Quaternary geology and neotectonic activity along the Fish Lake Valley fault zone, Nevada and California: Reno, University of Nevada, M.S. thesis, 379 p.

Sawyer, T.L., 1991, Quaternary faulting and Holocene paleoseismicity of the northern Fish Lake Valley fault zone, Nevada and California, in Guidebook for field trip to Fish Lake Valley, California-Nevada: Pacific Cell, Friends of the Pleistocene, p. 114-138.

Slate, J.L. 1991, Quaternary stratigraphy, geomorphology, and geochronology of alluvial fans, Fish Lake Valley, Nevada and California, in Guidebook for field trip to Fish Lake Valley, California-Nevada: Pacific Cell, Friends of the Pleistocene, p. 94-113.

Spaulding, W.G., 1980, The presettlement vegetation of the California desert: Bureau of Land Management, Riverside, California, Contract Report #CA-060-CT8-65, 97 p.

LATE CENOZOIC HISTORY OF SLIP ON THE FISH LAKE VALLEY FAULT ZONE, NEVADA AND CALIFORNIA

by Marith C. Reheis and Edwin H. McKee

ABSTRACT

Recent geologic mapping and dating of upper Tertiary and Quaternary deposits in Fish Lake Valley, northern Eureka Valley, and Deep Springs Valley, Nevada and California, provide information on the early history of motion on the northern end of the right-lateral oblique Furnace Creek fault zone (herein called the Fish Lake Valley fault zone) and other associated faults. These deposits are interpreted to suggest the following history: Faulting began on the southern end of the Fish Lake Valley fault zone about 8-12 Ma. During the late Miocene and Pliocene, uplift caused deposition of coarse angular gravel on the southeast side of the fault zone. This gravel graded laterally into a drainage system flowing south from the White Mountains into Eureka Valley; Deep Springs Valley did not exist. Motion on the Fish Lake Valley fault zone and associated faults created another depositional basin on the northeast side of the fault zone into which streams flowed from the northwest end of the Sylvania Mountains. Sometime after 0.74 Ma, streams draining from the White Mountains into Eureka Valley were defeated by motion on the bounding faults of Deep Springs Valley and either began to pond in Deep Springs Valley or were captured by streams flowing into Fish Lake Valley.

Estimated lateral and vertical slip rates on the Fish Lake Valley fault zone and associated faults vary both temporally and spatially. The post-late Miocene right-lateral slip rate in southern Fish Lake Valley is most likely about 4-6 mm/yr, whereas in northern Fish Lake Valley it is about 1-3 mm/yr. The post-Bishop-ash (0.74 Ma) vertical slip rates are much higher than the long-term slip rate. Post-0.74-Ma vertical slip rates range from 0.3 to 0.7 mm/yr on several parts of the fault zone, whereas poorly constrained post-late Miocene vertical slip rates range from 0.05 to 0.2 mm/yr. These relations suggest that slip rates increased markedly in the Quaternary. The post-0.74-Ma vertical slip rate at the northern end of the Fish Lake Valley fault zone is about half the rate measured at the southern end.

INTRODUCTION

The Furnace Creek fault zone (FCFZ) is an active right-lateral oblique-slip fault system, over 250 km long, that strikes northwest near the southeast boundary of California (fig. 1). The northern part of this fault zone, herein referred to as the Fish Lake Valley fault zone (FLVFZ), forms the western margin of Fish Lake Valley, Nevada and California, and the eastern margin of the White Mountains. Other related Quaternary fault zones in this area include the Deep Springs normal fault zone (DSFZ) and the Emigrant Peak normal fault zone (EPFZ; Reheis, in press b). The southern end of the FCFZ merges with the right-oblique Death Valley fault zone (DVFZ).

Estimates of total right slip on the Furnace Creek and related Death Valley fault zones vary widely. The FCFZ ends in northern Fish Lake Valley and the DVFZ ends in southern Death Valley; hence, late Cenozoic total slip at the ends of these faults must be zero. From central Fish Lake Valley to northern Death Valley, estimates of total slip on the FCFZ based on various stratigraphic and geochemical markers range from 40 to 100 km (for example, Saleeby and others, 1986; McKee, 1968a; Stewart, 1967). The higher estimates (80-100 km) are based on isopach trends of Precambrian and early Paleozoic formations and are considered to be maximum values due to the uncertainties inherent in

such reconstructions (Stewart, 1967). In central Death Valley, Wright and Troxel (1967) estimated a maximum of 11 km of total right slip at the junction of the FCFZ and the DVFZ; Butler and others (1988) measured about 35 km of late Cenozoic right slip on the southern DVFZ.

If the spatial variations in slip dicussed above are correct, then tectonic models must be able to account for this variation. Burchfiel and Stewart (1966) suggested that central Death Valley experienced little strike-slip faulting because it is a pull-apart basin between the ends of the en echelon strike-slip FCFZ and DVFZ. Stewart (1983) later accounted for the increase in slip in northern Death Valley by northwestward translation of the Panamint Mountains block on the west side of Death Valley. Although satisfactory for Death Valley, these two models do not account for the decrease in slip in Fish Lake Valley, nor for the increase in slip in southern Death Valley.

Two different models that are applicable to the entire length of the FCFZ have been proposed by Stewart (1988) and by W.B. Hamilton (written commun., 1990). Stewart's model suggests that the various extension and strike-slip features of the Walker Lane belt, of which the FCFZ is a part, are related to temporal variation in the relative magnitudes of the S1 and S2 stress directions in a field where S3 (least principal stress) is oriented west-northwest. Lateral variability in right slip along the FCFZ would then be caused by temporal changes in faulting style from extension to shear. Hamilton's model, like those of Davis and Burchfiel (1973) and Guth (1981) in other areas, proposes that the FCFZ acts as a transform fault with varying amounts and times of extension on opposite sides of the fault. This model seems better able to accomodate the differing amounts of slip along the FCFZ. A corollary of Hamilton's model is that the steeply dipping FCFZ may flatten into a regional detachment fault at depth.

More work is needed to weigh the applicability of the two regional models. For example, Pleistocene directions of least principal stress appear to be nearly east-west along the FCFZ, but may be oriented northwest in the region east of the FCFZ (Reheis and Noller, in press); such variations in stress direction may help to explain the complex fault patterns in the area. This paper presents new information on lateral and temporal variations in fault history and slip rates of the FLVFZ that will help to evaluate the two regional models for the FCFZ.

McKee (1968a) estimated a post-Jurassic total lateral slip of about 50 km along the FCFZ at the southern end of Fish Lake Valley, based on (1) offset of the quartz monzonite of Beer Creek, which crops out extensively in the southern White Mountains and in the Sylvania Mountains, and (2) offset of Precambrian and Cambrian sedimentary rocks (fig. 1). He also believed that Pliocene arkosic sedimentary rocks in Willow Wash and at the mouth of Horse Thief Canyon (fig. 2) were deposited within the same drainage system, and inferred that this postulated drainage system was subsequently dismembered by right-lateral slip of about 1 km on the Furnace Creek fault zone. From the offset of both the Jurassic and the Pliocene rocks, McKee (1968a) calculated a lateral slip rate of about 0.3 mm/yr for the northern Furnace Creek fault zone. If the total post-Jurassic slip is about 50 km, then McKee's slip rate must be a minimum value because motion on the FCFZ probably did not begin before middle Miocene time (Hamilton, 1988; Wright, 1989).

New mapping of upper Tertiary and Quaternary deposits in northern Eureka Valley, Deep Springs Valley, and southern Fish Lake Valley (Reheis, in press a), provides age constraints for the onset of motion on the FLVFZ and permits new estimates of lateral slip rates. Mapping in central and northern Fish Lake Valley will not be discussed in detail in this paper, but this work (Reheis, in press b, and in progress) permits new estimates of late Cenozoic vertical and lateral slip rates on the FLVFZ and associated faults.

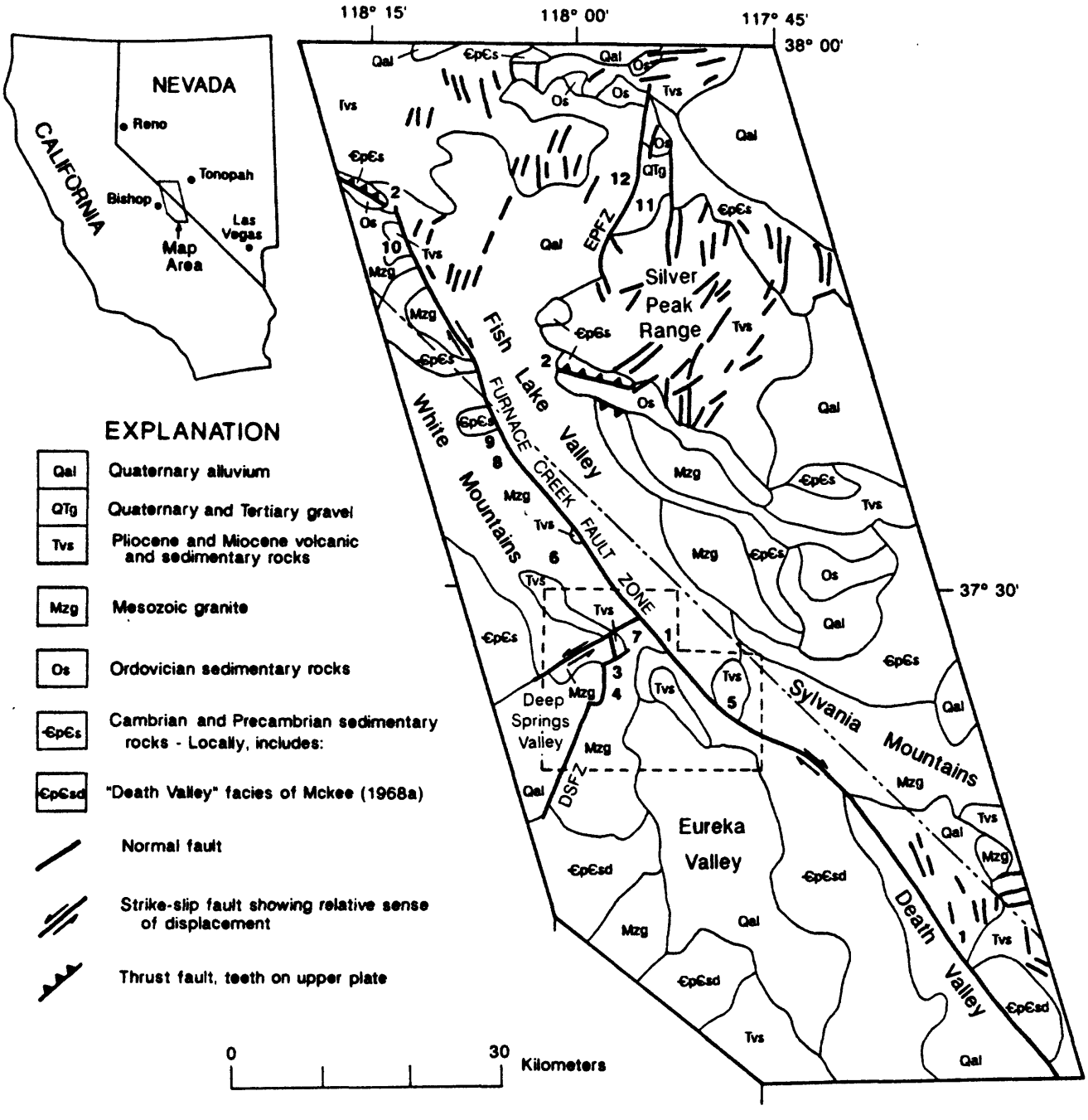

Figure 1. Geologic map of the northern Furnace Creek (Fish Lake Valley) fault zone (generalized from Stewart and Carlson, 1978). Additional faults in Quaternary deposits in northern Fish Lake Valley are from Reheis (in press b) and Reheis and Noller (in press). Number, location of slip-rate estimate (table 2). Short dashed line, area of figure 2. DSFZ, Deep Springs fault zone; EPFZ, Emigrant Peak fault zone. Thrust faults in northern Silver Peak Range and Sylvania Mountains not shown.

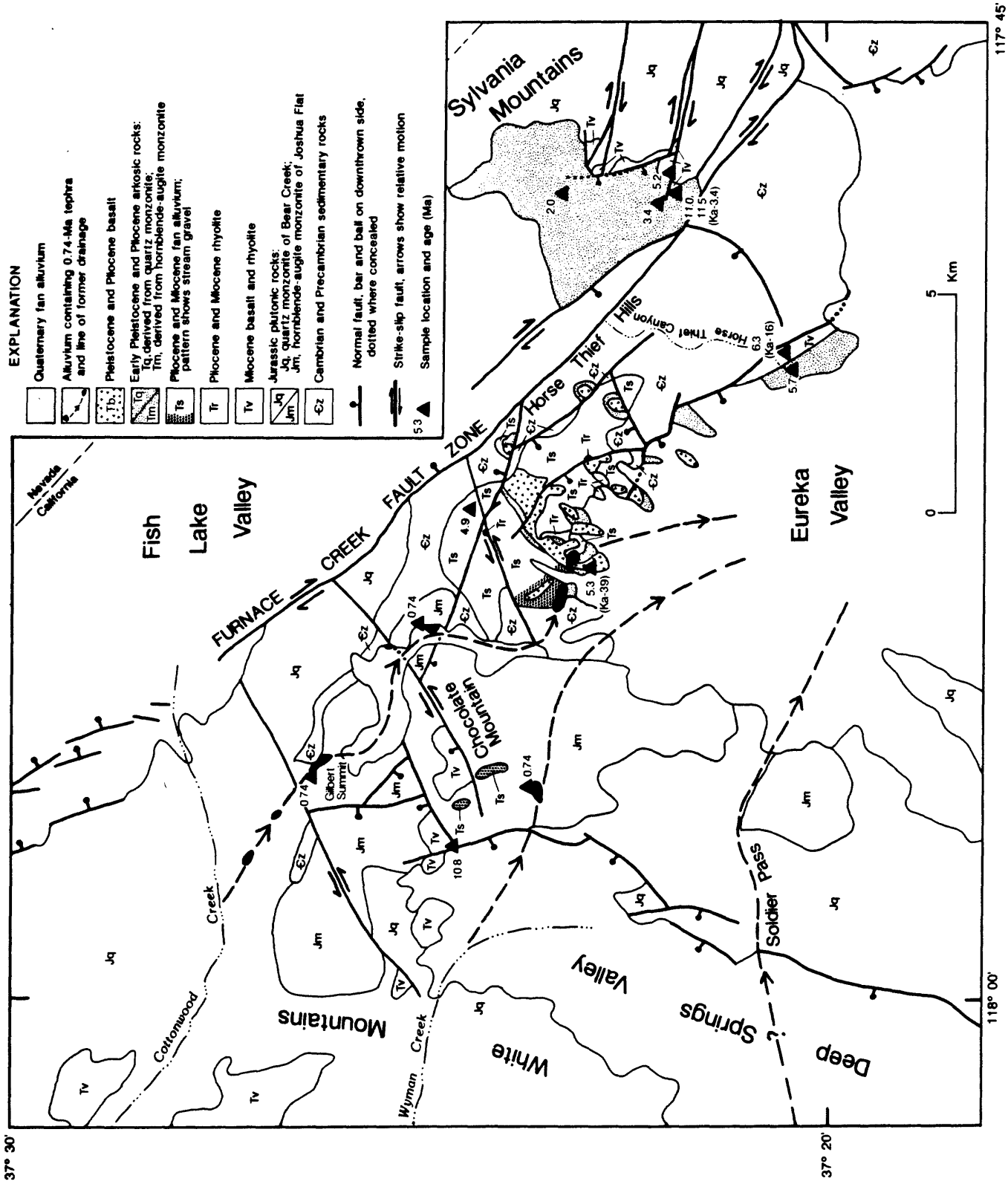

Figure 2. Geologic map of southern Fish Lake, Deep Springs and Eureka Valleys (modified from McKee and Nelson, 1967, Krauskopf, 1971, and McKee, 1985). Number (Ka-39) beside triangle denotes K-Ar dated samples obtained in this study (table 1).

STRATIGRAPHY AND STRUCTURE OF SOUTHERN FISH LAKE VALLEY AND SURROUNDING AREA

Deep Springs Valley Area

Outcrops of an 11.0±1.0 Ma basalt (Dalrymple, 1963; age converted to new constants; unit Tv, fig. 2), extend at least 30 km northwest from the north end of Deep Springs Valley (McKee and Nelson, 1967; Krauskopf, 1971), and are remnants of flows that were erupted onto a surface of low relief in the southern White Mountains. These basalt flows predate the formation of Deep Springs Valley (Dalrymple, 1963) and have been extensively disrupted by normal and left-lateral strike-slip faults between this valley and the FLVFZ. The gentle erosional surface on which these basalt flows were emplaced suggests that the basalt flows predate most, if not all, of the late Cenozoic motion on the FLVFZ. The basalt flows locally overlie a rhyolite flow dated at 11.1±0.2 Ma (Dalrymple, 1963; age converted to new constants).

Two small areas of stream gravel, mapped as unit Ts, crop out above the northeast corner of Deep Springs Valley (fig. 2; Miller, 1928). These gravels lie topographically about 40 m below the 10-12-Ma basalt at an elevation of about 2075 m (6805 ft). They are poorly to moderately consolidated and contain well-rounded to subrounded pebbles and large cobbles as well as less well rounded boulders. The smaller clasts include black and brown quartzite and black siltstone; the boulders are locally derived basalt and monzonite.

Wind gaps containing well-rounded stream gravel exist in three places on the hills bounding the east side and north end of Deep Springs Valley (Gilbert Summit, area south of Chocolate Mountain, and Soldier Pass, fig. 2). Based on their topographic positions and gravel lithologies, these wind gaps and fluvial deposits were most likely formed by streams flowing east and southeast from the southern White Mountains.

Deposits and preserved valleys of the paleodrainage of Cottonwood Creek (see road log, this volume), can be traced discontinuously from an elbow of capture above modern Cottonwood Creek in the southern White Mountains, along the present divide between Deep Springs Valley and Fish Lake Valley, and into Eureka Valley. Clast lithologies in the stream deposits at and northwest of Gilbert Summit (fig. 2) include abundant basalt, common quartz monzonite, granodiorite, quartzite, and phyllitic sandstone, and rare rhyolite. These lithologies are characteristic of formations exposed along the upper course of modern Cottonwood Creek in the White Mountains (Krauskopf, 1971). Deposits along the paleodrainage to the southeast have similar compositions, but the proportions of different lithologies vary and locally derived clasts are also present.

The gravel of ancestral Cottonwood Creek and associated alluvial-fan deposits commonly contain reworked tephra. Three deposits of tephra are correlated by glass major-oxide chemistry with the 0.74-Ma Bishop ash bed (A. Sarna-Wojcicki, written commun., 1988; age from Izett and others, 1988); several other tephra deposits resemble the dated deposits in grain size and in appearance and abundance of pumice clasts. Another wind gap south of Chocolate Mountain (fig. 2) contains stream gravel, probably from ancestral Wyman Creek, that is adjacent to, and may underlie, a deposit of Bishop ash. The tectonic significance of this deposit was recognized by Miller (1928).

Horse Thief Hills Area

Upper Miocene and Pliocene alluvial-fan deposits (Ts, fig. 2) overlie Precambrian and Cambrian rocks (McKee and Nelson, 1967; McKee, 1968a) in the Horse Thief Hills, and are the oldest Tertiary sedimentary rocks in the area (Reheis, in press a). These sedimentary rocks are moderately consolidated debris-flow and talus(?) deposits that consist primarily of unsorted angular clasts of Precambrian and Cambrian quartzite and

limestone. The thickness of the sedimentary section varies greatly. The basal contact is poorly exposed, but map relations of the basal fan alluvium with the subjacent bedrock suggest that the alluvium was deposited on an irregular topography. The fan alluvium generally coarsens (up to large boulders) both upward in the section and laterally to the northeast and feathers out near the present trace of the Furnace Creek fault zone. This apparent thinning to the northeast may be due to post-depositional erosion, inasmuch as the thinnest sections occur on present topographic highs. The alluvial-fan unit is as much as 120 m thick where well preserved.

Near Eureka Valley, the alluvial-fan facies of unit Ts grades to a round-pebble conglomerate facies. This conglomerate consists mainly of siliceous sedimentary rocks; black quartzite and siltstone are especially abundant, and carbonate rocks are rare or absent. Black quartzite and siltstone commonly, but not exclusively, occur in the Cambrian Campito Formation and the Late Proterozoic Deep Spring and Wyman Formations. These formations presently crop out in the southern White Mountains in the upper reaches of Wyman Creek (5 km west of the boundary of fig. 2; Nelson, 1966). They also crop out, in association with carbonate rocks of the Cambrian Bonanza King Formation or the Precambrian Reed Dolomite, along the north side of the Sylvania Mountains and the south side of Magruder Mountain (along the eastern edge and for about 15 km further east of the boundary of fig. 2; McKee, 1985; McKee and Nelson, 1967).

The clasts in the round-pebble facies of unit Ts are similar in lithology to the pebble- and cobble-sized fraction of the outcrops mapped as unit Ts on Chocolate Mountain, four kilometers to the northwest and about 550 m higher in elevation. Modern streams draining the White Mountains that carry pebble- to cobble-sized material have gradients of about 50-75 m/km. If the outcrops in Eureka Valley and on Chocolate Mountain represent deposits of the same drainage, their present topographic relations imply vertical uplift of the footwall of the Deep Springs Valley fault zone of about 250-350 m since Miocene time.

At two sites in the northwestern part of the outcrop area (fig. 2), clast imbrication and cross-bedding features in the round-pebble facies of unit Ts indicate stream flow to the south and southeast. Sedimentary structures indicative of flow direction were not observed in sediments of the alluvial-fan facies of unit Ts due to poor exposure and coarse grain size. However, the lithologic composition of the alluvial-fan facies is distinctly different from that of the round-pebble facies; hence, the alluvial-fan sediments must have been derived from a different source area.

Unit Ts contains at least one, and possibly as many as three, rhyolite units (Tr, fig. 2). The oldest rhyolite, interbedded with sediments near the base of unit Ts, yields a K-Ar age of 8.4 ± 0.2 Ma (Robinson and others, 1968; age converted to new constants). Another rhyolite, interbedded with sediments in the upper part of unit Ts, is correlated by glass chemistry to the 4.9 ± 0.2 Ma tuff of Springdale (K-Ar age, A. Sarna-Wojcicki, written commun., 1988; dated tuff collected by B. Hausback, California State University at Sacramento).

A section of moderately consolidated arkosic sedimentary rocks (Tm, fig. 2), of probable Pliocene age, overlies unit Ts on the crest and the western flank of the Horse Thief Hills (Reheis, in press a). On the crest, the arkosic unit is generally less than 50 m thick, but on the flanks of the hills along Eureka Valley, the unit locally exceeds 300 m in thickness. Unit Tm includes the sedimentary rocks described by McKee (1968a) at the mouth of Horse Thief Canyon. Unit Tm is in turn overlain by basalt and andesite flows (unit Tb, fig. 2), which have yielded a single K-Ar age of $5.3 \pm .16$ Ma (table 1).

Unit Tm consists mainly of subrounded to well-rounded gravel and sand, principally derived from the Jurassic hornblende-augite monzonite of Joshua Flat (Jm, fig. 2; McKee and Nelson, 1967)

Table 1. Analytical data for K-Ar age determinations.

Sample number[1]	Material dated	K_2O (wt. %)	$^{40}Ar^*$ (mole/g·10^{-11})	$^{40}Ar^*/E^{40}Ar$ (%)	Age (Ma±o)
FL-KA-1	whole rock	2.842	1.2928	20.0	3.2±0.12
FL-KA-2	whole rock	2.749	1.5606	28.1	3.9±0.13
FL-KA-3	glass	5.36	8.5464	66.5	11.0±0.3[2]
FL-KA-4	whole rock	1.223	2.0339	44.2	11.5±0.4
FL-KA-6	whole rock	3.73	1.5984	21.8	3.0±0.11
FL-KA-8	whole rock	3.35	1.4337	36.3	3.0±0.10
FL-KA-9	whole rock	3.02	1.3997	30.0	3.2±0.11
FL-KA-10	whole rock	1.754	2.4737	59.9	9.8±0.3
FL-KA-16	whole rock	3.36	3.0961	51.1	6.3±0.2
FL-KA-39	whole rock	2.363	1.8154	51.2	5.3±0.16

[1] Sample localities are shown on figs. 1 and 2.
[2] Originally dated by Robinson and others (1968) at 13.3±.08 Ma (age converted to new decay constants).

which crops out to the west and northwest of the Horse Thief Hills. The unit also contains quartzite and phyllitic clastsderived from Cambrian and Precambrian sedimentary rocks, especially in the northern part of the outcrop area, clasts derived locally from quartzite and limestone cropping out in the Horse Thief Hills in the southern part of the outcrop area, and some coarse-grained arkosic material possibly derived from the quartz monzonite of Beer Creek. Clast imbrication and cross-bedding in several outcrops of unit Tm along the northeastern margin of Eureka Valley indicate a consistent south to southeast direction of stream flow (Reheis, in press a). Robinson and others (1968; age converted to new decay constants) reported a K-Ar age of 5.9±0.6 Ma on biotite from a tephra near the base of unit Tm. This age is in good agreement with a K-Ar age of 6.3±0.2 Ma recently obtained on a basalt flow (unit Tv, which includes all Miocene volcanic rocks in the area) that underlies the unit at the mouth of Horse Thief Canyon (table 1).

Willow Wash Area

Over 800 m of upper Miocene to lower Pleistocene arkosic and volcanic rocks (described by McKee, 1968a, b) were deposited in a small basin on the north side of the Sylvania Mountains (figs. 2 and 3). New mapping of this area, summarized here, is described in detail in Reheis and others (this volume, a) and Reheis (in press a). The oldest rocks (Tv, fig. 2) in this basin are of Miocene age and overlie the Jurassic quartz monzonite of Beer Creek (Jq), which crops out extensively in the Sylvania Mountains (McKee and Nelson, 1967). These rocks include a biotite-rich rhyolite and an overlying basalt dated at 11.0±0.3 and 11.5±0.4 Ma, respectively (table 1; the rhyolite was originally dated at 13.3±.08 Ma, Robinson and others, 1968; age converted to new K radioactive decay constants).

Limited exposures show that the overlying sedimentary rocks (Tq, fig. 2) either lie unconformably on the Miocene volcanic rocks or are in fault contact with them. These sedimentary rocks grade upward from moderately to poorly consolidated and were derived primarily from the quartz monzonite of Beer Creek in the Sylvania Mountains. They

consist chiefly of silt, sand, and gravel, and commonly include large, intact feldspar and quartz phenocrysts derived from the quartz monzonite.

The lower half of the sedimentary section contains interbedded basalt and lithic tuff. The volcanic rocks lie about 30 m above an unconformity that bounds the top of a 145-m-thick section of fluvial sediments; these fluvial sediments in turn rest unconformably on the 11-12-Ma volcanic rocks.

The age control for the lower part of the sedimentary section is contradictory. The basalt flow interbedded with these sediments has a K-Ar age of 9.8±0.3 Ma (table 1), whereas tephra layers above and below the volcanic rocks are believed to be about 3.4 Ma and 5.2 Ma, respectively (fig. 3). The anomalously old K-Ar age of the basalt, the disturbed bedding in parts of these volcanic layers, and the tephrochronologic ages suggest that the interbedded volcanics may be landslides from topographically high parts of the basal volcanic rocks (fig. 2).

The middle part of the section consists of gypsiferous mudstones of an alkaline lake or playa, and the upper part of the section consists of coarse, bouldery alluvial-fan deposits. These deposits contain numerous beds of reworked tephra that constrain the age of the upper sedimentary sequence to late Pliocene and early Pleistocene time (figs. 2 and 3; Reheis and others, this volume, a). The bedding, composition, coarse grain size, and poor rounding of most of the alluvial deposits indicate that they were probably deposited by streams draining northwest from the Sylvania Mountains (Robinson and others, 1968). A sedimentary source in outcrop areas of the quartz monzonite of Beer Creek in the White Mountains is also possible. However, restoration of 10-30 km of right slip (based on slip rate estimates, discussed below) places the Willow Wash area adjacent to parts of the White Mountains with extensive outcrops of Precambrian and Cambrian sedimentary rocks or very fine-grained quartz monzonite that do not occur in the Willow Wash sediments.

The basal volcanic rocks in the Willow Wash area are extensively faulted by right-lateral faults of the FLVFZ. In many places the volcanic rocks are faulted against quartz monzonite (fig. 2), but in other locations, the volcanic rocks are in depositional contact with quartz monzonite. Where exposed, the topography of this contact appears to be gentle, and the underlying quartz monzonite is highly weathered.

The K-Ar ages of the basalt and rhyolite flows at the base of the Willow Wash section are very similar to the ages of the basalt and rhyolite in the southern White Mountains (table 1). In addition, preliminary results from major-oxide and trace-element analyses of several ~10-12-Ma basalts from the southern White Mountains, Deep Springs Valley, and Willow Wash suggest that the basalts are from the same flow or group of flows (R.A Thompson, written commun., 1991). The 11-12-Ma basal rhyolite may also be correlative with biotite-rich rhyolites within Tertiary sediments at the northern end of Fish Lake Valley; these rhyolites were dated at 11.3±0.2 and 11.6±0.2 Ma (Robinson and others, 1968; ages converted to new decay constants). These Tertiary sediments were inferred to represent a late Miocene period of tectonic stability, an environment which may also be indicated in Willow Wash by the weathered quartz monzonite and the gentle topography on which the basal volcanics were emplaced.

Structural relations in the basal 200 m of the Pliocene to early Pleistocene sedimentary rocks in Willow Wash are complex (see Reheis and others, this volume, a). Locally, the basal fluvial deposits appear to lie unconformably on eroded fault scarps. In other places, faults offset the basal sedimentary rocks but do not offset the upper 500 m of the section (fig. 2). Hence, deposition of the basal deposits appears to have been contemporaneous with early motion on splays of the FLVFZ.

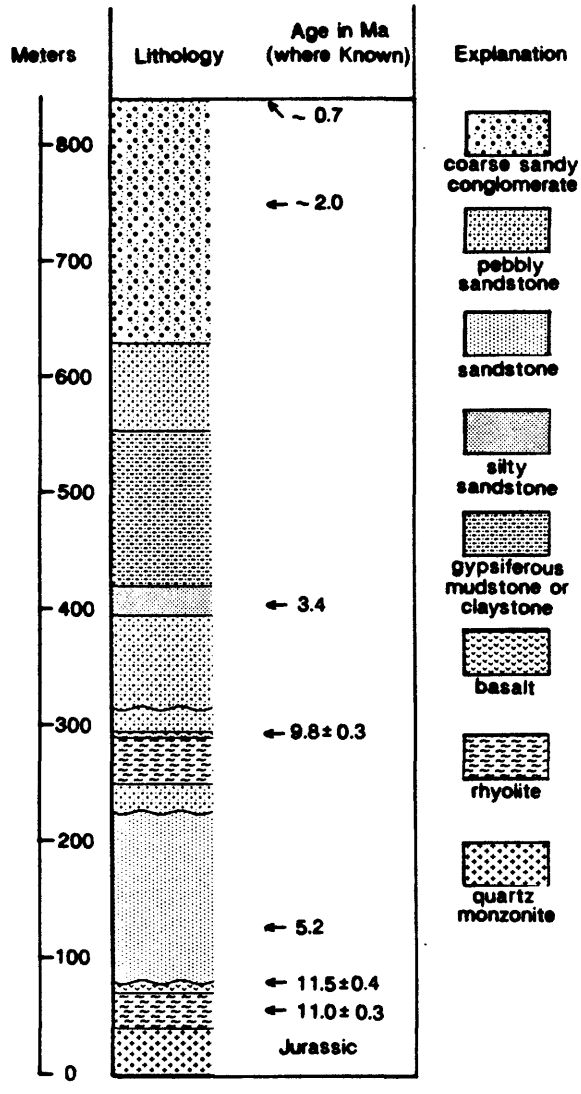

Figure 3. Composite stratigraphic section of upper Miocene to lower Pleistocene rocks in Willow Wash (see fig. 2). Dates on basalts and basal rhyolite are listed in table 1; dates within sediments are from tephrochronologic correlations (Reheis and others, this volume, a). 9.8-Ma basalt and underlying lithic tuff may be slide blocks derived from the basal volcanic flows.

Interpretation of Deposits and Faults

10-12-Ma basalt and rhyolite flows were erupted onto an extensive surface of low relief, mainly cut on the quartz monzonite of Beer Creek, in the southern White Mountains. These flows and the subjacent erosion surface were probably coextensive with the 11-12-Ma volcanic rocks overlying the same quartz monzonite at the base of the Willow Wash section, and may have been coextensive with Tertiary sediments and rhyolites of similar age at the northern end of Fish Lake Valley. These relations suggest a tectonically inactive late Miocene landscape of low relief that predated motion on the FLVFZ.

Moderately consolidated upper Miocene and Pliocene fan alluvium in the Horse Thief Hills (Ts, fig. 2) consists of Precambrian and Cambrian clasts deposited on a landscape of moderate relief. The composition, distribution, coarse grain size, and angularity of this alluvium suggests that it was deposited as a piedmont adjacent to a range front composed of Cambrian and Precambrian rocks bounded by an active range-front fault which lay in the vicinity of the present trace of the FLVFZ. Thus, the basal sediments of the fan alluvium in the Horse Thief Hills may record the onset of faulting along the southern FLVFZ. The fan alluvium contains interbedded rhyolite flows, including two tuffs dated at 8.4$\pm$0.2 Ma (Robinson and others, 1968; age converted to new constants) and

4.9±0.2 Ma (A.M. Sarna-Wojcicki, written commun., 1988). Hence, we infer that the Furnace Creek fault zone, or a range-front fault near the present position of the Furnace Creek fault zone, became active at or just prior to about 8.4 Ma.

The alluvial-fan facies of unit Ts grades laterally southwestward into a round-pebble conglomerate with distinctive black quartzite pebbles. Although black quartzites are found in Cambrian and Late Paleozoic formations that crop out in several areas around the Horse Thief Hills, the closest sources are to the east and northeast in the Last Chance Range and the northern Sylvania Mountains where large areas of carbonate rocks also crop out (McKee and Nelson, 1967; McKee, 1985). The round-pebble conglomerate of the Horse Thief Hills contains almost no carbonate clasts. Hence, it seems most likely that the source of this conglomerate was in the more distant southern White Mountains, where carbonate rocks are present but the greater distance of fluvial transport may have removed more carbonate clasts by solution. A source in the southern White Mountains for the round-pebble conglomerate is also favored by sedimentary structures that indicate southeastward flow.

If the round-pebble facies of unit Ts in northeastern Eureka Valley is correlative with stream gravel mapped as unit Ts that are inset into a 11.0±1.0 Ma basalt on the northeastern corner of Deep Springs Valley (fig. 2), then the drainage was established after the eruption of this basalt. The compositions of both the alluvial-fan and the round-pebble facies of unit Ts demonstrate that this depositional basin, although now adjacent to Willow Wash across the Furnace Creek fault zone, was distinct from that of Willow Wash throughout Pliocene time.

Scattered outcrops of Pliocene arkosic rocks (Tm, fig. 2) overlie the upper Miocene and Pliocene sediments (unit Ts) in and on the southwest margin of the Horse Thief Hills. Although McKee (1968a) believed that Willow Wash was the source area of these arkosic rocks, three observations suggest that this belief is incorrect: (1) The arkosic rocks contain clasts derived from the hornblende-augite monzonite of Joshua Flat. This monzonite does not crop out in the area of Willow Wash nor anywhere in the Sylvania Mountains, but only to the north and west of Eureka Valley (fig. 2). (2) Clast imbrications and cross-bedding in outcrops adjacent to Eureka Valley indicate a south to southeast flow direction, parallel to the Horse Thief Hills. (3) Horse Thief Canyon is similar to other drainages that are eroding headward from Eureka Valley into southern Fish Lake Valley. The youthful appearance of these drainages (steep narrow canyons, twisting stream courses) and the presence of ongoing stream captures in this area suggest that Horse Thief Canyon is too young to have served as a conduit for arkosic material from Willow Wash in Pliocene time. Horse Thief Canyon could, however, have been part of a subsequently dismembered drainage that crossed the fault in Pleistocene time.

In summary, the Pliocene arkosic rocks of unit Tm in the Horse Thief Hills and Eureka Valley were probably deposited by streams that flowed southeast from the southern White Mountains into Eureka Valley. In contrast to the drainage that deposited the older round-pebble facies of unit Ts, this later stream deposited arkosic rocks with monzonitic detritus derived from the hills along the east side of Deep Springs Valley. The addition of monzonitic detritus, however, need not have required a large change in source area. Uplift along the bounding faults of Deep Springs Valley, across the course of the paleodrainage, would result in the gradual exposure of a large area of monzonite bedrock to weathering and stream erosion. Thus, younger deposits of the paleodrainage should contain progressively larger amounts of monzonitic detritus.

In Willow Wash, a sequence of Pliocene and upper Pleistocene arkosic rocks (Tq, fig. 2) unconformably overlies upper Miocene basalt and rhyolite flows, which in turn overlie the Jurassic quartz monzonite of the Sylvania Mountains (figs. 3 and 3). The basal

volcanic rocks are extensively faulted and tilted, and deformation decreases upward and eventually dies out in the sedimentary section.

The arkosic rocks of Willow Wash are mainly composed of sediment derived from the quartz monzonite of Beer Creek and were probably deposited by streams draining northwesterly from the Sylvania Mountains. The basin in which the Willow Wash sediments crop out is fault-bounded on the west, south, and southeast (fig. 2) by the main Furnace Creek fault and associated west-striking strike-slip faults and north-striking normal faults. The distribution of these faults and the decrease in faulting upward in the Willow Wash section suggest that motion on faults associated with the FLVFZ was responsible for the formation of the depositional basin that now coincides with the southern end of Fish Lake Valley. A system of active basin-bounding faults would also help to explain the deposition of lacustrine or playa sediments so close (less than 0.5 km) to the western front of the Sylvania Mountains in Pliocene time. In summary, we infer that the basal sedimentary rocks of the Willow Wash section provide a minimum age of latest Miocene or earliest Pliocene for the inception of motion on the southern FLVFZ.

Streams continued to flow from the southern White Mountains into Eureka Valley until sometime after the eruption of the Bishop ash (0.74 Ma). The wind gaps and stream gravels in high divides between Deep Springs Valley and Fish Lake and Eureka Valleys collectively demonstrate that Deep Springs Valley and southern Fish Lake Valley did not exist in their present form until sometime after 0.7 Ma.

ESTIMATIONS OF SLIP RATES

Right-lateral slip rates on the FLVFZ

Volcanic rocks that underlie the faulted basal sediments of unit Tq in Willow Wash have a maximum age of 11.9 Ma, and rhyolite that crops out near the base of the alluvial-fan facies of unit Ts in the Horsethief Hills has a minimum age of 8.2 Ma (fig. 2 and table 1). The total right slip on the FLVFZ in southern Fish Lake Valley is probably about 50 km (McKee, 1968b), but may range from 40 km (Saleeby and others, 1985) to 100 km (Stewart, 1967). Hence, the slip rate in this area may range from 3-12 mm/yr, but has a range of only 4-6 mm/yr if the total slip is 50 km (sites 1, fig. 1 and table 2). This slip rate is similar to a rate of 4.1-4.4 mm/yr reported for the Furnace Creek fault zone in northern Death Valley by Oakes (1987), who based his calculation on offset of a granitic stock dated at 7.3-7.9 Ma (McKee, 1985).

These average slip rates are only applicable to the FLVFZ in southern Fish Lake Valley, because the fault zone ends at the northern end of the valley (fig. 1). We speculate that the total right slip in northern Fish Lake Valley is no more than 15-25 km, based on the northwest-southeast width of the northern part of the valley and on the apparent northwest-southeast separation of a thrust-fault contact in Paleozoic rocks on the east and northwest sides of the valley (sites 2, fig. 1). If faulting was initiated between 8.2 and 11.9 Ma, then the minimum slip rate on the northern FLVFZ is 1-2 mm/yr and the maximum slip rate is 2-3 mm/yr (table 2).

Table 2. Late Cenozoic slip rates for the Fish Lake Valley, Deep Springs, and Emigrant Peak fault zones. (X, no rate calculated. Site numbers are shown on fig. 1.)

Site no.	Area and fault zone	Offset marker	Offset distance or height (km) minimum	maximum	Age (Ma)	Slip rate (mm/yr) minimum	maximum
		Right-lateral Slip Rates					
1	southern FLVFZ	.706 Sr line, Precambrian facies, Jurassic pluton[1]	~40	~100	8.2-11.9[2]	0.3[1]	3-12
				~50	8.2-11.9		4-6
2	northern FLVFZ	Width of northern valley; separation of thrust fault	~15	~25	8.2-11.9	1-2	2-3
		Vertical Slip Rates					
3	Deep Springs fault zone	Basalt on Chocolate Mtn.;	0.71	X	10-12[5]	.06-.07	X
		offset near Soldier Pass	1.62[4]	X	10-12	.1-.2	X
4	Deep Springs fault zone	Wind gap of paleo-Wyman Creek	.20	X	.74[6]	.3	X
5	southern FLVFZ	Basalt on Chocolate Mtn. and in Willow Wash	.68	.68	10-12	.06	.07
6	southern FLVFZ	Basalt in southern White Mountains	.51-.58	1.14[7]	10-12	.04-.06	.09-.11
7	southern FLVFZ	Paleovalley of Cottonwood Creek[8,9]	X	.54	.74	X	.7
8	central FLVFZ	Pluvial-lake deposits at McAfee Creek[9]	.24	.55	.74	.3	.7
9	central FLVFZ	Pre-Bishop alluvium of Perry Aiken Creek	.31	X	~1.0[10]	.3	X
10	northern FLVFZ	Andesite of Davis Mountain	.54	.75[7]	2.9-3.3[3]	.15-.2	.2-.3
11	Emigrant Peak fault zone	Displaced tephras in old gravel[11]	.41	X	2.0[6]	.20	X
12	West strand of EPFZ	Pluvial-lake deposits[9,11]	.12	X	.74	.2	X

1 Saleeby and others, 1986; Stewart, 1967; McKee (1968a)
2 K-Ar age range of volcanics underlying or interbedded with fault-derived sediments
3 K-Ar age range of youngest andesites of Davis Mountain (table 1; Robinson and Crowder, 1973)
4 Height of bedrock ridge above valley floor plus depth to bedrock below valley floor from geophysics (Wilson, 1975)
5 Dalrymple (1963; converted to new constants)
6 Age of tephras reported by Izett and others (1988) and Sarna-Wojcicki and others (in press)
7 Estimated maximum depth to bedrock of fault from exposed bedrock elevations and well-log interpretation
8 Reheis (1991a)
9 Reheis and others (1991b)
10 Estimated age of pre-Bishop alluvium of Perry Aiken Creek
11 Reheis (1991b)

Vertical Slip Rates on the Fish Lake Valley fault zone

Estimates of long-term (millions of years) vertical slip on the FLVFZ are difficult to make, because a piercing point may have been translated laterally along the fault zone into an area with vertical offset different than the area of origin. Hence, the following long-term slip rate estimates are tentative and subject to change. Post-Bishop-ash vertical-slip rates are less subject to this type of error, because deposits of this age can have moved no more than 9 km, and probably less than 5 km, along the fault zone.

Southern Fish Lake Valley

The long-term vertical-slip rate on the southern end of the FLVFZ is estimated from the difference in elevations of the 10-12-Ma basalt (unit Tv) in the southern White Mountains and in Willow Wash and from the difference in elevations of deposits containing the Bishop ash on Gilbert Summit and in Fish Lake Valley.

Unit Tv lies at an elevation of 2348 m (7703 ft) on Chocolate Mountain (site 3, fig. 1). A correlative basalt, based on age and preliminary chemical data, lies at the base of the Willow Wash section (site 5, fig. 1) at an elevation of about 1670 m (5480 ft). These basalts both overlie the quartz monzonite of Beer Creek and, if right slip on the FLVFZ is restored, may once have been part of the same broad basalt-capped erosion surface at similar elevations. If so, then about 680 m of vertical offset has occurred across the southern FLVFZ since the eruption of these basalts, and the vertical slip rate since 10-12 Ma is 0.06-0.07 mm/yr.

Unit Tv crops out extensively at an elevation of about 3017 m (9900 ft) north of Deep Springs Valley (site 6, fig. 1; Krauskopf, 1971). These flows have surface slopes of about 80-90 m/km (420-480 ft/mi) perpendicular to the range front and the FLVFZ. One basalt outcrop is faulted by an active strand of the FLVFZ and is probably buried beneath alluvium of the valley floor somewhere east of the fault zone. The difference between the projected elevation of the top of the basalt at the range front and the elevation of the valley floor at the fault is 505-575 m. This minimum displacement gives a minimum vertical slip rate of 0.04-0.06 mm/yr (table 2). The estimated elevation of bedrock buried beneath alluvium near the fault, based on projections of exposed bedrock and well logs in the valley, is probably not less than 1097 m (3600 ft). This value gives a maximum vertical displacement of 1140 m and a maximum slip rate of 0.09-0.11 mm/yr since 10-12 Ma.

Stream gravel of the paleodrainage of Cottonwood Creek, including deposits of the Bishop ash, crops out at an elevation of 1914 m (6280 ft) near Gilbert Summit, the modern topographic divide between southern Fish Lake Valley and Deep Springs Valley (fig. 2; site 7, fig. 1). The elevation of southern Fish Lake Valley may have been about the same as that of the paleodrainage of Cottonwood Creek at 0.74 Ma. If the valley had been much lower, Cottonwood Creek would probably not have been able to maintain its southeasterly course at that time; if much higher, Fish Lake Valley probably could not have contained a pluvial lake north of the latitude of Deep Springs Valley at 0.74 Ma (Reheis and others, this volume, b). Buried fluvial deposits of the Bishop ash are inferred to exist at an elevation of about 1308 m (4555 ft) from records of a water well drilled in Fish Lake Valley near a line projected from Gilbert Summit perpendicular to the FLVFZ (Reheis and others, this volume, b). The difference in elevation of about 540 m between the inferred ash and the ash on Gilbert Summit should represent the maximum post-Bishop-ash displacement, so the vertical slip rate on this part of the FLVFZ must be less than 0.7 mm/yr (table 2).

The estimated post-0.74 Ma vertical slip rates on the southern FLVFZ are higher than the estimated post-10-12-Ma slip rates (table 2). At the post-0.74-Ma slip rate, all vertical slip on the southern FLVFZ could be accumulated in about 2.5 million years. This

result is in conflict with geologic relations in the Horse Thief Hills (discussed above), which suggest that initiation of movement on the FLVFZ began no later than about 8 Ma. Hence, it seems likely either that vertical slip rates increased markedly sometime late in the history of the fault zone, or that the estimates of vertical slip based on the assumed topographic relation of southern Fish Lake Valley to the Cottonwood paleovalley are in error.

Central Fish Lake Valley

The central part of the FLVFZ (from just south of site 8 to just north of the state line, fig. 1) has the highest scarps in Quaternary alluvium and is adjacent to the highest peaks of the White Mountains. Hence, short-term vertical slip rates are likely to be highest along this part of the fault zone. Slip rates (table 2) can be estimated with confidence from the offset of a thick bed of Bishop ash at McAfee Creek, and with less confidence from the offset of a pre-Bishop-ash fluvial gravel of Perry Aiken Creek (sites 8 and 9, fig. 1).

At least 30 m of fluvially deposited Bishop ash are faulted against bedrock by an inactive strand of the FLVFZ at the mouth of McAfee Creek (site 8, fig. 1; detailed map shown in fig. 3 of road log, this volume). This ash is believed to have been deposited as deltaic sediments in a pluvial lake, and is correlated to another deposit of Bishop ash in northern Fish Lake Valley whose elevation (1463 m, 4800 ft) represents the original shoreline elevation of the lake (Reheis and others, this volume, b). The ash bed at McAfee Creek is overlain by a fan gravel that also is present, but without the underlying ash, on the footwall of the fault. The ash bed is faulted internally by another inactive strand and is cut off by the active strand of the FLVFZ on the east.

The minimum offset across the three strands of the FLVFZ at McAfee Creek is represented by the difference in elevation between the exposed base of the footwall deposit of the post-Bishop-ash alluvium of McAfee Creek (1707 m, 5600 ft) and the original elevation of the pluvial lake (1463 m, 4800 ft). The elevation difference of 244 m represents the minimum offset, because the present elevation of buried shoreline deposits on the east side of the fault zone is unknown; the minimum vertical slip rate is 0.3 mm/yr (table 2). The maximum offset can be estimated from the inferred elevation of lake sediments in water wells in central Fish Lake Valley; this elevation is approximately 1219 m (4000 ft; Reheis and others, this volume, b). Hence, the maximum slip rate is 0.7 mm/yr. This maximum rate is almost certainly too high, because it does not account for the water depth of the at which the sediments in the wells were deposited.

A minimum vertical slip rate can also be estimated from the offset of pre-Bishop-ash alluvium of Perry Aiken Creek, just north of McAfee Creek (site 9, fig. 1; fig. 3 of road log, this volume). From relations of alluvium and tephras in northern Fish Lake Valley, the age of alluvium of Perry Aiken Creek is inferred to be about 1 Ma. A deposit of this gravel is at an elevation of 2012 m (6600 ft) south of Perry Aiken Creek in the footwall of the FLVFZ. The gradient of the modern creek in this area is about 75 m/km (400 ft/mi). If the deposit of pre-Bishop-ash stream gravel is projected eastward at this gradient, then the projected elevation at the active fault is about 1890 m (6200 ft). The difference between the projected elevation and the elevation of the modern surface at the fault (1585 m, 5200 ft) yields a minimum vertical offset of 305 m in the past one million years and a minimum slip rate of 0.3 mm/yr (table 2).

Northern Fish Lake Valley

At the northern end of the FLVFZ, fault scarps in Quaternary alluvium (Sawyer, 1990) are not as high as those in deposits of comparable age to the south. Thus, it seems likely that vertical slip is lower in northern Fish Lake Valley. Long-term vertical slip rates can be estimated from the age and elevation of the 3-Ma andesite of Davis Mountain (Tvs, site 10, fig. 1; Robinson and Crowder, 1973).

Andesite flows at the top of Davis Mountain slope eastward at a gradient of about 85 m/km (450 ft/mi); at this gradient, these flows project to an elevation of about 2454 m (8050 ft) at the fault zone. The difference between the projected elevation and the elevation of the ground surface on the hanging wall (1914 m, 6280 ft) yields a minimum vertical offset of 540 m since 3 Ma. This vertical offset and the age of the youngest andesite flows (table 1) yield a minimum slip rate of 0.15-0.2 mm/yr (table 2). The elevation of andesite flows beneath alluvium in the hanging wall is estimated at 1707 m (5600 ft) from projection of the elevations of exposed bedrock and of bedrock in water wells in northern Fish Lake Valley. This elevation gives a maximum vertical offset of about 750 m and maximum slip rates of 0.2-0.25 mm/yr.

Vertical Slip Rates on Other Fault Zones

Deep Springs fault zone

The Deep Springs fault zone (DSFZ) is a set of north-striking normal faults that bound the east side of Deep Springs Valley (figs. 1 and 2). Movement on the fault zone has created an intermontane basin that may represent a rhombochasm in the southern White Mountains between the right-oblique FLVFZ and the right-lateral Owens Valley fault zone to the west.

The long-term vertical slip rate for the DSFZ can be estimated from offset of the 10-12 Ma basalt (unit Tv) on the north end of the valley (site 3, fig. 1) and from the height of the wind gap containing 0.74-Ma Bishop ash that represents the former drainage of Wyman Creek on the east side of the valley (fig. 2; site 4, fig. 1).

The basalt crops out at 2348 m (7703 ft) on top of Chocolate Mountain (fig. 2), its highest elevation east of Deep Springs Valley, and is probably buried beneath alluvium in northern Deep Springs Valley (McKee and Nelson, 1967). The lowest surface elevation on the hanging wall of the fault west of Chocolate Mountain is about 1634 m (5360 ft). Hence, the minimum offset along this fault is 714 m, which yields a minimum slip rate since 10-12 Ma of 0.06-0.07 mm/yr (table 2). Wilson (1975) used gravity data to infer a depth to bedrock of about 792 m (2600 ft) adjacent to the fault near Soldier Pass (fig. 2). The highest elevation of bedrock on the footwall ridge near Soldier Pass is about 2387 m (7830 ft), and the surface of the valley floor is at about 1554 m (5100 ft). Hence, the minimum offset is about 1625 m; the maximum offset is unknown because the depth of erosion on the footwall ridge is unknown. Because Deep Springs Valley must have formed after the eruption of unit Tv, the minimum slip rate since 10-12 Ma is 0.13-0.16 mm/yr.

The wind gap containing 0.74-Ma Bishop ash south of Chocolate Mountain, on the footwall of the fault, is 201 m (660 ft) above the valley floor on the hanging wall, which is an estimate of minimum offset. Thus, the minimum slip rate on the fault since 0.74 Ma is 0.3 mm/yr (table 2). This rate is twice as large as the post-late Miocene rate. In order to attain a post-late Miocene rate similar to the younger rate, about 1.5 km of rock would have had to be removed from the top of the footwall ridge of Deep Springs Valley. Such erosion seems extremely unlikely in view of the gentle topography on the top of this ridge and the absence of large streams. These relations suggest that either (1) the post-0.74-Ma vertical slip rate has been much faster than that in late Miocene and Pliocene time or (2) if

the slip rate has been constant, the DSFZ did not begin to move until about 6 Ma or later. The presence of fresh, uneroded scarps cut on Holocene and late Pleistocene deposits along the Deep Springs fault zone indicates a relatively high late Pleistocene slip rate (Bryant, 1989).

Emigrant Peak fault zone

The Emigrant Peak fault zone (EPFZ) in northeastern Fish Lake Valley is a group of north-striking normal faults that offset alluvial and lacustrine deposits of Pliocene and Quaternary age (fig. 1; Reheis, in press b). This fault zone apparently serves as part of a pull-apart basin that transfers slip on the FLVFZ to slip on faults of the Walker Lane to the northeast (Reheis and Noller, 1979; Sawyer, 1990).

There are four major, parallel faults that offset upper Pliocene and Pleistocene alluvial and lacustrine deposits in northeastern Fish Lake Valley (fig. 1; only easternmost and westernmost faults bounding unit QTg are shown; Reheis, in press b). Slip-rate estimates on these faults are derived from the elevations of silicic tephra beds interbedded within unit QTg.

Sediments in the footwall of the westernmost fault (site 12, fig. 1) contain beach sands composed chiefly of Bishop ash (Reheis and others, this volume, b) that crop out as high as 1585 m (5200 ft; Reheis, in press b). The shoreline of the pluvial lake in which these sands were deposited is presently at 1463 m (4800 ft) in the hanging wall. Thus, the minimum post-Bishop offset on the western fault is 122 m, giving a minimum slip rate of 0.15 mm/yr (table 2).

The three other faults also offset unit QTg (site 11, fig. 1), but estimates of slip are less accurate because several assumptions must be made about erosion and continuity of deposition. The alluvial-fan deposits offset by the faults contain several tephra beds derived from the Long Valley caldera that predate the Bishop ash. These beds include one tephra of the ~1-Ma Glass Mountain eruptions and several tephras of the ~2-Ma Tuff of Taylor Canyon eruptions (Reheis, in press b, and tephra analyses by A.M. Sarna-Wojcicki). The easternmost fault places unit QTg against older Tertiary rocks, so the displacement of QTg across this fault is unknown. The next fault west offsets unit QTg a minimum of 74 m, based on the projection of the base of unit QTg in the footwall; the base of unit QTg is not exposed in the hanging wall. At the second fault west, Glass Mountain tephra is exposed in the hanging wall but has been eroded from the top of unit QTg in the footwall. Vertical displacement on this fault is a minimum of 213 m.

The minimum cumulative displacement on the three westernmost faults in the EPFZ is 409 m since 2 Ma and the minimum slip rate is 0.2 mm/yr. The total slip rate across the whole fault zone is probably much larger, because slip on the easternmost fault is unknown, and because critical marker beds that would permit more accurate estimates of slip on the two middle faults have been buried or removed by erosion.

Discussion of Slip Rates

The estimated right-lateral slip rate of the FLVFZ in southern Fish Lake Valley since initiation of faulting in the late Miocene is about 4-6 mm/yr. The lateral slip rate in northern Fish Lake Valley, assuming that movement there began at about the same time as in the southern part of the valley, is about 1-3 mm/yr (table 2). The northern slip rates are greater than rates of 0.6-0.8 mm/yr calculated using offset of late Pleistocene deposits at the northern end of the FLVFZ (Sawyer, 1990). These younger slip rates are for a single strand of the FLVFZ, however, so it is likely that cumulative late Pleistocene displacement across the whole fault zone in this area approaches the long-term late Cenozoic rate.

Estimated vertical slip rates on the FLVFZ are much higher since 0.74 Ma than in the interval from 10.8 Ma to 0.74 Ma (table 2). Post-0.74-Ma slip rates range from 0.3 to 0.7 mm/yr, whereas post-late Miocene slip rates range from 0.05 to 0.15 mm/yr. Extrapolation of Quaternary slip rates back in time yields estimates for the onset of motion on the FLVFZ and related faults that do not agree with older estimates obtained from ages of presumably fault-derived sediments in Willow Wash and the Horse Thief Hills. These relations suggest that slip rates increased markedly in Quaternary time and possibly after the eruption of the Bishop ash, a conclusion also reached by dePolo (1989) in a study of the White Mountain fault zone bounding the west side of the White Mountains and by Gillespie (in press) for Quaternary subsidence of Owens Valley.

Post-Bishop-ash vertical slip rates are similar for the DVFZ and EPFZ and for all parts of the FLVFZ (table 2), and they are the same as a Holocene vertical slip rate of 0.4-0.8 mm/yr reported for the northern FLVFZ (Sawyer, 1990). They are also similar to a vertical slip rate calculated for the White Mountains fault zone from an erosion surface on the east side of the White Mountains (dePolo, 1989), but are lower than dePolo's preferred Quaternary slip rate of 1 mm/yr for this fault zone. The vertical slip rate calculated for the southern part of the FLVFZ seems anomalously high when compared to the relatively subdued fault scarps and the low elevation of the White Mountains in this area. This anomalously high rate may be caused by an incorrect assumption about the elevation of southern Fish Lake Valley relative to the paleovalley of Cottonwood Creek at the time of eruption of the Bishop tuff. The vertical slip rate measured for the northern FLVFZ is about half that measured for the central FLVFZ; this decline in rates to the north is compatible with the smaller Quaternary scarps and more subdued topography of the range front to the north.

The estimated long-term right-lateral slip rates are roughly an order of magnitude larger than the vertical slip rates (table 2). Some lateral:vertical displacement ratios estimated for late Pleistocene offsets on individual fault strands on the northern end of the FLVFZ are as high as 10:1, but ratios may be as low as 1:1 (Sawyer, 1990).

SUMMARY

Preliminary interpretation of the upper Tertiary and lower Quaternary deposits in Fish Lake Valley, northern Eureka Valley, and Deep Springs Valley suggests the following history of motion on the FLVFZ: (1) Faulting began after about 12 Ma but before about 8 Ma in southern Fish Lake Valley. Before this time, the Horse Thief Hills were part of a large region of Precambrian and Cambrian rock of low relief (McKee, 1968a). On the east side of the Furnace Creek fault zone, the northern boundary of these rocks is on the northeastern side of Death Valley (fig. 1). Relative uplift on the northeast along the FLVFZ, or along a range-front fault located near the present trace of the FLVFZ, caused deposition of coarse angular gravel (unit Ts), derived from the Precambrian and Cambrian rocks, in the area of the present Horse Thief Hills. Streams drained south from the White Mountains into Eureka Valley (the round-pebble facies of unit Ts); Deep Springs Valley did not exist. (2) During Pliocene time, oblique motion on the Furnace Creek fault zone and associated faults created a depositional basin (represented by unit Tq, the Willow Wash section) into which streams flowed from the northwest end of the Sylvania Mountains. A shift to deposition of arkosic sediment (unit Tm) in the area of the Horse Thief Hills in the Pliocene may have been caused by the onset of motion on the bounding faults of Deep Springs Valley, but streams continued to flow from the White Mountains into Eureka Valley. (3) Sometime after 0.74 Ma, streams draining from the White Mountains into Eureka Valley were defeated by continued faulting and either began to pond in Deep Springs Valley or were captured to flow into Fish Lake Valley.

Estimated lateral and vertical slip rates on the Fish Lake Valley fault zone and associated faults vary both temporally and spatially. The post-late Miocene right-lateral slip rate in southern Fish Lake Valley is about 4-6 mm/yr, whereas in northern Fish Lake Valley it is about 1-3 mm/yr. The post-0.74-Ma vertical slip rates are much higher than the long-term slip rates. Post-Bishop-ash vertical slip rates range from 0.3 to 0.7 mm/yr on the FLVFZ, the DSFZ, and the EPFZ, whereas post-late Miocene vertical slip rates range from 0.05 to 0.2 mm/yr. These relations suggest that slip rates increased markedly in the Quaternary.

ACKNOWLEDGEMENTS

We thank R. Thompson (U.S. Geological Survey) for interpretation of trace-element analyses and major-oxide chemistry (the latter performed by personnel of the Branch of Geochemistry) of basalt and andesite samples prepared by S. Schilling (U.S. Geological Survey) for chemical analysis. A. Sarna-Wojcicki performed tephrochronologic analyses of volcanic ashes in the sedimentary units. Several field assistants participated in mapping and sample collection: J. Slate (University of Colorado), D. Rennie and T. Rennie (University of Nevada at Reno), A. Stein, E. Skov, and L. Von Wald (Humboldt State University), and T. McCamant (U.S. Geological Survey).

REFERENCES CITED

Bryant, W.A., 1989, Deep Springs fault, Inyo County, California--An example of the use of relative-dating techniques: California Geology, v. 42, no. 11, p. 243-255.

Burchfiel, B.C., and Stewart, J.H., 1966, "Pull-apart" origin of the central segment of Death Valley, California: Geological Society of America Bulletin, v. 77, p. 439-442.

Butler, P.R., Troxel, B.W., and Verosub, K.L., 1988, Late Cenozoic history and styles of deformation along the southern Death Valley fault zone, California: Geological Society of America Bulletin, v. 100, p. 402-410.

Dalrymple, G.B., 1963, Potassium-argon dates of some Cenozoic volcanic rocks of the Sierra Nevada, California: Geological Society of America Bulletin, v. 74, p. 379-390.

Davis, G.A., and Burchfiel, B.C., 1973, Garlock fault--An intracontinental transform structure, southern California: Geological Society of America Bulletin, v. 84, p. 1407-1422.

dePolo, C.M., 1989, Seismotectonics of the White Mountains fault system, east-central California and west-central Nevada: Reno, University of Nevada, M.S. thesis.

Gillespie, A.R., in press, Quaternary subsidence of Owens Valley, California: Proceedings of the White Mountain Research Station Symposium, Fall 1989, p. 356-382.

Guth, P.L., 1981, Tertiary extension north of the Las Vegas Valley shear zone, Sheep and Desert Ranges, Clark County, Nevada: Geological Society of America Bulletin, v. 92, part 1, p. 763-771.

Hamilton, W.B., 1988, Detachment faulting in the Death Valley region, California and Nevada, *in* Carr, M.C., and Yount, J.C., eds., Geologic and hydrologic investigations of a potential nuclear waste disposal site at Yucca Mountain, southern Nevada: U.S. Geological Survey Bulletin 1790, p. 51-85.

Izett, G.A., Obradovich, J.D., and Mehnert, H.H., 1988, The Bishop ash bed (middle Pleistocene) and some older (Pliocene and Pleistocene) chemically and mineralogically similar ash beds in California, Nevada, and Utah: U.S. Geological Survey Bulletin 1675, 37 p.

Krauskopf, K.B., 1971, Geologic map of the Mt. Barcroft quadrangle, California-Nevada: U.S. Geological Survey Geologic Quadrangle Map GQ-960, scale 1:62,500.

McKee, E.H., 1968a, Age and rate of movement of the northern part of the Death Valley-Furnace Creek fault zone, California: Geological Society of America Bulletin, v. 79, p. 509-512.
McKee, E.H., 1968b, Geology of the Magruder Mountain area, Nevada-California: U.S. Geological Survey Bulletin 1251-H, 40 p., scale 1:62,500.
McKee, E.H., 1985, Geologic map of the Magruder Mountain quadrangle, Esmeralda County, Nevada, and Inyo County, California: U.S. Geological Survey Geologic Quadrangle Map GQ-1587, scale 1:62,500.
McKee, E.H., and Nelson, C.A., 1967, Geologic map of the Soldier Pass quadrangle, California and Nevada: U.S. Geological Survey Geologic Quadrangle Map GQ-654, scale 1:62,500.
Miller, W.J., 1928, Geology of Deep Spring Valley, California: Journal of Geology, v. 36, p. 510-525.
Nelson, C.A., 1966, Geologic map of the Blanco Mountain quadrangle, Inyo and Mono Counties, California: U.S. Geological Survey Geologic Quadrangle Map GQ-529, scale 1:62,500.
Oakes, E.H., 1987, Age and rates of displacement along the Furnace Creek fault zone, northern Death Valley, California: Geological Society of America Abstracts with Programs, v. 19, no. 6, p. 437.
Reheis, M.C., in press a, Geologic map of late Cenozoic deposits and faults in parts of the Soldier Pass and Magruder Mountain 15' quadrangles, Inyo and Mono Counties, California, and Esmeralda County, Nevada: U.S. Geological Survey Miscellaneous Investigations Map I-2268, scale 1:24,000.
Reheis, M.C., in press b, Geologic map of late Cenozoic deposits and faults in the western part of the Rhyolite Ridge 15' quadrangle, Esmeralda County, Nevada: U.S. Geological Survey Miscellaneous Investigations Map I-2183, scale 1:24,000.
Reheis, M.C., and Noller, J.S., 1989, New perspectives on Quaternary faulting in the southern Walker Lane, Nevada and California, *in* Ellis, M.A., ed., Late Cenozoic evolution of the southern Great Basin--Selected papers from the workshop: Nevada Bureau of Mines and Geology Open File 89-1, p. 57-61.
Reheis, M.C., and Noller, J.S., in press, Aerial photographic interpretation of lineaments and faults in the eastern part of the Benton Range 1:100,000 quadrangle and the Goldfield, Last Chance Range, Beatty, and Death Valley Junction 1:100,000 quadrangles, Nevada and California: U.S. Geological Survey Open-file Report 90-41, scale 1:100,000.
Reheis, M.C., Sarna-Wojcicki, A.M., Burbank, D.M., and Meyer, C.E., 1991a, The late Cenozoic section at Willow Wash, west-central California: A tephrochronologic rosetta stone: U.S. Geological Survey Open-file Report 81-290, this volume.
Reheis, M.C., Slate, J.L, Sarna-Wojcicki, A.M., and Meyer, C.E., 1991b, An early Pleistocene pluvial lake in Fish Lake Valley, Nevada-California: Ringside resort for the eruption of the Bishop Tuff: U.S. Geological Survey Open-file Report 81-290, this volume.
Robinson, P.T., and Crowder, D.F., 1973, Geologic map of the Davis Mountain quadrangle, Esmeralda and Mineral Counties, Nevada, and Mono County, California: U.S. Geological Survey Geologic Quadrangle Map GQ-1078, scale 1:62,500.
Robinson, P.T., McKee, E.H., and Moiola, R.J., 1968, Cenozoic volcanism and sedimentation, Silver Peak region, western Nevada and adjacent California, *in* Coats, R.R., Hay, R.L., and Anderson, C.A., Studies in Volcanology: Geological Society of America Memoir 116, p. 577-611.
Saleeby, J.B., and many others, 1986, C-2 central California offshore to Colorado Plateau: Geological Society of America, Centennial Continent/Ocean Transect #10, 63 p., scale 1:500,000.

Sarna-Wojcicki, A.M., Lajoie, K.R., Meyer, C.E., Adam, D.P., and Rieck, H.J., in press, Tephrochronologic correlation of upper Neogene sediments along the Pacific margin, conterminous United States, in Morrison, R. B., ed., Quaternary non-glacial geology--Conterminous U.S.: Geological Society of America, Decade of North American Geology, v. K-2.

Sawyer, T.L, 1990, Quaternary geology and neotectonic activity along the Fish Lake Valley fault zone, Nevada and California: Reno, University of Nevada, M.S. thesis, 379 p.

Stewart, J.H., 1967, Possible large right-lateral displacement along fault and shear zones in the Death Valley-Las Vegas area, California and Nevada: Geological Society of America Bulletin, v. 78, p. 131-142.

Stewart, J.H., and Carlson, J.E., 1978, Geologic map of Nevada: U.S. Geological Survey and Nevada Bureau of Mines and Geology, scale 1:500,000.

Stewart, J.H., 1983, Extensional tectonics in the Death Valley area, California--Transport of the Panamint Range structural block 80 km northwestward: Geology, v. 11, p. 153-157.

Stewart, J.H., 1988, Tectonics of the Walker Lane belt, western Great Basin: Mesozoic and Cenozoic deformation in a zone of shear, in Ernst, W.G., ed., Metamorphism and Crustal Evolution of the Western United States: Rubey Volume VII, New Jersey, Prentice Hall, p. 683-711.

Wilson, D.V., 1975, Geophysical investigation of the subsurface structure of Deep Springs Valley, California: Los Angeles, University of California, M.S. thesis, 65 p.

Wright, L.A., 1989, Overview of the role of strike-slip and normal faulting in the Neogene history of the region northeast of Death Valley, California-Nevada, *in* Ellis, M.A., ed., Late Cenozoic evolution of the southern Great Basin (selected papers from the workshop): Nevada Bureau of Mines and Geology Open File 89-1, p. 1-11.

Wright, L.A., and Troxel, 1967, Limitations on right-lateral, strike-slip displacement, Death Valley and Furnace Creek fault zones, California: Geological Society of America Bulletin, v. 78, p. 933-950.

THE LATE CENOZOIC SECTION AT WILLOW WASH, WEST-CENTRAL CALIFORNIA: A TEPHROCHRONOLOGIC ROSETTA STONE

Marith C. Reheis, Andrei M. Sarna-Wojcicki, Douglas M. Burbank, and Charles E. Meyer

ABSTRACT

Over 50 different tephra layers crop out in a sequence of about 735 m of sedimentary rocks that overlie ~11-Ma volcanic rocks in Willow Wash, near the California-Nevada border north of Death Valley. Preliminary analyses of major-oxide chemistry indicate that these tephra layers are derived from eruptions in at least five, perhaps six of the major silicic volcanic centers of the western United States, and were episodically deposited in a sequence of fluvial, lacustrine, and alluvial-fan deposits from about 5.5 Ma to about 0.7 Ma. The sediments were deposited in a basin adjacent to the northern part of the Furnace Creek fault zone and provide information on the inception of right-lateral motion on the fault zone and on subsequent tectonic history.

The general stratigraphic correlations among several short measured sections in Willow Wash are established by tephrochronology and by physical tracing of beds between sections. The ages of sediments based on tephrochronology are confirmed and elaborated upon by paleomagnetic analyses. When the correlations and age assignments of the tephra layers have been confirmed and refined by further chemical analyses and isotopic dating, this section will serve as an exposed, on-land reference section for late Neogene tephra layers found in other areas.

INTRODUCTION

About 800 m of late Miocene to early Quaternary arkosic, tuffaceous sedimentary rocks and volcanic flows crop out along upper Willow Wash at the southern end of Fish Lake Valley, in west-central California (fig. 1). This section was first mapped by McKee and Nelson (1967) and described as part of the late Miocene to late Pliocene Esmeralda Formation by McKee (1968) and Robinson and others (1968). The Willow Wash section rests unconformably on the Jurassic quartz monzonite of Beer Creek and is truncated on the northeast by active faults of the Furnace Creek fault zone.

The rocks exposed in Willow Wash were examined and mapped in detail as part of an ongoing project to investigate the late Cenozoic history of the northern end of the Furnace Creek fault zone (here referred to as the Fish Lake Valley fault zone, or FLVFZ; fig. 1). The sedimentary beds contain several tens of silicic tephra layers, mostly reworked, that are evenly distributed throughout the section (fig. 2).

The tephra beds are derived from at least five and perhaps six major rhyolitic eruptive centers of late Cenozoic age in the western United States (table 2, below). The Silver Peak volcanic center is only 30 to 50 km north of Willow Wash (Robinson and others, 1968); the chemistry of rhyolite flows from this center is being investigated, but is not yet well enough known to permit correlations to tephra layers in Willow Wash. The southern end of Fish Lake Valley is only about 80 km east-southeast of the Long Valley caldera and hence is ideally situated to preserve tephra erupted from the Long Valley area (Sarna-Wojcicki and others, 1984, in press; Izett and others, 1988); most of the tephra beds in the upper one-third of the Willow Wash section are derived from this source. Some layers containing tephra tentatively identified as erupted from the Sonoma volcanic field north of San Francisco (Sarna-Wojcicki, 1976; Sarna-Wojcicki and others, in press) have been identified in the Willow Wash section (table 1). Tephra derived from the southern

Cascade Range of northeastern California (Sarna-Wojcici, 1976) has also been identified in the Willow Wash section. Tephra from the Timber Mountain-Black Mountain-Oasis caldera complex in southern Nevada has been identified 2 km to the south of the Willow Wash section in sediments equivalent to those in the basal part of the section (Reheis, in press a). Southern Fish Lake Valley is well within the geographic distribution of several widespread tephra layers that have not yet been found in this area. For example, a tephra layer in northern Fish Lake Valley has been provisionally correlated with the 2.0-Ma Huckleberry Ridge Tuff in the eastern Snake River Plain-Yellowstone area (Reheis and others, this volume), and tephra derived from this tuff and from the 0.6-Ma Lava Creek Tuff (Christiansen and Blank, 1972) are found in lake sediments in the Tecopa Basin (Sarna-Wojcicki and others, 1984, 1987; Izett and Wilcox, 1982), about 200 km to the southeast.

Because the Willow Wash section is in the overlap area of tephra fallout from several major rhyolitic eruptive centers of late Cenozoic age and contains many tephra beds, it can serve as a calibration and reference section--a "Rosetta stone"--for correlation and dating of tephra layers in the western United States. Although tephra layers of Pliocene and early Quaternary age are commonly found in this area, few exposed sites contain more than a half-dozen tephra layers (Sarna-Wojcicki and others, in press). In the past, determining the stratigraphic relationships of these tephras required piecing together incomplete information from many different sites. Characterization and dating of the tephra layers in the Willow Wash section, by glass chemistry, paleomagnetism, and laser-fusion K-Ar dating, will permit more secure identification of tephra layers and correlation of their host sedimentary sections in the western U.S.

Finally, the structural setting and age of deposits in the Willow Wash area provide important information on the initiation of right-lateral motion on the FLVFZ and provide data on sedimentation patterns associated with the fault zone.

Methods

Sampling and mapping

The composite section of sedimentary rocks in Willow Wash (fig. 2) is combined from several shorter measured sections. The sections were measured using an Abney level and Jacobs staff. Tephra beds were sampled as they were encountered; in general, the sample numbers increase upward within each segment, but the numbering system is complicated by discovery of additional tephra layers in subsequent visits.

Individual sections (figs. 1 and 2) were measured where unconformities were thought to be absent and where exposures were best. Where possible, the sections were connected by physically tracing beds. These connections were subsequently confirmed when matches of glass chemistry were made between tephra layers in different sections. Syn- and post-depositional faulting and folding have disrupted the Willow Wash sequence. Two significant unconformities exist within the basal part of the sedimentary section. Missing strata between these unconformities are in part represented by the "Candy Cliff" section (fig. 2); tephra and paleomagnetic samples from this section have not yet been analyzed.

Tephrochronology

Tephra samples were examined under the petrographic microscope. Glass shards in samples containing isotropic glass were separated from other components and analyzed by electron microprobe for SiO_2, Al_2O_3, Fe_2O_3, MgO, MnO, CaO, TiO_2, Na_2O, and K_2O, using methods described by Sarna-Wojcicki and others (1984). Results of analyses and other analytical data are presented in table 1. Sample compositions were compared against a data base of previously analyzed tephra layers using numerical programs (Sarna-Wojcicki and others, 1984) and the best matches were identified. Correlations were made on the basis of similarity in chemical composition, petrographic characteristics (primarily shard morphology), and other available stratigraphic and numerical-age data.

Values for glass compositions in table 1 are normalized to 100 percent, to correct for the variable amounts of hydration of the volcanic glass. Original totals, all significantly lower than 100 percent, are approximate guides to the degree of hydration of each sample--the lower the total, the greater the degree of hydration. In addition to hydration, some post-depositional alkali exchange has occurred in many of the samples. Variability in sodium and potassium contents are particularly apparent in tephra layers about 2 Ma or older. Because of this variability, comparisons of sample compositions were done in at least two stages. An initial comparison was made using six oxides (silicon, aluminum, iron, calcium, sodium, and potassium). Follow-up comparisons were made excluding sodium and potassium, but including one or more of the minor oxides of magnesium, titanium, and manganese where the concentration of these oxides was sufficiently high (0.1-0.2 weight percent) to allow a reasonably precise comparison.

Because some compositionally closely related suites of tephra layers cannot be distinguished by electron-microprobe analysis of volcanic glass, the results presented here should be considered preliminary, pending further analysis. Analyses of these tephra layers by energy-dispersive X-ray fluorescence (a more sensitive technique for minor and trace elements) and laser-fusion $^{39}Ar/^{40}Ar$ dating are planned or are in progress.

Paleomagnetism

The objective of the magnetostratigraphic studies was to place locally determined chronological constraints on both the tephra succession and the overall stratigraphic record. Samples were collected at ~10-m intervals, depending on available exposures and appropriate lithologies (mudstones, siltstones, and fine-grained sandstones). Three to four oriented samples were collected at each sampling site, such that a total of ~200 specimens was obtained. Where the sediments were very friable, especially in the upper part of the section, specimens were collected following soaking and cementation with sodium silicate.

Three specimens from each of 12 sites were selected as pilot specimens for demagnetization analysis. The criteria for selection were that (1) various sample lithologies would be represented and (2) nearly the entire stratigraphic extent of the section would be spanned. Two of the pilot specimens from each site were subjected to stepwise, thermal demagnetization in 50°C steps between 100°C and 500°C and then 25° steps up to 600°C. The third specimen from each site was subjected to alternating-field (AF) demagnetization at 100, 200, 400, 600, and 800 oe.

In general, consistent behaviors were revealed by these demagnetization procedures. Most of the specimens were relatively strongly and stably magnetized (~10^{-5} emu/cc), and specimens from the same site revealed similar magnetic orientations during both thermal and AF demagnetization (fig. 3). Decreases in magnetic intensities appeared to be about linear during demagnetization, such that the initial magnetic intensities were reduced to about 50% by either 300°C or 300 oe. For many of the specimens, the initially determined remanent directions persisted throughout the demagnetization. This behavior suggests that these specimens had undergone very little overprinting since deposition.

Some of the reversely magnetized specimens revealed a weak normal overprint that was removed by about 200-250°C, at which point a maximum in intensity was observed. The majority of the reversely magnetized sites, however, displayed initial remanence directions that were oriented south and up and that remained stable throughout demagnetization. A few of the sites displayed weak initial intensities. Although some of these displayed increasingly coherent directions after demagnetization, most of them appeared to become more random.

A conspicuous loss of remanence intensity between 500°C and 575°C in many specimens suggests that magnetite carries the primary depositional remanence in these specimens. Some of the more weakly magnetized specimens show only minor decreases in intensity during thermal demagnetization. The magnetic directions revealed by such specimens appear to be largely random and appear to result from the presence of post-depositional hematite.

The coherence of the specimen data for each site was assessed using Fisher (1953) statistics. Sites were classified as "Class I", if Fisher $k \geq 10$; "Class II", if $k < 10$ but the site showed an unambiguous polarity; and "Class III", if the polarity was indeterminate. The mean inclination and declination of Class I and II sites were used to calculate the virtual geomagnetic pole (VGP) for each (fig. 4 below). The latitude of the VGP formed the basis for the local magnetic polarity stratigraphy (MPS). An alpha-95 error envelope was calculated and plotted for each VGP latitude.

Antipodal directions displayed by stereonet plots of the Class I data (fig. 3) indicate that these data pass a reversal test (McElhinny, 1975). Within the uncertainties of these data, a small (~11°), counter-clockwise rotation can be defined. Because of the gentle and rather uniform dips of the strata, the magnetic data do not pass a fold test. The successful reversal test and the observation that, among the numerous, juxtaposed magnetozones uncovered by this sampling program, there are no apparent correlations between lithology, apparent alteration, and magentic polarity indicates that reliable characteristic remanences have been delineated for these sites and that these directions are depositional or very early post-depositional in nature.

DESCRIPTION OF THE WILLOW WASH SECTION

Stratigraphy and sedimentology

The oldest volcanic rocks of the Willow Wash section are of Miocene age and rest on the Jurassic quartz monzonite of Beer Creek (McKee and Nelson, 1967; figs. 1 and 2). These volcanics include a biotitic rhyolite and an overlying basalt dated at 11.0 ± 0.3 and 11.5 ± 0.4 Ma, respectively (Reheis and McKee, this volume). The aggregate thickness of the two flows ranges from less than 15 m to several tens of meters.

About 735 m of sedimentary rocks overlie the Miocene volcanics (fig. 2). Limited exposures show that these sedimentary rocks are either unconformable on the volcanic rocks or are in fault contact with them. The sedimentary rocks grade upward from moderately to poorly consolidated. They are dominantly sandstone and conglomerate, commonly including large, euhedral feldspar and quartz phenocrysts weathered and eroded from the quartz monzonite of Beer Creek, with minor rhyolite and basalt clasts. The angular nature of the sand and gravel indicates they were transported only a short distance.

The sedimentary rocks are divided into three units characterized by different depositional styles (Reheis, in press a): Unit Te, the oldest, consists mainly of fluvial deposits; unit Tm consists of alkaline lake or playa deposits; and unit Tl, the youngest, consists of alluvial-fan deposits with fluvial deposits locally preserved at the base.

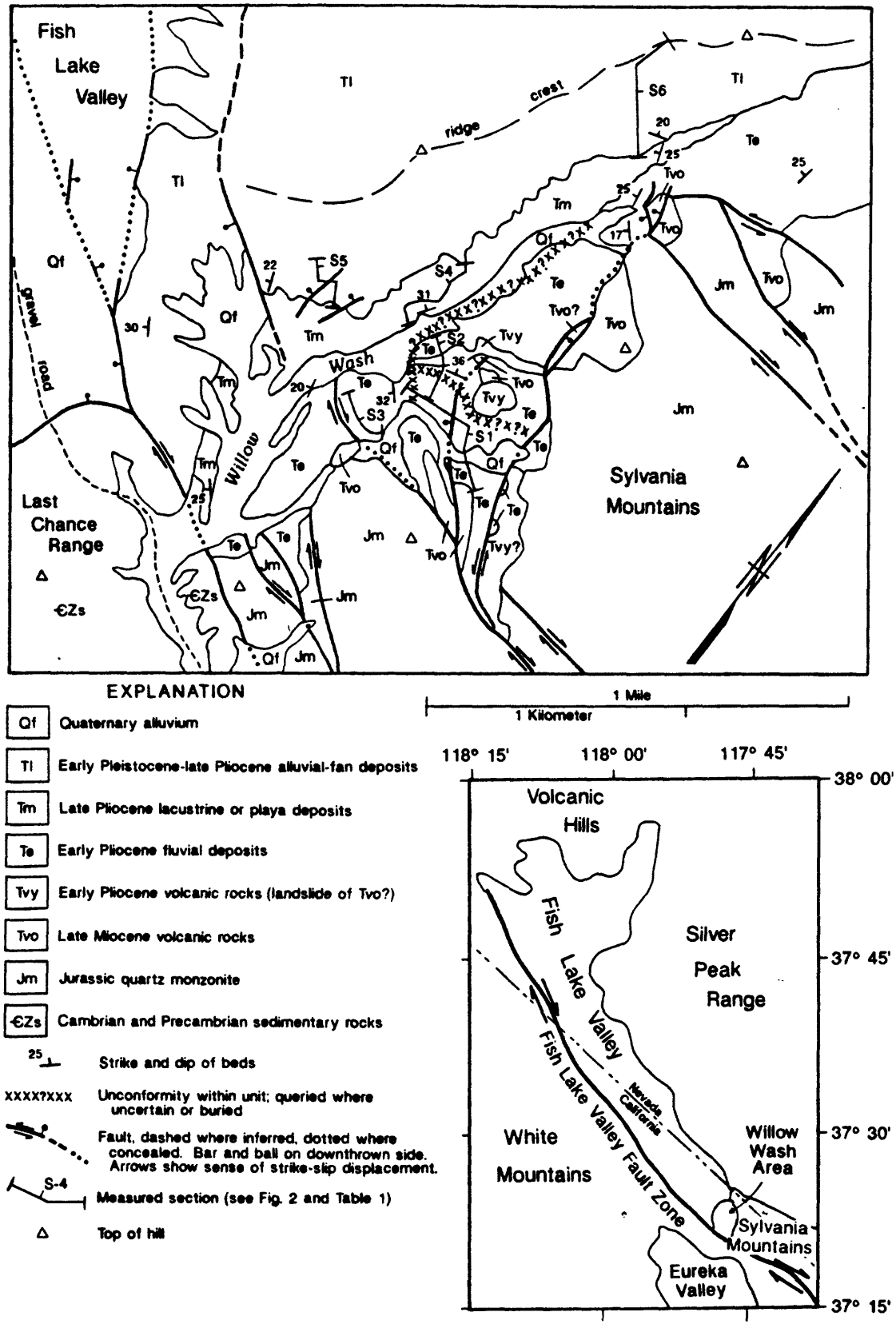

Figure 1. Generalized geologic map of the Willow Wash area (modified from Reheis, in press a).

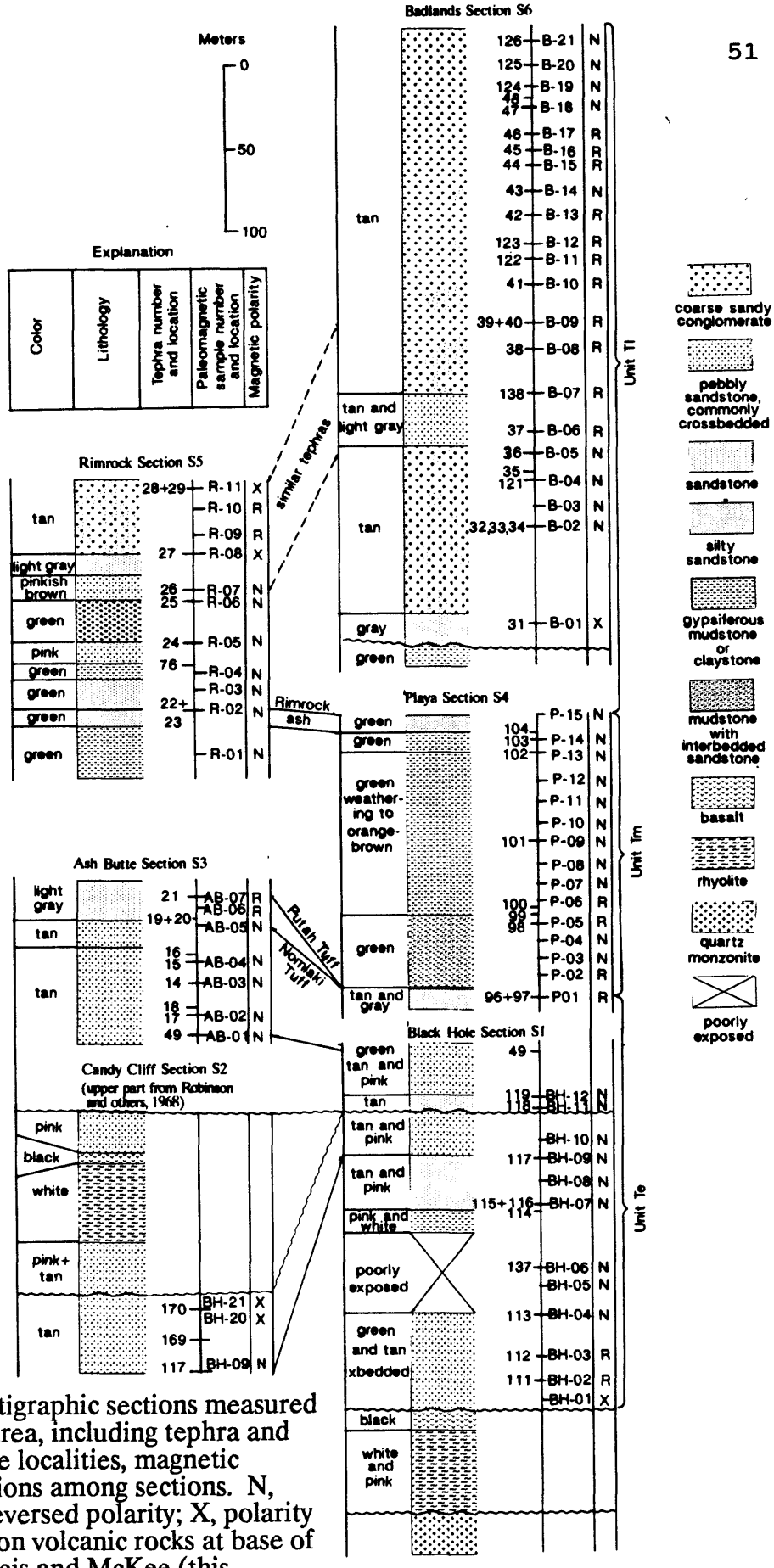

Figure 2. Stratigraphic sections measured in the Willow Wash area, including tephra and paleomagnetic sample localities, magnetic polarity, and correlations among sections. N, normal polarity; R, reversed polarity; X, polarity not measured. Ages on volcanic rocks at base of section are from Reheis and McKee (this volume).

Unit Te

The oldest sedimentary rocks in the Willow Wash section are at least 340 m thick (fig. 2) and crop out mainly on the east side of Willow Wash (fig. 1). These rocks apparently rest unconformably on the 11-Ma volcanic rocks and locally on quartz monzonite, but the base of the section is not exposed. The upper contact with unit Tm is marked by the upper contact of the ash bed here identified as the Nomlaki Tuff (table 2; Sarna-Wojcicki and others, in press). Unit Te is represented by the "Black Hole", "Candy Cliff", and "Ash Butte" sections (figs. 1 and 2; S1 to S3).

The deposits consist of moderately indurated, interbedded grayish-orange, orange-pink, and greenish-yellow arkosic conglomerate, sandstone, and minor siltstone, and commonly contain lenses and extensive beds of volcanic ash and tuffaceous sandstone. The clasts in unit Te are dominantly quartz monzonite, but locally include basalt and rhyolite. The sedimentary rocks are well sorted and stratified, and are inferred to represent fluvial deposition (Reheis, in press a).

The Candy Cliff section contains interbedded basalt and lithic tuff. This section is bounded above and below by angular unconformities (figs. 1 and 2); the interbedded volcanic rocks lie about 30 m above an unconformity that bounds the top of a 145-m-thick section of fluvial sediments (the basal two-thirds of the Black Hole section). The basalt flow in the Candy Cliff section has a K-Ar age of 9.8$\pm$0.3 Ma (Reheis and McKee, this volume), whereas tephra layers above and below the volcanic rocks in the upper and lower parts of the Black Hole section are about 3.4 Ma and 5.2 Ma, respectively (table 2 below). The anomalously old K-Ar age of the basalt, the disturbed bedding in parts of these volcanic layers, and the tephrochronologic ages suggest that the interbedded volcanics may be landslides from topographically high parts of the basal volcanic rocks (fig. 1).

Unit Tm

Unit Tm is about 145 m thick (fig. 2) and crops out as badlands just above the valley floor on the west side of Willow Wash (fig. 1). It consists of distinctive green beds weathering to a thick, expansive "popcorn" surface layer that obscures the bedding underneath. The upper and lower contacts of unit Tm appear to be conformable at the south end of the outcrop area, but this unit pinches out to the north. The lower contact appears to rise gradually in stratigraphic position, whereas the upper contact becomes an angular unconformity (fig. 1). The thickness of unit Tm also decreases to the south before the sediments are cut off against the active strand of the FLVFZ. The upper contact with unit Tl is marked by the "Rimrock ash", locally named for its distinctive, continuous outcrop on top of the green beds (fig. 2). This ash is apparently cut out in the northern part of the outcrop. Unit Tm is represented by the "Playa" section (S4, figs. 1 and 2). The base of this section is marked by two closely spaced tephra layers that are identified as correlative to the Putah and Nomlaki Tuffs (table 2).

The deposits consist primarily of swelling, gypsiferous, pale-olive to grayish-olive mudstone, siltstone, and minor sandstone; sandstone beds are most abundant below the "Rimrock ash" at the top of the unit and above the Putah and Nomlaki ash beds at the base. Thin (3-60 cm) but laterally extensive, white tuffaceous fine-grained sandstones crop out locally within unit Tm (for example, tephra samples 98-, 99-, and 102-WW, fig. 2); these sandstones weather to orange in color and are very fractured. Other sandstones are purplish-gray and very fine-grained (100-WW and 101B-WW, fig. 2); they are also thought to be tephra layers, perhaps from a distant source area such as the Snake River Plain. Based on the swelling clays, the presence of gypsum and other salts, and the continuous nature of individual beds, unit Tm is inferred to have been deposited in an alkaline lake or a playa (Reheis, in press a).

Unit Tl

The youngest sedimentary rocks overlie unit Tm and are exposed in steep, unstable cliffs on the west side of Willow Wash (fig. 1). The maximum preserved thickness is about 340 m. Unit Tl is represented by two measured sections: the "Rimrock" section (S5) on the west and the "Badlands" section (S6) on the east (figs. 1 and 2).

The deposits consist primarily of interbedded grayish-orange sandy gravel and sand, with lenses of volcanic ash and tuffaceous sand. Induration decreases from moderate to poor upward in the section. These deposits are coarsely stratifieds and poorly to moderately sorted. The clasts, commonly pebbles and cobbles but as large as 1 m in diameter, are dominantly quartz monzonite but also include basalt, rhyolite, and sparse sedimentary rocks (Reheis, in press a). At the base of the "Rimrock" section are about 75 m of pinkish-brown to greenish-yellow sandstones and gravelly sandstones. These sandstones are cross-bedded and are better sorted than higher deposits. The stratigraphic interval occupied by these sandstones to the west appears to be represented by less well sorted, gravelly beds to the east ("Badlands" section, fig. 2).

We infer that most of the beds in unit Tl were deposited in alluvial fans shed northward from the Sylvania Mountains, based on the clast composition, relatively poor sorting, and stratification (Reheis, in press a). The well sorted, crossbedded strata at the base of the "Rimrock" section, however, were probably deposited by streams of relatively low gradient. These stream deposits were subsequently buried by alluvial and debris-flow deposits.

Structure

On its southwest side, the Willow Wash section is juxtaposed against the right-lateral strike-slip Fish Lake Valley fault zone (FLVFZ; the northern part of the Furnace Creek fault zone). The entire section ends abruptly against the active strand of this fault zone and has clearly been cut off by the fault.

The basal 11.0-11.5-Ma volcanic rocks in Willow Wash rest unconformably on the quartz monzonite of Beer Creek, but are extensively deformed by inactive faults of the FLVFZ. The depositional contact of the volcanic rocks with the quartz monzonite is always gently sloping. Several high-angle right-lateral strike-slip faults offset these volcanics. Locally, the volcanic rocks are overturned by drag along two closely spaced faults (Tvo near base of section S1, fig. 1), or are overlain by quartz monzonite along a high-angle reverse fault (northernmost outcrop of Tvo in fig. 1).

The oldest sedimentary rocks in the Willow Wash section, those in unit Te, are also greatly deformed by motion on inactive faults of the FLVFZ. Offsets are nearly pure strike-slip on northwest-trending faults, locally show components of high-angle reverse motion on east-west faults, and are normal and down to the west on north-trending faults (fig. 1). The normal faults splay from, and locally connect the ends of, strike-slip faults; the best example of this is the north-trending fault that bounds the east side of the Syvania Mountains and forms the contact between unit Te and subjacent volcanics to the north. Sediments of unit Te were locally deposited on the stripped surface of this fault. A similar north-trending fault, buried under modern alluvium, may connect two strike-slip faults south of the base of section S3. In one exposure near this buried fault, sediments near the top of unit Te rest unconformably on the volcanics, possily on a stripped fault surface. Two angular unconformities occur within unit Te (figs. 1 and 2).

None of the inactive strike-slip and normal faults that offset the basal volcanic rocks and unit Te extend upward into the younger sedimentary rocks. Units Tm and Tl are cut by the two westernmost strands of the FLVFZ; these strands also show Quaternary offset. There are two minor normal faults near section S5 (fig. 1).

Older sedimentary rocks appear to be more folded than younger rocks. Section S1, in unit Te, was measured roughly along the axis of a northwest-trending syncline within and parallel to the axis of a large anticline; dips of beds in this area are as much as 35^{o}. Beds of unit Tl, in contrast, define a simple, broad northwest-trending anticline; dips of beds are typically between 20 and 25^{o} except near active strike-slip faults. Bedding-plane attitudes are difficult to measure in the youngest, least consolidated sediments near the top of unit Tl; however, dips appear to remain relatively constant within vertical sections such as section S6 (fig. 1).

CORRELATION OF TEPHRA LAYERS WITHIN THE WILLOW WASH SECTION, AND TO TEPHRA AT OTHER SITES

Electron-microprobe analyses of glass in tephra layers of the Willow Wash section are presented in table 1, in approximate stratigraphic order from youngest (1) to oldest (61). Figure 2 shows how the measured sections in Willow Wash are correlated by means of the tephra layers. Several tephra layers can be traced continuously or nearly continuously between sections.

The uppermost part of the Badlands section (tephra 47 and above, fig. 2) contains multiple layers and lenses of impure, reworked tephra interbedded with fan gravel. These tephra layers are chemically similar to the 0.74-Ma Bishop ash bed (nos. 1 and 2, table 2; Izett and others, 1988) erupted from the Long Valley caldera, and to 0.9-1.0-Ma tephra (no. 3, table 2; Sarna-Wojcicki and others, 1984; Izett and others, 1988) erupted from the Glass Mountain source area, a predecessor to the caldera and in part contiguous with it (table 2; Metz and Mahood, 1985). On the basis of their major-oxide compositions, the two uppermost samples, FLV-125- and -126-WW, may correlate with either the Bishop ash bed or the younger of several layers erupted from Glass Mountain, for example the Glass Mountain D or G ash bed (table 2). Paleomagnetic analysis, however (see below), indicates that the uppermost 40 m of the Badlands section (tephra 47 and above) has normal polarity. Thus, the uppermost four tephra layers in this section may all be reworked from the Bishop ash.

Tephra layers within the middle part of the Badlands section, particularly FLV-122- and -123-WW (no. 6, table 2), and perhaps two layers immediately above and three below these two (fig. 2) appear to correlate well on the basis of glass chemistry with older tephra layers from the area of Glass Mountain (nos. 5 and 7, table 2), specifically with the thick complex of airfall tephra layers found east of that source at the Cowan Pumice Mine near Benton Springs, west of Fish Lake Valley. This compound unit is referred to as the tuff of Taylor Canyon (Krauskopf and Bateman, 1977; Izett, 1981; Sarna-Wojcicki and others, 1984; Izett and others, 1988). Its age is 2.0 to 2.1 Ma by conventional K-Ar dating and by single-grain laser-fusion dating on sanidines from pumice clasts in the tuffs, and on associated obsidian clasts (Izett and others, 1988; C.E. Meyer, J.K. Nakata, and A.M. Sarna-Wojcicki, unpublished data, 1991). Near-source correlative flow rocks from the Glass Mountain source range from 0.8 to 2.2 Ma (Metz and Mahood, 1985), based on conventional K-Ar analysis.

The upper part of the Rimrock section generally correlates with the middle to lower part of the Badlands section on the basis of correlations between several tephra layers: FLV-36-WW through FLV-40-WW and FLV-138-WW in the Badlands section with FLV-26-WW through FLV-29-WW in the Rimrock section (fig. 2 and table 1).

Table 1. Results of electron-microprobe analysis of volcanic glass shards from upper Neogene tephra layers of the Willow Wash section, Fish Lake Valley, California. Values given are in weight-percent oxide, recalculated to 100 percent on a fluid-free basis. Original oxide totals before recalculation are given to indicate approximate degree of hydration of volcanic glass. Approximately 15 glass shards were analyzed for each sample. Sodium and potassium concentrations in most samples were highly variable from shard to shard of the same sample, and suggest that alkalies have been mobile within the glass of these samples. For estimate of analytical error, see Table 2. Sample compositions are presented in stratigraphic order, from uppermost to lowermost in each section. Tephra layers in Candy Cliff section (fig. 2) are not yet analyzed. C. E. Meyer, U.S.G.S., Menlo Park, California, analyst.

Sample	SiO_2	Al_2O_3	Fe_2O_3	MgO	MnO	CaO	TiO_2	Na_2O	K_2O	Total
Badlands Section, S6 on fig. 2										
1. FLV-126-WW	77.8	12.1	0.78	0.05	0.03	0.45	0.07	3.7	5.0	93.4
2. -125-	78.0	12.1	0.76	0.05	0.04	0.39	0.05	3.9	4.8	93.6
3. -124-	77.6	12.6	0.76	0.02	0.05	0.34	0.06	4.0	4.6	94.9
4. -48-	77.4	12.8	0.71	0.04	0.06	0.32	0.06	3.8	4.8	95.2
5. -47-	78.0	12.3	0.72	0.03	0.07	0.31	0.04	3.8	4.7	90.6
6. -46-	77.9	12.4	0.68	0.02	0.08	0.30	0.07	3.8	4.7	91.3
7. -45-	78.0	12.3	0.67	0.02	0.10	0.29	0.07	3.9	4.7	91.2
8. -44-	77.8	12.6	0.64	0.04	0.10	0.29	0.05	3.9	4.5	91.3
9. -43-	78.0	12.3	0.56	0.03	0.08	0.32	0.06	3.8	4.8	91.9
10. -42-	77.9	12.3	0.61	0.04	0.07	0.36	0.06	3.6	5.2	91.5
11. -123-	77.5	12.5	0.59	0.03	0.08	0.35	0.08	3.8	5.0	94.7
12. -122-	77.5	12.6	0.59	0.02	0.08	0.34	0.07	3.8	5.0	94.7
13. -41-	77.7	12.7	0.55	0.04	0.11	0.31	0.09	3.6	5.0	93.5
14. -40-	78.0	12.6	0.55	0.04	0.10	0.34	0.09	3.8	4.6	93.6
15. -39-	77.6	12.6	0.53	0.06	0.09	0.35	0.10	2.8	5.9	93.2
16. -38-	79.2	12.7	0.54	0.05	0.08	0.42	0.10	2.2	4.8	92.2
17. -138-	76.8	13.0	0.56	0.04	0.09	0.42	0.09	2.7	6.4	93.5
18. -37-	77.7	12.7	0.55	0.05	0.08	0.40	0.09	3.2	5.3	93.9
19. -36-	77.5	12.8	0.58	0.05	0.09	0.43	0.11	3.7	4.8	94.0
20. -35-	77.6	12.7	0.60	0.06	0.07	0.49	0.10	3.8	4.7	94.1
21. -121-	76.6	13.0	0.65	0.04	0.06	0.57	0.07	2.9	6.2	94.4
22. -34-	76.9	12.9	0.62	0.08	0.06	0.62	0.10	2.5	6.2	93.2
23. -33-	76.9	13.0	0.64	0.07	0.07	0.62	0.12	2.7	6.0	93.0
24. -32-	77.2	12.9	0.61	0.07	0.08	0.62	0.12	2.8	5.7	93.9
25. -31-	77.5	12.0	2.01	0.02	0.05	0.35	0.15	3.4	4.5	93.2
Rimrock Section, S5 on fig. 2										
26. -29-	76.9	12.7	0.55	0.06	0.08	0.41	0.06	2.2	7.1	94.2
27. -28-	77.5	12.6	0.53	0.06	0.08	0.39	0.09	2.2	6.7	94.0
28. -27-	77.9	12.4	0.54	0.05	0.08	0.43	0.10	3.0	5.7	94.1
29. -26-	77.9	12.4	0.54	0.05	0.08	0.39	0.10	2.9	5.7	93.7
30. -25-	77.6	12.5	0.61	0.07	0.07	0.56	0.10	2.9	5.7	94.2
31. -24-	76.7	13.0	0.67	0.07	0.07	0.63	0.08	3.2	5.6	94.8
32. -76-	77.9	12.2	0.86	0.11	0.02	0.46	0.18	3.2	5.1	94.3
33. -23-	75.7	13.9	0.77	0.08	0.09	0.63	0.07	4.1	4.6	92.9
34. -22-	75.5	14.0	0.78	0.08	0.10	0.64	0.08	4.2	4.6	93.3
Playa Section, S4 on fig. 2 (Note: glass of tephra samples FLV-98 through 104-WW in this section was completely altered)										
35. -97-	76.9	13.2	1.15	0.21	0.01	1.07	0.24	4.0	3.2	92.4
36. -96-	76.3	12.9	1.76	0.07	0.03	0.61	0.16	4.4	3.8	92.7
Ash Butte Section, S3 on fig. 2										
37. -21-	77.2	12.9	1.10	0.22	0.05	0.99	0.21	4.0	3.4	93.2
38. -20-	75.0	13.6	1.77	0.11	0.03	0.72	0.14	4.0	4.6	93.3
39. -19-	77.3	13.2	0.72	0.04	0.08	0.48	0.06	3.8	4.3	93.6
40. -16- -MS[1]	69.6	15.0	3.97	0.81	0.11	2.37	0.78	4.4	3.0	91.8
41. -16- -SS[2]	77.2	12.8	0.75	0.07	0.05	0.49	0.10	3.1	5.4	96.7
42. -15-	76.7	13.1	1.19	0.08	0.02	0.57	0.12	3.7	4.4	93.8
43. -14-	74.7	13.9	1.69	0.31	0.06	1.25	0.32	4.3	3.5	93.2
44. -18-	67.7	15.8	4.12	1.34	0.09	3.56	0.65	4.3	2.5	92.9
45. -17-	71.9	15.9	2.30	0.60	0.05	2.15	0.29	3.7	3.2	91.1
46. -49-	77.1	13.1	0.90	0.16	0.05	0.97	0.12	3.4	4.2	94.5
Black Hole Section, S1 on fig. 2										
47. -119-	76.6	13.1	1.14	0.17	0.02	0.92	0.21	3.3	4.5	92.2
48. -119- SS[2]	76.9	13.0	1.07	0.16	0.05	0.89	0.19	3.4	4.4	92.7
49. -118- MS[1]	77.1	12.7	0.81	0.04	0.04	0.50	0.10.	3.2	5.6	96.8
50. -118- SS[2].	77.2	12.6	0.78	0.06	0.06	0.52	0.09	3.3	5.4	96.1
51 -117-	76.6	12.8	1.15	0.18	0.05	0.94	0.21	3.1	5.0	92.8
52. -116-	76.9	12.4	1.31	0.09	0.02	0.49	0.21	3.0	5.6	93.5
53. -115-	77.1	12.4	1.27	0.08	0.01	0.47	0.19	2.9	5.6	93.4
54. -114-	72.7	15.1	1.67	0.07	0.06	0.59	0.11	3.9	5.8	92.2
55. -137-	70.9	14.8	3.19	0.65	0.09	2.12	0.67	4.4	3.2	91.6
56. -113-	71.2	14.5	3.52	0.12	0.09	1.04	0.21	5.0	4.3	92.6
57. -112- MS[1]	77.2	12.5	0.81	0.04	0.04	0.49	0.08	3.0	5.8	96.5
58. -112- SS[2]	77.0	12.7	0.80	0.03	0.07	0.46	0.06	3.0	6.0	95.4
59. -111-	77.0	12.5	0.82	0.02	0.08	0.46	0.06	2.9	6.2	95.0
60. -111B-	76.8	13.0	0.80	0.02	0.02	0.47	0.07	3.1	5.9	93.7
61. FLKA-3	77.5	12.3	0.62	0.07	0.04	0.47	0.09	3.5	5.4	94.9

[1]MS - Mafic, or less silicic shards, in bimodal sample.
[2]SS - Albic, or more silicic shards, in bimodal sample.

Table 2. Glass composition of tephra layers chemically similar to those present in the Willow Wash section, Fish Lake Valley. Other comments as in Table 1. Multiple analyses of a homogenous natural glass standard, RLS 132, are given below, and provide a close estimate of the analytical error for each oxide in electron-probe analysis. Comparative values based on wet-chemical analysis of the same sample are also given (28). C. E. Meyer, U.S.G.S., Menlo Park, California, electron-probe analyst.

Sample	SiO_2	Al_2O_3	Fe_2O_3	MgO	MnO	CaO	TiO_2	Na_2O	K_2O	Total
Bishop ash bed (0.74 Ma) from Fish Lake Valley (1) and from several known distal and proximal localites (2); average of two proximal samples of Glass Mountain ash beds (D, 0.9 Ma, and G, 1.0 Ma) (3); and tephra layer from Willow Wash section, uppermost in Badlands Section, S6 (4)										
1. Average of 5	77.8	12.7	0.72	0.03	0.03	0.43	0.07	3.7	4.6	93.8
2. Average of 6	77.5	12.7	0.73	0.03	0.04	0.43	0.06	3.8	4.7	93.6
3. Average of 2	77.6	12.7	0.74	0.03	0.03	0.43	0.07	3.7	4.7	95.0
4. FLV-126-WW	77.8	12.1	0.78	0.05	0.03	0.45	0.07	3.7	5.0	93.4
Tephra layers similar to Tuff of Taylor Canyon from several localities in Fish Lake Valley (5), chemically similar tephra from Willow Wash section, middle part of Badlands Section, S6 (6), and Tuff of Taylor Canyon (~1.9-2.1 Ma) from proximal and distal localities (7)										
5. Average of 8	77.3	12.6	0.59	0.04	0.09	0.33	0.06	3.4	5.6	94.4
6. Average of 2	77.5	12.6	0.59	0.03	0.08	0.35	0.08	3.8	5.0	94.7
7. Average of 7	77.5	12.6	0.59	0.04	0.09	0.34	0.07	3.7	5.0	93.7
Tephra layer in Willow Wash section near base of Playa Section, S4 (8), near top of Ash Butte Section, S3 (9), and Nomlaki Tuff (Member of the Tuscan and Tehama Formations; 3.4 Ma), Sacramento Valley, CA (10)										
8. FLV-97-WW	76.9	13.2	1.15	0.21	0.01	1.07	0.24	4.0	3.2	92.4
9. FLV-21-WW	77.2	12.9	1.10	0.22	0.05	0.99	0.21	4.0	3.4	93.2
10. OP84-193A	76.8	13.0	1.15	0.22	0.04	1.08	0.23	4.1	3.4	94.4
Tephra layer in Willow Wash section at base of Playa Section, S4 (11), near top of Ash Butte Section, S3 (13), and Putah Tuff (Member of the Tehama Formation; 3.4 Ma), southwestern Sacramento Valley, CA (12, 14), closest matches to samples 11 and 13										
11. FLV-96-WW	76.3	12.9	1.76	0.07	0.03	0.61	0.16	4.4	3.8	92.7
12. 758-287D	76.3	12.7	1.76	0.09	0.02	0.61	0.18	4.1	4.3	92.9
13. FLV-20-WW	75.0	13.6	1.77	0.11	0.03	0.72	0.14	5.1	3.3	93.3
14. 758-292	74.9	13.9	1.76	0.09	0.03	0.72	0.14	4.1	4.4	92.9
Tephra layers in Willow Wash section near the top of Black Hole Section, S1 (15, 17, 18); biotite-vitric tuff near top of Tassajara Fm., Livermore Valley, west-central California (16); and Nomlaki Tuff (Member of the Tehama and Tuscan Formations; 3.4 Ma), Sacramento Valley, CA (19)										
15. FLV-119-WW ss[1]	76.9	13.0	1.07	0.16	0.05	0.89	0.19	3.4	4.4	92.7
16. 758-328(2)	78.4	13.0	1.02	0.16	0.03	0.82	0.19	4.0	2.3	91.9
17. FLV-119-WW	76.6	13.1	1.14	0.17	0.02	0.92	0.21	3.3	4.5	92.2
18. FLV-117-WW	76.6	12.8	1.15	0.18	0.05	0.94	0.21	3.1	5.0	92.8
19. 758-324(2)	77.5	12.9	1.14	0.17	0.03	0.95	0.22	3.8	3.4	94.6
Tephra layers in Willow Wash section, middle part of Black Hole Section, S1 (20, 21), and undated tephra layer from eastern Snake River Plain, Idaho, west of Yellowstone National Park, Wyo. (22)										
20. FLV-116-WW	76.9	12.4	1.31	0.09	0.02	0.49	0.21	3.0	5.6	93.5
21. FLV-115-WW	77.1	12.4	1.27	0.08	0.01	0.47	0.19	3.0	5.6	93.4
22. ER-6	76.6	12.4	1.36	0.08	0.03	0.51	0.23	3.2	5.5	94.0
Tephra layer in Willow Wash section, lower part of Black Hole Section, S1 (23), and tephra layers erupted from the Sonoma Volcanics: the Pinole Tuff (5.2 Ma) (24), the basal tephra layers in the Monticello Road section (5.4 Ma) (25), and a tuff from near Healdsburg, CA (26)										
23. FLV-113-WW	71.2	14.5	3.52	0.12	0.09	1.04	0.21	5.0	4.3	92.6
24. 758-178B	71.3	14.4	3.56	0.09	0.08	1.09	0.23	5.8	3.5	94.0
25. 758-365(2)	72.1	14.9	3.55	0.11	0.05	1.09	0.22	3.0	5.0	91.2
26. HEALDS-1	72.2	14.4	3.25	0.11	0.09	0.98	0.21	5.1	3.6	95.7
Internal glass standard used: probe analysis (27) and wet-chemical analysis (28)										
27. RLS 132 (Av. 18)	75.4	11.2	2.12[2]	0.06	0.16	0.11	0.19	4.9	4.4	98.6
±1 std. dev.:	0.1	0.2	0.04	0.01	0.01	0.01	0.01	0.1	0.01	
28. RLS 132 (wet chemical)	75.7	11.4	2.12	0.05	0.15	0.12	0.21	5.3	4.5	99.6

[1]Only composition of silicic shards is reported.
[2]Iron in the standard reported as FeO, rather than Fe_2O_3

The chemical composition of volcanic glass in the tephra layers within the Badlands section appears to change systematically with stratigraphic position; only the composition of the basal layer in this section, FLV-31-WW, is very different, which suggests that it was derived from a different or genetically unrelated source (table 1). The same type of systematic variation is apparent in the partly correlative Rimrock section, where the variation continues downward into tephra layers older than those in the Badlands section. Despite these systematic variations, the tephra compositions of layers in these sections are each relatively homogeneous. The systematic variation probably reflects chemical evolution with time within the magmatic system that produced this suite of tephra layers. Thus, it seems unlikely that the layers and lenses within the Badlands and Rimrock sections are reworked from one or a few large tephra layers, but rather they represent a temporal sequence of eruptions from a single source. However, some minor mixing may have occurred among stratigraphically adjacent tephra layers within the Badlands and Rimrock sections, particularly within the middle part of the former and the upper part of the latter.

The Rimrock ash bed (FLV-22- and 23-WW) can be traced physically from near the base of the Rimrock section to the top of the Playa section (fig. 2). All the tephra layers within the Playa section, except for the basal two layers, however, are altered, presumably by the saline, alkaline waters that were once contained in the lake or playa, and no isotropic glass is preserved.

The two unaltered, basal ash beds in this section, FLV-97-WW and FLV-96-WW (nos. 8 and 11, table 2), correlate chemically with the Nomlaki Tuff Member of the Tehama and Tuscan Formation, and the Putah Tuff Member of the Tehama Formation, respectively (nos. 10, 12, and 14, table 2). Both latter units are present in deformed late Cenozoic alluvium of the Sacramento Valley of California. At one locality in that valley, near the town of Orland, these two layers are present in a core in the same stratigraphic order as in the Willow Wash section: the Putah is at a depth of about 440 m, the Nomlaki at a depth of about 430 m. Both are dated directly and indirectly at about 3.4 Ma (K-Ar; Evernden and others, 1964; Miller, 1966; Sarna-Wojcicki, 1976; Obradovich and others, 1978; Sarna-Wojcicki and others, in press). The Putah Tuff Member is composed of two compositional variants, and both variants are present within the Willow Wash section (table 2, samples 11 through 14). Tephra of the Nomlaki Tuff Member was erupted from the southern Cascade Range, probably from a region in northeastern California, southeast of Lassen Peak. Tephra of the Putah Tuff Member was erupted from the Sonoma volcanic field, within the central Coast Ranges of California north of San Francisco Bay; it formed one of the last widespread units derived from that source (Sarna-Wojcicki and others, in press).

The two tephra layers in the Willow Wash section that are here provisionally correlated with the Nomlaki and Putah Tuff Members also correlate the base of the Playa section with the top of the Ash Butte section (fig. 2 and tables 1 and 2; FLV-97-WW with -21-WW, and -96-WW with -20-WW. The section between these two tuffs thins considerably from the Ash Butte to the Playa section (fig. 2).

Within the Ash Butte section there are several tephra layers below the putative Nomlaki and Putah Tuff Members that appear to correlate on the basis of their glass chemistry with much younger tephra layers (middle Pleistocene) than their stratigraphic positions would allow. Unless there are serious problems with the correlations and the sequence of measured sections as we present them here (fig. 2), such as an undetected younger section that is inset into an older one, the similarities to the younger layers must be considered spurious.

Tephra bed FLV-49-WW can be traced continuously between the base of the Ash Butte section and the top of the Black Hole section, the lowermost section within Willow Wash. An unresolved problem in correlation of the base of the Playa, the upper part of the

Ash Butte, and the top of the Black Hole sections is the presence of two tephra layers within the upper part of the Black Hole section, FLV-119- and -117-WW (nos. 15, 17, and 18, table 2), which have glass chemistry very similar to that of FLV-21-WW in the top of the Ash Butte section, and FLV-97-WW in the base of the Playa section. All four samples have chemistry similar to that of the Nomlaki Tuff Member (nos. 16 and 19, table 2). FLV-119-WW is bimodal, having shards similar in chemistry to both the Nomlaki and to an undated biotite-vitric tuff present in Livermore Valley, in the central Coast Ranges of California. This last tuff is situated stratigraphically above the Huichica Tuff within the Coast Ranges, the latter being dated by K-Ar at about 4.0 Ma (Sarna-Wojcicki, 1976), but the biotite-vitric tuff has no limiting age above it. FLV-117-WW in the Black Hole section is a particularly impressive, 3-m-thick tuff, and must represent a sizeable eruption compared to other tephra layers in the Willow Wash section. If the tie between the base of the Ash Butte section and the top of the Black Hole section based on the continuous exposure of tehpra layer FLV-49-WW is correct--and it is difficult to see how it could be incorrect--then there must be more than one tephra layer having glass composition similar to that of the Nomlaki Tuff within the Willow Wash section. Further work is needed to resolve the puzzle as to which layer is the real Nomlaki Tuff.

Below FLV-117-WW, within the middle part of the Black Hole section, there are two tephra layers, FLV-116- and -115-WW (nos. 20 and 21, table 2), that are similar in glass composition and shard morphology to tephra layers erupted from the eastern Snake River Plain-Yellowstone National Park area of east-central Idaho and northwestern Wyoming. These tephra layers are most similar to, and probably correlate with, an undated tephra layer found in east-central Idaho, ER-6 (T. Yancey, written commun., 1979; no. 22, table 2). They are also similar to the informally named Alturas ash bed, the age of which is estimated to be 4.8 Ma (Sarna-Wojcicki and Meyer, unpublished data), but the iron content in the Alturas ash bed is too high. They are also similar to the tuff of Wolverine Creek, which is between 4.3 and 6.0 Ma (Hackett and Morgan, 1989), but the titanium content of this tuff is too high to allow a match.

A poorly-exposed interval intervenes between the middle and lower part of the Black Hole section. Below this interval, the chemistry of tephra layer FLV-113-WW (no. 23, table 2) matches well with those of several tephra layers erupted from the Sonoma volcanic field. The matches are to the Pinole Tuff (758-178B), dated at 5.2 Ma by K-Ar (Evernden and others, 1964), and to a tuff at the base of the Monticello Road section (758-365), dated at 5.4 Ma (Sarna-Wojcicki, 1976), as well as to an undated tephra layer near Healdsburg, Calif. (nos. 24-26, table 2). The Pinole Tuff and the tuff at the base of the Monticello Road section have been previously correlated on the basis of multiple criteria (Sarna-Wojcicki, 1976).

PALEOMAGNETISM

High-quality, stable magnetic directions were obtained from most of the sampling sites. Of the 66 sites that were sampled, 83% are Class I, 8% are Class II, and 9% yielded unusable results (fig. 4). The demagnetized Class I data exhibit antipodal clustering of the normally and reversely magnetized sites (fig. 5). There appears to be a minor ($\sim 10^{0}$) clockwise rotation of the mean directions with respect to the average dipole-field direction. This rotation, although small, is consistent with dextral shear along the FLVFZ. The section is dominated by normal polarity, but includes a long, reversed magnetozone near the top and encompasses a total of ten magnetozones. Four of the short magnetozones (< 10 m) are represented by fewer than three sites. The correlation of the Willow Wash magnetic polarity stratigraphy (MPS) with the magnetic polarity time scale (MPTS, fig. 6; Berggren and others, 1985) is aided by the presence of tephra that are recognizable based on their geochemical characteristics.

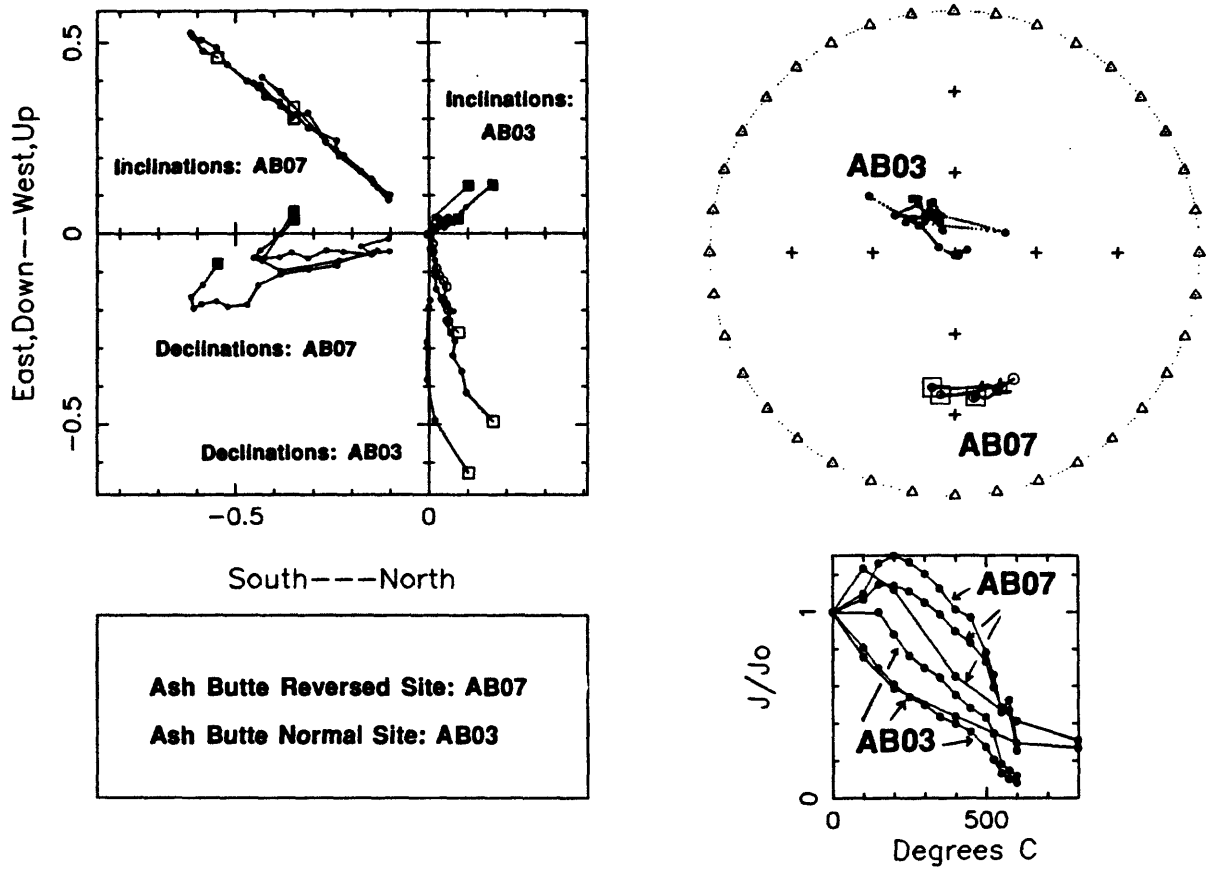

Figure 3. Demagnetization plots for six specimens from two sites (AB03 and AB07) in the Ash Butte section (fig. 2). Two specimens from each site were thermally demagnetized, and one was demagentized in an alternating field. All show very consistent and coherent results. Stereonet displays the approximately antipodal orientation of the data, and intensity plot shows that a weak overprint on the reversely magnetized specimens is removed by 200°C or 200 oe.

The lowermost normal magnetozone (N1, fig. 4) includes a major unconformity (represented by two unconformities in the Black Hole section, fig. 2) along which at least 100 m of strata have been erosionally removed. The presence of tephra layers that appear correlative with the Pinole Tuff and others tuffs of the Sonoma volcanic field suggest that the portion of the section below this unconformity should be about 5.2 Ma. Based on these relations, it is likely that R1 and the basal portion of N1 (fig. 4) correlate with the basal Gilbert chron or with the upper part of chron 5 (fig. 6).

Tephra correlated with the Putah and Nomlaki tuffs (dated at 3.4 Ma elsewhere) are present at ~325 m in both the Ash Butte and Playa sections (fig. 4). Their presence requires that this portion of the section be correlative with part of the Gauss chron. The absence of any reversely magnetized strata between these tuffs and the underlying unconformity indicates that these strata are younger than the base of the Gauss chron. In fact, they occur near the base of the lower reversed subchron within the Gauss, and thus they appear to have an age of ~3.2 Ma based on the MPTS (Berggren and others, 1985). The longest reversely magnetized zone (R4 and R5, 550-710 m, fig. 4) would then correlate with the Matuyama chron (fig. 6). It appears that relatively continuous sedimentation prevailed in the vicinity of Willow Wash from ~3.4 to 2.0 Ma; during this interval, 500 m of strata accumulated at an average rate of 36 cm/kyr.

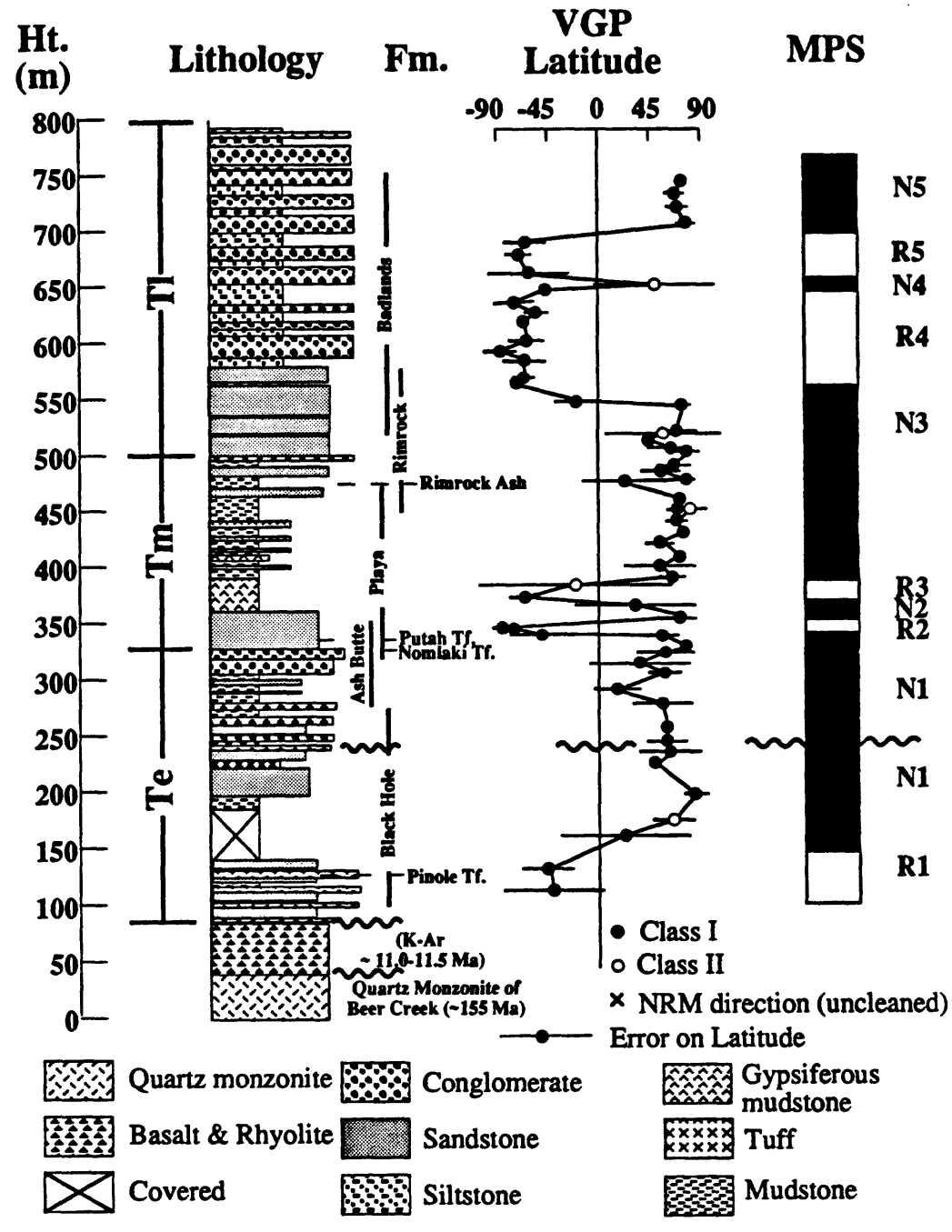

Figure 4. Preliminary magnetic polarity stratigraphy (MPS) for the Willow Wash section. Schematic lithologies and the stratigraphic extent of each of the measured sections is depicted on the left. The NRM polarity of each site that has not been demagnetized is marked by an X. Wavy lines mark unconformities.

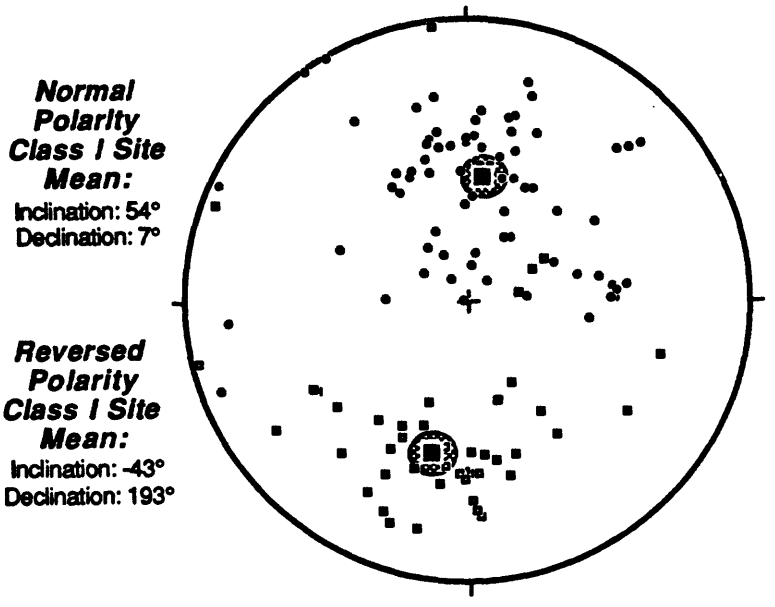

Figure 5. Stereoplot of the individual specimen magnetic directions for the Class I sites. The mean direction of the normally and reversely magnetized sites are plotted with a 95% confidence envelope. Filled dots are lower hemisphere projections and open squares are upper hemisphere projections.

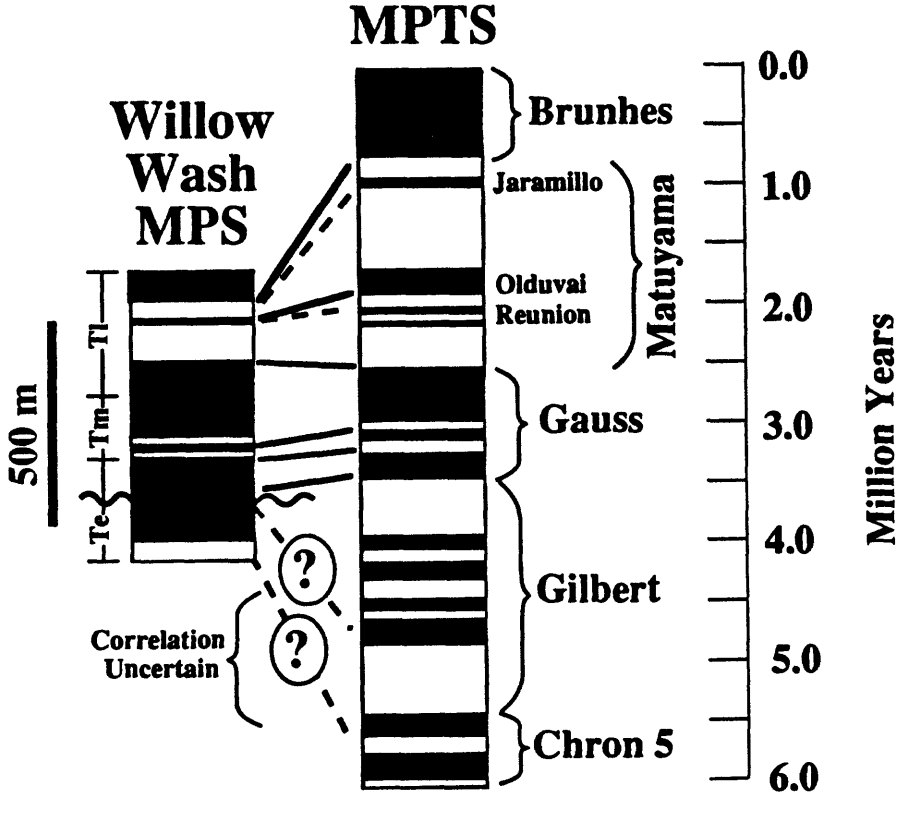

Figure 6. Correlation of the Willow Wash MPS with the magnetic polarity time scale (MPTS) of Berggren and others (1985). Wavy line marks unconformity.

Tephra layers 122 and 123 (fig. 2) are correlated to the 2.0-2.1-Ma tuff of Taylor Canyon (table 2) and lie in the middle of a long part of the Badlands section with reversed polarity. These tephra layers are overlain by a single tephra (43, fig. 2) with normal polarity that is also chemically similar to the tuff of Taylor Canyon. Based on their tephrochronologic age and polarity, the reversely polarized beds of the R4 magnetozone correlate to the lower part of the Matuyama chron, and tephra 43 (N4) may correlate to the Olduvai or to one of the Reunion subchrons (fig. 6). Samples from the topmost 40 m of the Badlands section have normal polarity. The tephra layers in this part of the section (47 and above, fig. 2) are chemically similar to the Bishop and the older Glass Mountain ash beds, but of these beds only the Bishop has normal polarity. Thus, the upper part of the N5 magnetozone (fig. 4), and perhaps all of it, must correlate with the Brunhes chron (fig. 6). If these correlations are correct, then the 30-m-thick reversely magnetized R5 magnetozone (fig. 4) must either contain one or more unconformities or represent a period of slow sedimentation that spans nearly all of the latter part of the Matuyama chron. Mean compacted sediment accumulation rates during this interval are only 2-3 cm/kyr. This is an order of magnitude lower than during the previous 1.5 million years, suggesting that the rate of subsidence had slowed dramatically and was nearly equal to and sometimes exceeded by the rate of uplift of the basins.

DISCUSSION AND CONCLUSIONS

Age of the Sedimentary Rocks in Willow Wash

The alluvial-fan deposits of unit Tl are late Pliocene to early Pleistocene in age. The highest tephra beds in the section (125 and 126, fig. 2) are correlated to the 0.74-Ma Bishop Tuff (Izett and others, 1988) in Long Valley, Calif., based on their chemistry and normal polarity. Because there is more than one tephra layer with chemistry similar to that of the Bishop Tuff and with normal polarity, it appears that this tephra may have been episodically reworked after the eruption. Several tephra beds in the upper part of unit Tl (39-43 and 122-123, fig. 2) correlate to tuffs ranging in age from 1.8 to 2.2 Ma (table 2), beds of the tuff of Taylor Canyon in the Long Valley area. Of these beds, 43-WW has normal polarity whereas the beds above and below have reversed polarity. The interval of normal polarity may correspond to the Olduvai or one of the Reunion subchrons (fig. 6) between 1.7 and 2.2 Ma.

The lacustrine or playa beds of unit Tm are of late Pliocene age. These beds overlie tephra layers provisionally correlated to the 3.4-Ma Putah and Nomlaki Tuff Members of the Tehama Formation (Sarna-Wojcicki and others, in press) and are capped by the "Rimrock ash" (fig. 2). This ash was dated by K-Ar on biotite at 4.3 ± 0.4 Ma (Robinson and others, 1968). If the correlations to the Putah and Nomlaki Tuff Members are correct, the "Rimrock ash" must be much younger than the K-Ar age. Sediments of unit Tm are nearly all normally magnetized, except for two beds near the base. Based on the paleomagnetic data and relations to the Putah and Nomlaki tephra layers, these sediments correspond to younger portion of the Gauss chron and span about 2.7 to 3.2 Ma (fig. 6).

The uppermost tephra layers of unit Te are provisionally correlated to the Putah and Nomlaki Tuff Members. These tuffs occur in a short section of sediments containing a transition from normal polarity (N1) to reversed polarity (R2) in Willow Wash (fig. 4). A thick section of normally magnetized sediments (N1 above unconformity, fig. 4; lower part of Ash Butte and upper part of Black Hole sections) underlies the Putah and Nomlaki tephra layers; these sediments probably belong to the lower part of the Gauss Chron. These relations are somewhat in conflict with the reported age of 3.4 Ma for the Gauss-Gilbert chron boundary (Berggren and others, 1985). The conflict could be due either to uncertainty in the reported age of the Putah and Nomlaki Tuffs and (or) the chron

boundary, or to our uncertainty as to whether FLV-117-WW, in the Black Hole section, is the "real" Nomlaki.

The oldest sedimentary rocks in the Willow Wash section, fluvial deposits of unit Te, are probably of early Pliocene age. Tephra FLV-113-WW is tentatively correlated with the 5.2-Ma Pinole Tuff (table 2). The tephra correlative with the Pinole Tuff is normally magnetized, whereas two underlying beds are reversely magnetized; this magnetic boundary may represent a boundary at about 4.9 Ma (Berggren and others, 1985) within the basal part of the Gilbert chron or one within the older Chron 5 (5.5-6.0 Ma). Two uncorrelated tephra beds and at least 30 m of sedimentary rocks occur underneath tephra FLV-113-WW; thus, it is possible that the oldest exposed sediments are latest Miocene in age.

The tephra beds indicate that the upper part of the Willow Wash section is much younger than was previously thought (McKee and Nelson, 1967; McKee, 1968; Robinson and others, 1968). These sedimentary rocks were mapped as the Esmeralda Formation, dated in the area of Fish Lake Valley as old as 13.1 Ma and as young as somewhat less than 4.3 Ma (Robinson and others, 1968). Based on the tephrochronology, only the basal volcanic rocks and unit Te fall within this time span.

Unit Tl is correlated to a thick sequence of gravelly debris-flow deposits in northeastern Fish Lake Valley (unit QTg, Reheis, in press b) based on tephra correlations. These gravelly deposits overlie greenish lacustrine sediments (Robinson and others, 1968) similar to those of unit Tm in Willow Wash; hence, it is possible that this lake occupied all of Fish Lake Valley.

Implications of Structure and Stratigraphy

The age of the basal rhyolite and basalt flows is roughly coincident with the resurgence of local (Robinson and others, 1968) and regional (Carr, 1984) volcanism in the late Miocene. The nature of the depositional contact of the volcanics with the subjacent quartz monzonite suggests, but does not prove, that motion on the FLVFZ did not begin until after the eruption of the flows (Reheis and McKee, this volume).

The distribution of the inactive strike-slip and normal faults in the area of Willow Wash suggests that they once formed a single coherent pull-apart basin in which the late Cenozoic sediments accumulated. The north-trending faults of this pull-apart basin may have been later disrupted by continued motion on the strike-slip faults, resulting in the stair-step appearance of the faults and of the volcanic-sedimentary contact. This reconstruction is supported by the intense faulting of unit Te and the sharp unconformity of the base of unit Te with underlying rocks, locally occurring on stripped fault surfaces. Hence, the age of the basal sedimentary rocks of the Willow Wash area (about 5.5 Ma?) provide a minimum age, perhaps a closely limiting minimum age, for the onset of motion on the Furnace Creek fault zone in this area.

Sedimentary relations suggest ongoing uplift and faulting along the north-trending normal faults during deposition of units Tm and Tl in the late Pliocene and early Pleistocene. Angular unconformities and the presence of layers of volcanic rock within the sediments of unit Te, apparently due to landsliding, attest to active tectonism during deposition of this unit. An active range-front fault is implied by the occurrence of lacustrine or playa sediments so close to the faults and the bedrock high of the Sylvania Mountains. In addition, the large clasts and relatively poor bedding and sorting that characterize unit Tl suggest alluvial-fan deposition near a mountain front.

Bedding attitudes in the sedimentary rocks suggest progressive folding and tilting that accompanied depositon. The older rocks of unit Te have steeper dips than the younger rocks of unit Tl, and folds in unit Te do not appear to extend upward into unit Tl. Unit Tl is broadly warped along a northwest axis and dips in this unit are relatively uniform (20-25ø) away from active strike-slip faults. Hence, compression and northwestward tilting must have occurred following deposition of unit Tl, in middle and late Pleistocene time.

Implications for Tephrochronology

Fish Lake Valley, including Willow Wash at the southern end, is situated in a unique geographic location between several major sources of Neogene explosive silicic volcanism within the western conterminous United States. The known distribution patterns for several widespread Neogene tephra layers derived from different sources overlap at or near Fish Lake Valley. Not coincidentally, a large number of tephra layers are found within Willow Wash and in other areas of Fish Lake Valley (Reheis, in press a, b). Consequently, this area is favorable for the development of a tephrochronologic framework that can be used for detailed stratigraphic mapping and correlation on a local scale, and the area provides a unique opportunity for stratigraphic and structural analysis with a degree of precision that is difficult to achieve at other sites. Furthermore, the large number of tephra layers found within the Willow Wash section and elsewhere in Fish Lake Valley provide a detailed reference sequence to which tephra from other regions can be correlated and placed within a stratigraphically controlled and (eventually) well-dated sequence.

The presence in the Willow Wash section of multiple, relatively coarse tephra layers erupted from the Long Valley-Glass Mountain source area is expected, because the Willow Wash section is only about 80 km and downwind from this source. The presence in the Willow Wash section of Pliocene tephra layers such as the Putah Tuff Member and the Pinole Tuff, erupted from the Sonoma volcanic field in west-central California, should also be expected; Fish Lake Valley and the Willow Wash section are due east of the Sonoma field, in the direction of the prevailing winds that exist today and probably existed at the times of these eruptions. During those times, about 3-6 Ma, both the Sierra Nevada and the White Mountains were probably much lower in elevation that they are now (e.g. Axelrod and Ting, 1960; Putnam, 1962; Huber, 1981), which would allow transport of volcanic ash even from small eruptions by low-level winds.

The presence in the Willow Wash section of tephra layers from other source areas, such as the Cascade Range or the area of the eastern Snake River Plain-Yellowstone National Park, requires transport under special conditions, such as specific positioning of high- or low-pressure systems relative to the sources, or eruption of tephra plumes above the tropopause, where counter-winds can transport them in directions opposite to those of the prevailing winds. Such conditions, however, occur rather frequently in historic times and have been documented for historic eruptions (for example, the eruptions of Mount St. Helens in May of 1980; McCormick, 1981; Sarna-Wojcicki and others, 1983).

The tuffaceous sedimentary sequence in Willow Wash rests unconformably on volcanic rocks dated at about 11.0-11.5 Ma (Reheis and McKee, this volume). If the ages and correlations presented here are correct, the unconformity beneath the sedimentary section represents a time gap of about 5.5 to 6 Ma. The section thus represents intermittent sedimentation during a period from about 5.5 to about 1 Ma, under diverse conditions controlled largely by variations in tectonic and climatic factors. Once we have been able to confirm and refine the correlations and age assignments of tephra layers in the Willow Wash section, we can not only use this section as a reference for tephra layers found in other areas, but also begin to determine the nature and sequence of tectonic and climatic events that are represented in the Willow Wash section and the greater Fish Lake Valley area.

ACKNOWLEDGEMENTS

We are grateful for the help of several field assistants: J. Slate (University of Colorado), and A. Stein, E. Skov, and L. Von Wald (Humboldt State University). R. Hobbs was responsible for the paleomagnetic sampling, and Hobbs, S. Henyey, and K. Young for sample processing (University of Southern California). E.H. McKee (U.S. Geological Survey) dated the volcanic rocks (Reheis and McKee, this volume) and provided valuable comments on his early work and these new ideas.

REFERENCES

Anderson, C.A., and Russell, R.D., 1939, Tertiary formations of northern Sacramento Valley, California: California Journal of Mines and Geology, v. 35, no. 3, p. 215-253.

Axelrod, D.I., and Ting, W.S., 1960, Late Pliocene floras east of the Sierra Nevada: University of California Publications in Geological Sciences, v. 39, no. 1, p. 1-117.

Berggren, W.A., Kent, D.V., Flynn, J.J., and van Couvering, J.A., 1985, Cenozoic geochronology: Geological Society of America Bulletin, v. 96, p. 1407-1418.

Carr, W.J., 1984, Regional structural setting of Yucca Mountain, southwestern Nevada, and late Cenozoic rates of tectonic activity in part of the southwestern Great Basin, Nevada and California: U.S. Geological Survey Open-File Report 84-854, 109 p.

Christiansen, R.L., and Blank, H.R., Jr., 1972, Volcanic stratigraphy of the Quaternary rhyolite plateau in Yellowstone National Park: U.S. Geological Survey Professional Paper 729-B, 18 p.

Evernden, J.F., Savage, D.E., Curtis, G.H., and James, G.T., 1964, Potassium-argon dates and the Cenozoic mammalian chronology of North America: American Journal of Science, v. 262, p. 145-198.

Fisher, R.A., 1953, Dispersion on a sphere: Proceedings of the Royal Society of London, v. A217, p. 295-305.

Hackett, W.R., and Morgan, L.A., 1989, Explosive basaltic and rhyolitic volcanism of the eastern Snake River Plain, Idaho, *in* Link, P.K., and Hackett, W.R., eds., Guidebook to the geology of central southern Idaho: Idaho Geological Survey Bulletin 27, p. 283-301.

Huber, N.K., 1981, Amount and timing of late Cenozoic uplift and tilt of the central Sierra Nevada, California--evidence from the upper San Joaquin basin: U.S. Geological Survey Professional Paper 1197, 28 p.

Izett, G.A., 1981, Volcanic ash beds: recorders of upper Cenozoic silicic pyroclastic volcanism in the Western United States: Journal of Geophysical Research, v. 86, no. B11, p. 10,200-10,222.

Izett, G.A., Obradovich, J.D., and Mehnert, H.H., 1988, The Bishop ash bed (middle Pleistocene) and some older (Pliocene and Pleistocene) chemically and mineralogically similar ash beds in California, Nevada, and Utah: U.S. Geological Survey Bulletin 1675, 37 p.

Izett, G.A., and Wilcox, R.E., 1982, Map showing localities and inferred distributions of the Huckleberry Ridge, Mesa Falls, -and Lava Creek ash beds (Pearlette family ash beds) of Pliocene and Pleistocene age in the Western United States and Southern Canada: U.S. Geological Survey Miscellaneous Investigations Map I-1325, scale 1:4,000,000.

Krauskopf, K.B., and Bateman, P.C., 1977, Geologic map of the Glass Mountain quadrangle, Mono County, California, and Mineral County, Nevada: U.S. Geological Survey Geologic Quadrangle Map GQ-1099, scale 1:62,500.

McCormick, P.M., 1981, Lidar measurements of Mount St. Helens effluents: Proceedings of the International Society for Optical Engineering, v. 278, p. 19-22.

McElhinny, M.W., 1975, Palaeomagnetism and plate tectonics: Cambridge University Press, 358 p.

McKee, E.H., 1968, Age and rate of movement of the northern part of the Death Valley-Furnace Creek fault zone, California: Geological Society of America Bulletin, v. 79, p. 509-512.

McKee, E.H., and Nelson, C.A., 1967, Geologic map of the Soldier Pass quadrangle, California and Nevada: U.S. Geological Survey Geologic Quadrangle Map GQ-654, scale 1:62,500.

Metz, J.M., and Mahood, G.A., 1985, Precursors to the Bishop Tuff eruption: Glass Mountain, Long Valley, California: Journal of Geophysical Research, v. 90, no. B13, p. 11,121-11,126.

Miller, W.L., 1966, Petrology of the Putah Tuff Member of the Tehama Formation, Yolo and Solano Counties, California: University of California, Davis, M.S. thesis, 85 p.

Obradovich, J.D., Naeser, C.W., and Izett, G.A., 1978, Geochronology of late Neogene marine strata in California, *in* Correlation of tropical through high latitude marine Neogene deposits of the Pacific basin: IGCP Project 14, Stanford University, Calif., p. 40-41.

Putnam, W.C., 1962, Late Cenozoic geology of McGee Mountain, Mono County, California: California University Publications in Geological Sciences, v. 40, no. 3, p. 181-218.

Reheis, M.C., in press a, Geologic map of late Cenozoic deposits and faults in parts of the Soldier Pass and Magruder Mountain 15' quadrangles, Inyo and Mono Counties, California, and Esmeralda County, Nevada: U.S. Geological Survey Miscellaneous Investigations Map I-2268, scale 1:24,000.

Reheis, M.C., in press b, Geologic map of late Cenozoic deposits and faults in the western part of the Rhyolite Ridge 15' quadrangle, Esmeralda County, Nevada: U.S. Geological Survey Miscellaneous Investigations Map I-2183, scale 1:24,000.

Reheis, M.C., and McKee, E.H., 1991, Late Cenozoic history and slip rates of the Fish Lake Valley fault zone and surrounding areas of Nevada and California: U.S. Geological Survey Open-file Report 91-290, this volume.

Robinson, P.T., McKee, E.H., and Moiola, R.J., 1968, Cenozoic volcanism and sedimentation, Silver Peak region, western Nevada and adjacent California, in Coats, R.R., and others, eds., Studies in volcanology: Geological Society of America Memoir 116, p. 577-611.

Sarna-Wojcicki, A.M., 1976, Correlation of late Cenozoic tuffs in the central Coast Ranges of California by means of trace- and minor-element chemistry: U.S. Geological Survey Professional Paper 972, 30 p.

Sarna-Wojcicki, A.M., Champion, D.E., and Davis, J.O., 1983, Holocene volcanism in the conterminous United States and the role of silicic volcanic ash layers in correlation of latest-Pleistocene and Holocene deposits, *in* Wright, H.E., Jr., ed., Late Quaternary Environments of the United States, v. 2, The Holocene: University of Minnesota Press, Minneapolis, Minn., p. 52-77.

Sarna-Wojcicki, A.M., and nine others, 1984, Chemical analyses, correlations, and ages of upper Pliocene and Pleistocene ash layers of east-central and southern California: U.S. Geological Survey Professional Paper 1293, 40 p.

Sarna-Wojcicki, A.M., Lajoie, K.R., Meyer, C.E., Adam, D.P., and Rieck, H.J., in press, Tephrochronologic correlation of upper Neogene sediments along the Pacific margin, conterminous United States, in Morrison, R. B., ed., Quaternary non-glacial geology--Conterminous U.S.: Geological Society of America, Decade of North American Geology, v. K-2.

Sarna-Wojcicki, A.M., Morrison, S.D., Meyer, C.E., and Hillhouse, J.W., 1987, Correlation of upper Cenozoic tephra layers between sediments of the western United States and eastern Pacific Ocean, and comparison with biostratigraphic and magnetostratigraphic age data: Geological Society of America Bulletin, v. 98, p. 207-223.

AN EARLY PLEISTOCENE PLUVIAL LAKE IN FISH LAKE VALLEY, NEVADA-CALIFORNIA: RINGSIDE RESORT FOR THE ERUPTION OF THE BISHOP TUFF

Marith C. Reheis, Janet L. Slate, Andrei M. Sarna-Wojcicki, and Charles E. Meyer

ABSTRACT

The question of whether a pluvial lake existed in Fish Lake Valley, Nevada and California, has been debated for over 100 years. We have obtained stratigraphic evidence that a lake did exist in this valley at intervals during late Pliocene to middle Pleistocene time. This lake may have overflowed northward, or it may have been periodically contiguous with a pluvial lake to the north in Columbus Salt Marsh.

Proof of the existence of this lake, informally named Pluvial Lake Rennie, rests primarily on four outcrops of shallow-water lacustrine sediments, two outcrops of deep-water sediments, and drilling logs of sediments. The exposed and buried sediments contain beds of silicic tephra, which provide age control. Based on thickness, grain size, and major-oxide chemistry of glass shards, three of the shallow-water deposits consist mainly of tephra that was most likely derived from the 0.74-Ma eruption of the Bishop Tuff. These three deposits include deltaic, beach, and siliceous hot-spring sediments. One outcrop of beach sand is underlain by lacustrine (?) sediments believed to be about 1 Ma. The exposed deep-water sediments consist of green claystone, siltstone, and fine-grained sandstone containing tephra derived from the eruptions of the ~2.1-Ma tuff of Taylor Canyon and, provisionally, of the ~2.0-Ma Huckleberry Ridge Tuff. The drilling logs record numerous thick beds of clay and sandy clay, some containing beds interpreted to be volcanic ash; these clay beds are inferred to be deep-water lacustrine sediments.

From the outcrops and drilling logs, the history of Pluvial Lake Rennie is as follows: (1) At around 2 Ma, the lake was deep enough in its northeastern part that clay was deposited. The lake level in early Pleistocene time is not known, but a lake probably existed around 1 Ma. (2) At about 0.74 Ma, the lake had a high stand at an elevation of about 1440 m. The lake level must have dropped during or just after the eruption of the Bishop ash. (3) The lake may have persisted sporadically at a lower level until about 0.5 Ma, but no long-lived lake existed in Fish Lake Valley in late Pleistocene time. The late Pliocene and Pleistocene record of Pluvial Lake Rennie is reasonably parallel to that of Lake Tecopa, 200 km to the southeast.

INTRODUCTION

The existence of a pluvial lake in Fish Lake Valley, Nevada and California, and its relation to other nearby pluvial lakes such as Columbus Salt Marsh (fig. 1), have been topics of debate in Quaternary studies of the Great Basin for over a century. For example, Russell (1885) showed a very small pluvial lake confined to the valley; Hubbs and Miller (1948) proposed that a pluvial lake of uncertain size and age overflowed to Lake Lahontan; Mifflin and Wheat (1979) thought that there was no late Pleistocene lake, but that there may have been an early Pleistocene lake connected to Lake Lahontan. Most of the published studies included Fish Lake Valley in compilations of the pluvial lakes of large regions, and little work beyond interpretation of aerial photographs and limited field checking was done.

We have obtained stratigraphic evidence that substantiates the existence of a pluvial lake in Fish Lake Valley and that bears on its age during recent mapping of late Cenozoic deposits and faults of Fish Lake Valley (Reheis, in press a; J.L. Slate, thesis in progress). The purpose of this paper is to present the stratigraphic evidence for the existence

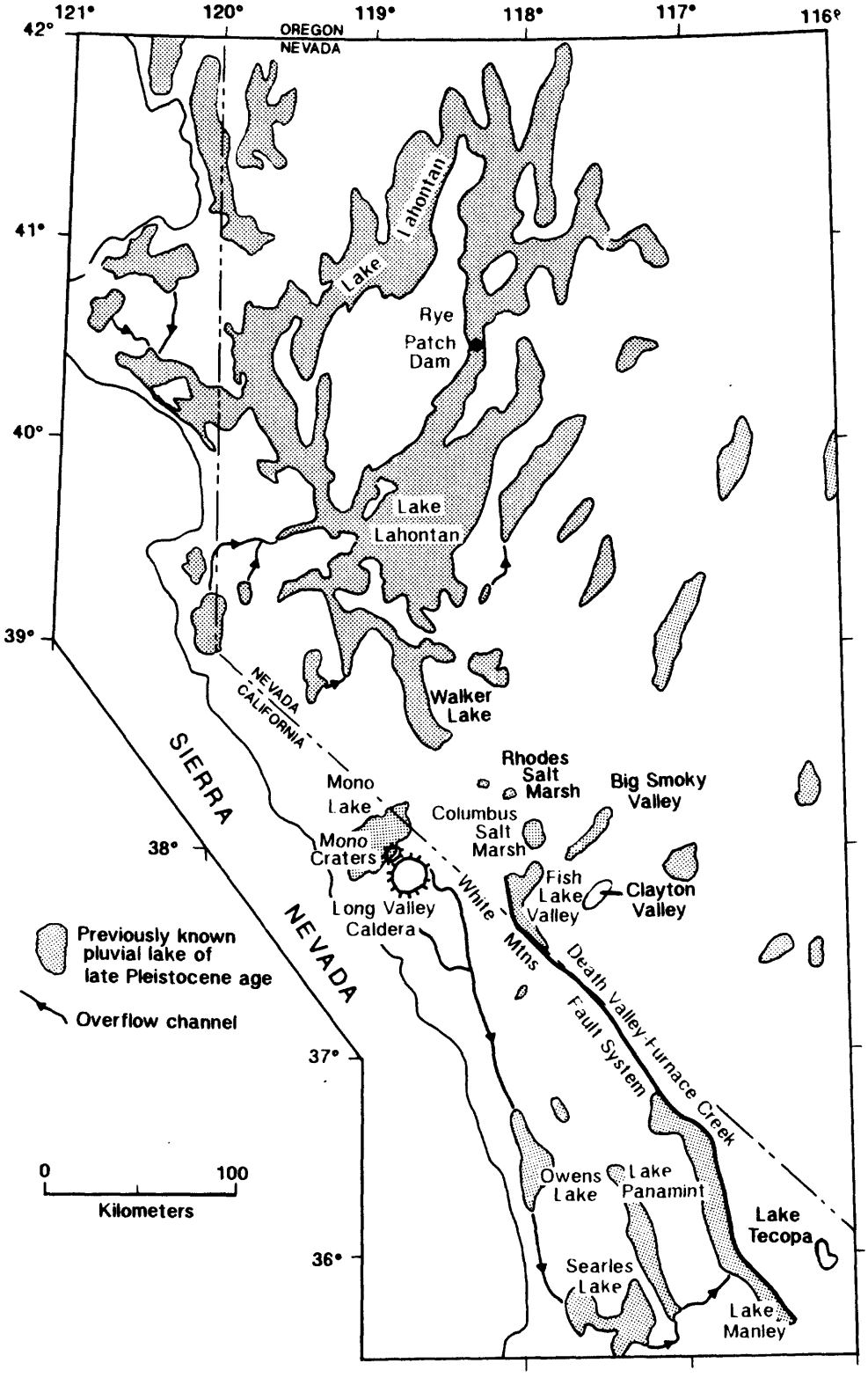

Figure 1. Regional location map showing selected late Pleistocene pluvial lakes and their connections in the western Great Basin, sources of silicic tephra in the Long Valley area, and the Death Valley-Furnace Creek fault system (modified from Morrison, 1965).

of this pluvial lake, to present tephrochronologic data on its age, and to infer its depth, its extent, and the nature of its connection to other lakes. We emphasize that some of the tephrochronologic correlations are preliminary, in particular the discrimination of the Bishop ash from the chemically similar Glass Mountain tephra layers. Other analyses that permit more confident identification of the Bishop ash are in progress.

We informally name this lake Pluvial Lake Rennie in honor of Douglas P. Rennie, who unstintingly gave his help and companionship in the field during 1987 and 1988 before his untimely death in a car accident. He must be excited to know where the early discoveries of mysteriously thick tephra layers in Fish Lake Valley have led us.

BACKGROUND AND METHODS

Geographic, Geologic, and Climatic Setting

Fish Lake Valley is a nearly closed basin about 70 km east of the Long Valley caldera and about 80 km east of the Mono Craters (fig. 1). The valley lies between the glaciated White Mountains (elevations as high as 4340 m) on the west and the lower, unglaciated Silver Peak Range on the east. Drainage from the valley is partly blocked on the north by the low Volcanic Hills (fig. 2), but overflows intermittently from the playa in the northeast corner northward through "The Gap" into Columbus Salt Marsh (Beaty, 1968).

Fish Lake Valley owes its existence and its remarkably well-exposed stratigraphy to right-oblique faulting along the Fish Lake Valley fault zone (Sawyer, 1990), which forms the northern end of the Death Valley-Furnace Creek fault system (fig. 1). Vertical offset along the faults that bound the east side of the White Mountains and the northwest side of the Silver Peak Range (fig. 2) expose coarse alluvial-fan and finer-grained sediments that blanket most of the valley floor and margins. These sediments are well preserved due to the arid climate of Fish Lake Valley, which lies in the rain shadow of the Sierra Nevada and the White Mountains. The sediments contain numerous beds of silicic volcanic tephra that were largely derived from the nearby Long Valley caldera and the Mono Glass Mountain area (fig. 1; Reheis, in press a,b). The tephra layers provide the chronologic framework for the alluvium and other sediments.

The magnitude and extent of glaciation in the White Mountains is a topic of debate. These mountains contained small valley glaciers of Tahoe and Tioga age (LaMarche, 1965; Elliott-Fisk, 1987). LaMarche (1965) suggested that the northern valleys of Indian and Chiatovich Creeks may have had glaciers extending to the range front in pre-Tahoe time. Elliott-Fisk (1987) defined the "Dyer Glaciation" of possible Sherwin age (>740 ka) based on "Glacial till...preserved as uplifted fans at canyon mouths..." of Perry Aiken and McAfee Creeks near Dyer (fig. 2). These deposits, however, are indistinguishable from alluvial-fan deposits elsewhere along the range (J.L. Slate, unpub. data).

Fish Lake Valley contains abundant groundwater, which is largely recharged by surface and subsurface flow from the White Mountains and discharged at springs and other areas of high water table in the northeastern part of the valley (fig. 2; Rush and Katzer, 1973). The only perennial standing water is Fish Lake, a spring-fed pond. Recharge to the valley sediments was probably greater during recent glaciations than at present, but little or no evidence supports surface flow northward into Columbus Salt Marsh during those times (discussed below).

Mean annual temperature on the valley floor is about 10.5 ^{o}C (National Climatic Data Center, 1986). Mean annual precipitation on the valley floor is about 12 cm, whereas on the White Mountain crest it is at least 40 cm (Rush and Katzer, 1973). Until now, little evidence was available regarding climatic conditions in the valley in Pleistocene time.

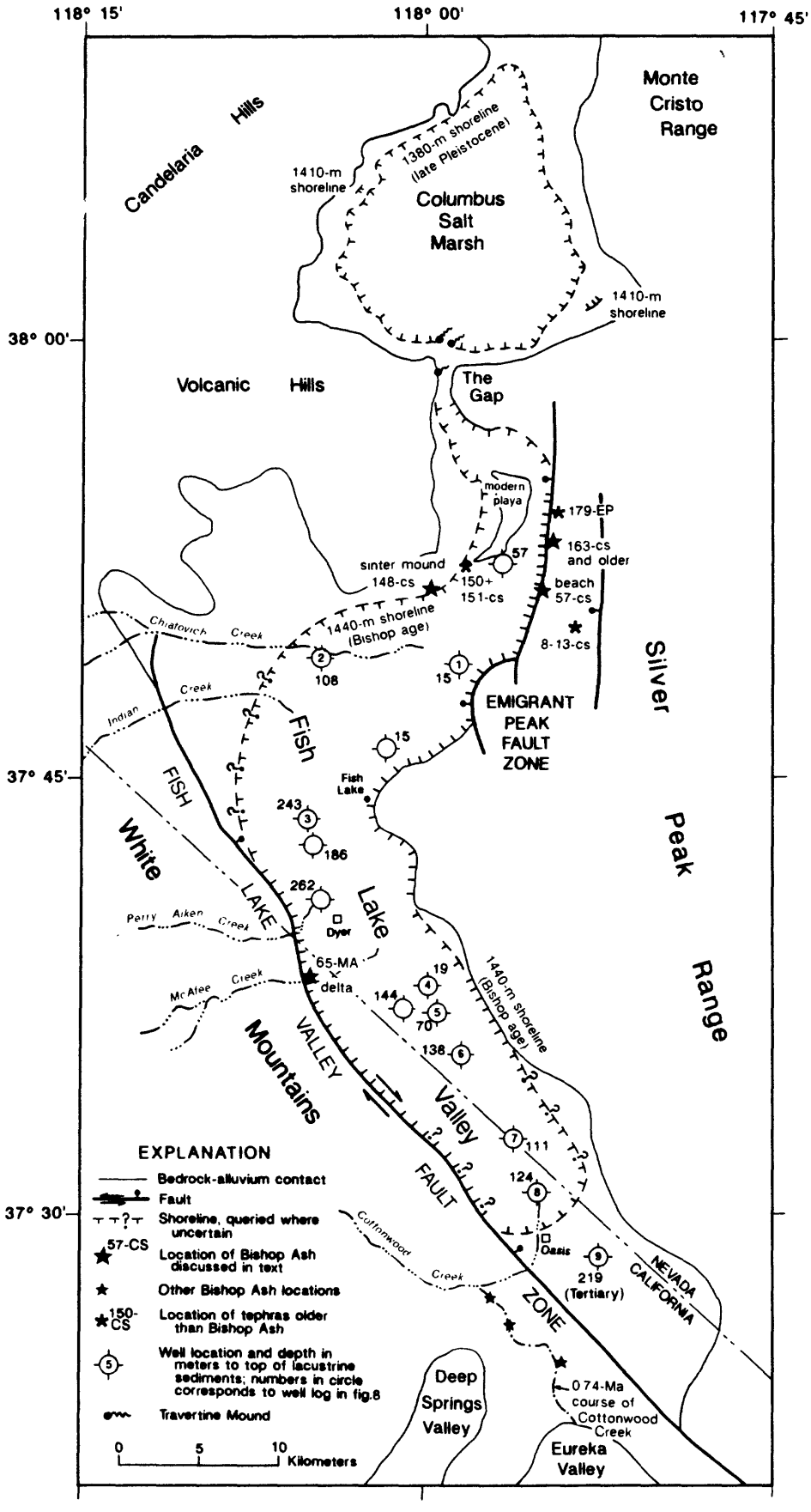

Figure 2. Sketch map of Fish Lake Valley and vicinity, showing locations discussed in text, selected well locations, and reconstructed pluvial-lake shorelines.

Packrat middens indicate a cooler late Pleistocene climate from the presence of juniper-shadscale woodland as late as 10,700 B.P. at the southern end of Fish Lake Valley, which is the present northern boundary of creosote bush (Spaulding, 1980). Mifflin and Wheat (1979) inferred a last-glacial climate for Nevada that was about 2.8°C lower in mean annual temperature and about 70% higher in precipitations than the modern climate. Clearly, these conditions were not sufficient to produce a large, long-lived, late Pleistocene lake in Fish Lake Valley, because it has no shorelines of this age (Mifflin and Wheat, 1979; this study). In late Pliocene and early Pleistocene time, however, the entire region may have been much wetter because the White Mountains (dePolo, 1989; Reheis and McKee, this volume) and to a lesser extent the Sierra Nevada (Huber, 1981) were lower in elevation, and the rain-shadow effect of these ranges was consequently weaker.

Previous Studies

Fish Lake Valley was identified as a site that might have had a pluvial lake as early as the late 1800's, and a connection between it and other pluvial lakes was suggested early in the 1900's. Russell (1885) and Meinzer (1922) mapped a small pluvial lake about the same size as the modern playa in northeastern Fish Lake Valley (fig. 2). Free (1914) proposed that a pluvial lake discharged northward through The Gap to a pluvial lake in Columbus Salt Marsh. Hubbs and Miller (1948) suggested that the pluvial lake may have had an early (pre-Lahontan, or pre-Illinoian; Morrison and Davis, 1984) or very temporary late Pleistocene pluvial connection to Lake Lahontan (fig. 1), based on the resemblance of a now-extinct fish (Siphateles sp.) in modern Fish Lake (fig. 2) to Lahontan fish. However, they discounted Free's (1914) suggestion of discharge through The Gap based on their observations of terraces.

Later in this century, the postulated lake grew in size. Snyder and others (1964), in a map of Pleistocene lakes of the Great Basin based on identification of shoreline features on aerial photographs and on limited field reconnaissance, showed a large (480 km^2) pluvial Fish Lake of unspecified age that overflowed northward into a pluvial lake in Columbus Salt Marsh. Late Pleistocene shorelines are prominent in Columbus Salt Marsh, but do not exist in Fish Lake Valley (Mifflin and Wheat, 1979; Reheis, in press a). We infer that their lake reconstruction in Fish Lake Valley was based on an incorrect identification of a curvilinear fault scarp east of the modern playa as a shoreline. This same inference was made by Mifflin and Wheat (1979, and M.D. Mifflin, oral commun., 1990), who omitted Fish Lake Valley from their detailed investigation of late Pleistocene pluvial lakes and pluvial climates of Nevada. These authors did, however, suggest that ancient Lake Lahontan may have extended as far south as Clayton Valley (fig. 1), including Fish Lake Valley, in pre-Lahontan time. They based their suggestion mainly on: (1) the presence of extensive evaporite deposits in valleys below 1500 m elevation that connect Clayton Valley with Walker Lake, the southernmost arm of Lake Lahontan in late Pleistocene time; and (2) the presence of lacustrine gravels at elevations well above that of the late Pleistocene Lahontan shoreline at Walker Lake.

Methods

Many beds of silicic volcanic tephra were found and sampled in the course of detailed mapping in the northern part of Fish Lake Valley. Of these, several were suspected to be ash derived from the eruption of the Bishop Tuff in the area of Long Valley, Calif. (fig. 1), based on the thickness and coarse grain size of the deposits. The stratigraphy and sedimentology of these outcrops of suspected Bishop ash, including measured sections at three well-exposed sites, were described.

Table 1. Electron-microprobe analyses of volcanic glass shards from middle Pleistocene and upper Pliocene tephra layers of Fish Lake Valley, California and Nevada, and comparative compositions of shards from near-source and distal tephra layers of the Long Valley--Mono Glass Mountain source area of California. Values given are in weight-percent oxide, recalculated to 100 percent fluid-free basis. Original oxide totals before recalculation are given to indicate approximate degree of hydration of volcanic glass. Approximately 15 individual glass shards were analyzed for each sample. [e] - glass shards of a sample are heterogenous with respect to this element. Homogeneity data are not available for some samples; these samples were analyzed with a MAC[1] three-channel electron microprobe. Other samples were analyzed with a nine-channel SEMQ[1] electron-microprobe. Multiple analyses of a homogenous natural glass standard, RLS 132, are given below (39) and provide a close estimate of the analytical error for each oxide in electron-probe analysis. Comparative values based on wet-chemical analysis of the same sample are also given (40). C. E. Meyer, U.S.G.S., Menlo Park, electron-probe analyst.

Sample	SiO_2	Al_2O_3	Fe_2O_3	MgO	MnO	CaO	TiO_2	Na_2O	K_2O	Total
Thick, coarse, water-deposited tephra in fan alluvium (1, 2), and thick, reworked ash and tuff in nearshore sands of Pluvial Lake Rennie (3-6); sample 6, hydrothermally altered and leached ash from sinter mound (see text); Bishop ash from Gilbert Summit, CA (7)										
1. FLV-65-MA	77.6	13.0	0.70	0.02	0.02	0.43	0.06	3.7	4.5[e]	92.6
2. FLV-66-MA	77.7	12.7	0.75	0.02	0.04	0.43	0.07	3.8	4.5[e]	94.1
3. FLV-57-CS	77.6	12.7	0.69	0.02	0.04	0.44	0.07	3.7	5.0	93.3
4. FLV-163-CS	77.6	12.9	0.79	0.02	0.05	0.41	0.06	3.5	4.8	93.4
5. FLV-148A-CS	77.8	12.6	0.72	0.03	0.03	0.43	0.07	3.7	4.7	94.9
6. FLV-148-CS	77.5	13.8[e]	0.43[e]	0.11[e]	0.00	0.51[e]	0.05	3.5[e]	4.2[e]	88.0
7. FLV-4-WP	77.9	12.5	0.74	0.05	0.04	0.44	0.06	3.7	4.5[e]	94.0
Mean (1-5, 7):	77.7	12.7	0.72	0.03	0.03	0.43	0.07	3.7	4.6	93.8
± standard dev.:	0.1	0.2	0.03	0.01	0.01	0.01	0.01	0.05	0.2	0.9
Proximal Bishop airfall ash bed at south end of tableland, southeast of Long Valley Caldera, north of Bishop, CA, at Owens River (8, 9), and at Insulating Aggregates Quarry (10); distal Bishop ash bed from Lake Tecopa, CA (11), Arches National Park, Utah (12), and Onion Creek, Utah (13)										
8. BT-11A1	77.6	12.7	0.69	0.03	0.04	0.43	0.06	3.7	4.8	94.4
9. BT-11C1	77.7	12.6	0.72	0.03	0.04	0.42	0.06	3.7	4.8	93.9
10. BT-8	77.8	12.5	0.73	0.03	0.05	0.44	0.05	3.8	4.7	94.3
11. TECO-28B	77.0	12.9	0.75	0.04	0.03	0.43	0.06	3.8	5.0	93.9
12. ARCH-88-1	77.4	12.7	0.74	0.04	0.03	0.43	0.07	4.2	4.4	92.2
13. 66W5	77.6	12.7	0.74	0.03	0.05	0.45	0.07	3.9	4.4	93.1
Mean (8-13):	77.5	12.7	0.73	0.03	0.04	0.43	0.06	3.8	4.7	93.6
± standard dev.:	0.3	0.1	0.02	0.01	0.01	0.01	0.01	0.2	0.2	0.9
Finer, thinner-bedded tephra layers at locality FLV-163-CS, stratigraphically below coarse beach sand of samples 3 and 4, above										
14. FLV-162-CS	77.4	12.9	0.77	0.03	0.07	0.46	0.07	3.4	5.0	93.5
15. FLV-161-CS	77.5	12.8	0.71	0.03	0.06	0.45	0.06	3.5	5.0	94.0
16. FLV-160-CS	77.4	12.8	0.73	0.01	0.06	0.50	0.07	3.5	4.9	93.8
17. FLV-147-CS	76.8	12.6	0.71	0.04	0.05	0.45	0.03	3.2	6.2	93.7
Glass Mountain D (18; ca. 0.9 Ma) and G (19, 20, 22, ca. 1.0 Ma) ash beds, stratigraphically below airfall Bishop ash bed at locality of samples 8, 9 above										
18. BT-2	78.0	12.3	0.71	0.03	0.05	0.41	0.06	3.5	5.0	95.4
19. BT-1	77.3	12.9	0.80	0.03	0.03	0.43	0.05	3.9	4.6	94.6
20. BT-1C	77.8	12.7	0.77	0.03	0.05	0.42	0.06	3.5	4.6	94.6
Volcanic ash beds in upper Pliocene alluvial-fan gravels underlying fan alluvium containing sample 3, 4, and 14 -17 (above) in northeastern Fish Lake Valley (21-28)										
21. FLV-8-CS	77.8	12.4	0.58	0.05	0.11	0.31	0.06	3.8[e]	5.0[e]	94.1
22. FLV-9-CS	77.4	12.3	0.56	0.05	0.10	0.32	0.06	2.8[e]	6.5[e]	93.7
23. FLV-10-CS	77.1[e]	12.6	0.57	0.05	0.08	0.34	0.07	2.8[e]	6.4[e]	94.3
24. FLV-11-CS	77.1[e]	12.7	0.57	0.05	0.09	0.34	0.07	2.8[e]	6.4[e]	93.7
25. FLV-12-CS	77.2	12.8	0.60	0.04	0.09	0.33	0.05	3.2[e]	5.8[e]	94.4
26. FLV-13-CS	77.5	12.8	0.60	0.04	0.08	0.33	0.04	3.9[e]	4.8[e]	95.2
27. FLV-150-CS	77.3	12.7	0.61	0.03	0.09	0.34	0.05	4.0[e]	5.0[e]	94.9
28. FLV-151-CS	77.3	12.7	0.60	0.04	0.09	0.34	0.05	4.1[e]	4.7[e]	95.2
Mean (21-28):	77.3	12.6	0.59	0.04	0.09	0.33	0.06	3.4	5.6	94.4
±standard dev.:	0.2	0.2	0.02	0.01	0.01	0.01	0.01	0.6	0.8	0.6
Proximal Tuff of Taylor Canyon, near Mono Glass Mountain (29-32; ca. 1.9-2.1 Ma); distal Waucoba ash beds (33, 34) in Owens Valley, east of Big Pine, CA., and distal ash (35) stratigraphically below Huckleberry Ridge ash bed (ca. 2.0 Ma) in Pico Fm., Ventura, southwestern CA.										
29. TTC-6	77.2	12.9	0.58	0.05	0.09	0.33	0.09	4.1	4.6[e]	94.6
30. TTC-9A	77.6	12.7	0.58	0.04	0.10	0.34	0.07	3.7	4.9[e]	93.2
31. TTC-18	77.9	12.5	0.59	0.05	0.10	0.35	0.07	3.5	5.1[e]	93.7
32. TTC-19	77.5	12.6	0.59	0.05	0.07	0.33	0.06	3.9	4.9[e]	93.2
33. WAC-6	77.2	12.7	0.60	0.04	0.06	0.34	0.09	4.0	4.9	95.2
34. W2A	77.4	12.5	0.60	0.03	0.08	0.34	0.08	3.3	5.7	93.0
35. P-169Q	77.6	12.6	0.58	0.04	0.10	0.33	0.06	3.9	4.9	92.8
Average (29-35):	77.5	12.6	0.59	0.04	0.09	0.34	0.07	3.7	5.0	93.7
± standard dev.:	0.2	0.2	0.01	0.01	0.02	0.01	0.01	0.3	0.3	0.9

Table 1 (continued)

Sample	SiO_2	Al_2O_3	Fe_2O_3	MgO	MnO	CaO	TiO_2	Na_2O	K_2O	Total
Fine-grained, bluish-gray, 0.5-m-thick tephra layer (36) in tuffaceous lake beds stratigraphically below dissected fan alluvium containing samples 3, 4 and 14 - 17 (above); Huckleberry Ridge ash bed in lake beds of Pleistocene Lake Tecopa (37) and in Pico Fm., Ventura County, CA (38)										
36. FLV-179-EP	76.61	12.14	1.72	0.01	0.04	0.59	0.11	2.8	6.0	93.86
37. TECO-12B	76.30	12.36	1.75	0.03	0.05	0.61	0.14	3.5	5.3	94.86
38. PICO-157	76.61	12.25	1.73	0.03	0.04	0.59	0.13	3.7	4.9	94.64
39. RLS 132 (Av. 18)	75.4	11.3	2.12[2]	0.06	0.16	0.11	0.19	4.9	4.4	98.6
standard dev.:	0.1	0.2	0.04	0.01	0.01	0.01	0.01	0.1	0.1	
percent st.d.:	0.2	1.4	1.9	17	6.3	9	5.3	2.7	1.4	
40. RLS 132 (wet chemical	75.7	11.4	2.12[2]	0.05	0.15	0.12	0.21	5.3	4.5	99.6

[1]Use of trade names by the U.S. Geological Survey does not represent an endorsement of the product.
[2]Iron reported as FeO for the standard.

Table 2. Comparison of the average of volcanic glass shard compositions of five unaltered samples of the Bishop ash bed in Fish Lake Valley (1) with the glass shard compositions of a hydrothermally altered sample, FLV-148-CS (2). Note that the original analyzed values are given below, not values normalized to 100 percent, in order to estimate the amounts of elements lost or gained in the altered sample during alteration. A-U - difference for each oxide between the altered and average of the unaltered samples. %A-U - the percentage difference between the altered and average of the unaltered samples. Other comments as in Table 1.

Sample	SiO_2	Al_2O_3	Fe_2O_3	MgO	MnO	CaO	TiO_2	Na_2O	K_2O	Total
1. Bishop ash bed	72.9	11.9	0.67	0.03	0.03	0.41	0.06	3.5	4.4	93.8
2. FLV-148-CS	68.1	12.1	0.38	0.10	0.00	0.45	0.04	3.1	3.7	88.0
A-U	-4.8	+0.2	-0.29	+0.07	-0.03	+0.04	-0.02	-0.4	-0.7	-5.9
%A-U	-6.5	+2	-43	+233	-100	+10	-33	-12	-16	

Tephra samples were examined under the petrographic microscope. Glass shards of samples that contained glass were separated from other components and analyzed by electron microprobe for major-oxide composition (tables 1 and 2) using methods described by Sarna-Wojcicki and others (1984). Sample compositions were compared against compositions in a data base of previously analyzed tephra layers using numerical programs, and the best matches were identified. Correlations were made on the basis of similarity in chemical composition, petrographic characteristics (for example, shard morphology, mineralogy; data not shown), and other stratigraphic and numerical-age data.

Values for glass compositions in Table 1 are normalized to 100 percent to correct for the variable amounts of hydration of the volcanic glass. Original totals, all significantly lower than 100 percent, are approximate guides to the degree of hydration of each sample. In addition to hydration, some post-depositional alkali exchange has occurred in many of the samples. Variability in sodium and potassium contents are particularly apparent for the older tephra layers, those correlative with the tuff of Taylor Canyon (table 1). One sample (FLV-148-CS), collected from a sinter mound where the pluvial shoreline deposits are particularly well preserved by silica and carbonate cementation, has been hydrothermally altered (Table 2).

Samples from the cemented strata of the sinter mound were examined in thin section. These samples were also ground and analyzed in powder mounts for whole-rock mineralogy by X-ray diffraction.

Over 100 driller's logs of irrigation and domestic wells deeper than 60 m in Fish Lake Valley were examined for evidence of lacustrine sediments. The sedimentology in these logs was plotted with depth and compared to more detailed logs of boreholes drilled in the area south of the modern playa during lithium investigations by the U.S. Geological Survey (fig. 2; Pantea and others, 1981).

EVIDENCE FOR AN EARLY PLEISTOCENE LAKE

The geologic evidence supporting an early Pleistocene lake in Fish Lake Valley derives from five outcrops, three of which represent deposition in shallow water and two in deeper water, and on sediments reported in water-well logs and cores. The five areas of outcrop are described in order from south to north, followed by description of the nature of the overflow or connecting channel.

The Delta at McAfee Creek

A dissected remnant of alluvial-fan gravel overlies, is channeled into, and is interbedded with, a thick (>30 m) deposit of fluvially deposited tephra on the north side of the mouth of McAfee Creek (figs. 2 and 3; map of area is in fig. 3, road log, this volume). The tephra and overlying gravel are in fault contact on the west with bedrock along an inactive strand of the Fish Lake Valley fault zone. A second inactive group of small faults cuts the tephra deposit but dies out in the overlying gravel in the area where the gravel channels most deeply into the tephra (fig. 3); hence, these faults were active during deposition of the tephra. A third fault, the presently active strand, bounds the tephra deposit and overlying gravel on the east.

Stratigraphy and sedimentology

A 71-m-thick section of gravel and tephra, divided into six subsections based on composition and bedding (fig. 3), was measured in the middle of the exposure on the north side of McAfee Creek. West of the measured section, the sediments consist mainly of tephra; east of the section, the sediments are chiefly coarse gravel. Gravel in most of the section consists mainly of granodiorite and quartz monzonite, whereas gravel in the uppermost 11 m consists mainly of dolomite, marble, and limestone. Normal faults with offsets ranging from 0.5 to 2 m are well exposed in the lower 35 m of the section but were not observed in higher beds.

The base of the measured section consists of at least 6.4 m (base not exposed) of nearly pure tephra, with pumice clasts 1-3 cm long, reworked into beds ranging from 10-30 cm thick. Above the tephra beds is 9.8 m of interbedded tephra and gravel with beds ranging from 10 cm to 2 m thick. Gravel beds are fairly well sorted and clast-supported. Rip-up clasts of pebbles and cobbles in a mud matrix are interbedded with tephra and gravel at the base, and crossbedded layers of tephra and gravel are scoured into massive beds of tephra near the top of this subsection.

The base of the subsection containing foreset tephra beds is marked by an abrupt, smooth contact at the base of a poorly sorted, matrix-supported deposit containing pebble- to boulder-size clasts. Two erosional scarps about 0.5 and 1.5 m high in this deposit are overlain by a total of 3.5 m of steeply dipping (N75^{o}E at 38^{o}SE) tephra beds that are truncated at the top by 70 cm of planar-bedded tephra. Such a configuration is typical of deltaic deposits of pluvial lakes elsewhere in the Basin and Range province

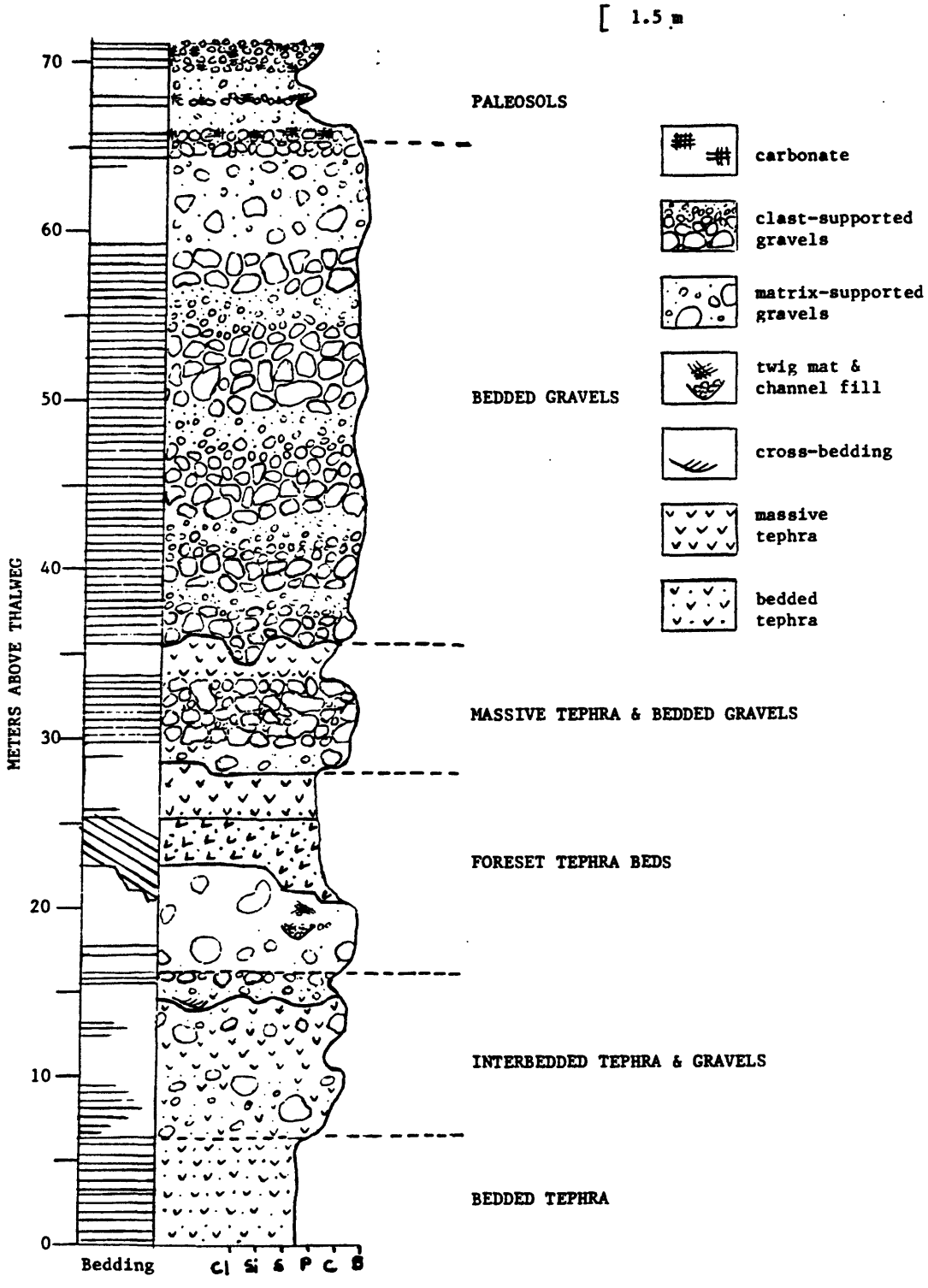

Figure 3. Stratigraphic section of deltaic and alluvial-fan deposits at the mouth of McAfee Creek (fig. 2), measured by Abney level and tape. Horizontal scale indicates range of clast size within a given bed (cl, clay; si, silt; s, sand; p, pebble; c, cobble; b, boulder).

(Russell, 1885; Gilbert, 1890). A poorly bedded, matrix-supported deposit containing cobbles and boulders overlies the topset and foreset tephra beds, and cuts off the tephra beds on the down-dip end.

The topset beds grade upward into massive tephra that is overlain and channeled into by matrix-supported and clast-supported gravel; this section is cut by at least four faults that do not penetrate the overlying 30-m-thick section of poorly bedded, mostly clast-supported, cobble-to-boulder gravel.

The uppermost 6 m of the section contains two buried soils and a stripped relict soil. The soils are marked by prominent carbonate-cemented horizons; horizons between these carbonate-rich horizons are poorly exposed but appear slightly reddened. The lowest buried soil is formed in poorly sorted gravel of granodiorite and quartz monzonite, whereas the upper buried soil and the surface relict soil are formed in fairly well-sorted gravel of carbonate rocks.

Dating

The major-oxide composition of glass from the tephra deposit at McAfee Creek (FLV-65- and 66-MA, table 1) matches with other Bishop ash samples (0.74 Ma; Izett and others, 1970, 1988), although correlation with older rhyolitic ashes from Glass Mountain (0.9-1.0 Ma; Sarna-Wojcicki and others, 1984; Izett and others, 1988), on the northeast rim of the Long Valley caldera (fig. 1), is not precluded. However, the great thickness (>30 m) and coarse grain size (pumice clasts as much as 7 cm long) of the tephra deposit favor a Bishop correlation, for the Bishop eruption was far larger volumetrically than those at Glass Mountain (Bailey and others, 1976). In comparison, maximum pumice clasts from the large eruption of Mount Mazama ash from Crater Lake, about 6,850 yrs B.P., at a comparable distance of 60 to 70 km from the source, are 4.5 to 6 cm in diameter (Fisher, 1964).

Interpretation

Based on the thickness, grain size, sorting, and locally steep bedding of the tephra deposit, we infer that it was deposited as a delta of McAfee Creek at the margin of a pluvial lake. Although the tephra deposit is reworked, its thickness and purity suggest that deposition occurred close to or at the time of the ash eruption. The major-oxide chemistry, coarse grain size, and thickness of the deposit suggest that this tephra is most likely the Bishop ash. This tephra deposit was first described, but not identified, by Elliott-Fisk (1987) as underlying "glacial outwash and till" correlated with the Sherwin Till of the eastern Sierra Nevada. Based on sorting and stratification, however, this gravel consists of alluvial-fan deposits like those elsewhere along the White Mountains (J.L. Slate, unpub. data). Nor can the gravel be correlative with outwash of Sherwin age, because Sherwin till underlies the Bishop Tuff at the type locality (Sharp, 1968). There is, however, a younger till that overlies the Bishop Tuff at Reds Meadow and at other sites near the Long Valley Caldera (Huber and Rinehart, 1967; Sarna-Wojcicki and others, 1984).

Beach Sands Along the Emigrant Peak Fault Zone

Normal faults that bound and lie west of the northern Silver Peak Range (fig. 2) expose a thick (at least 400 m) sequence of alluvial-fan gravel, derived from the Silver Peak Range, that locally contains interbeds of well-sorted sand and fine gravel in exposures along the westernmost fault (Reheis, in press a). The basal deposits are moderately indurated and cemented with carbonate, but the upper deposits are only slightly indurated. As a result, exposures are poor because lag gravel from the upper deposits blankets most slopes.

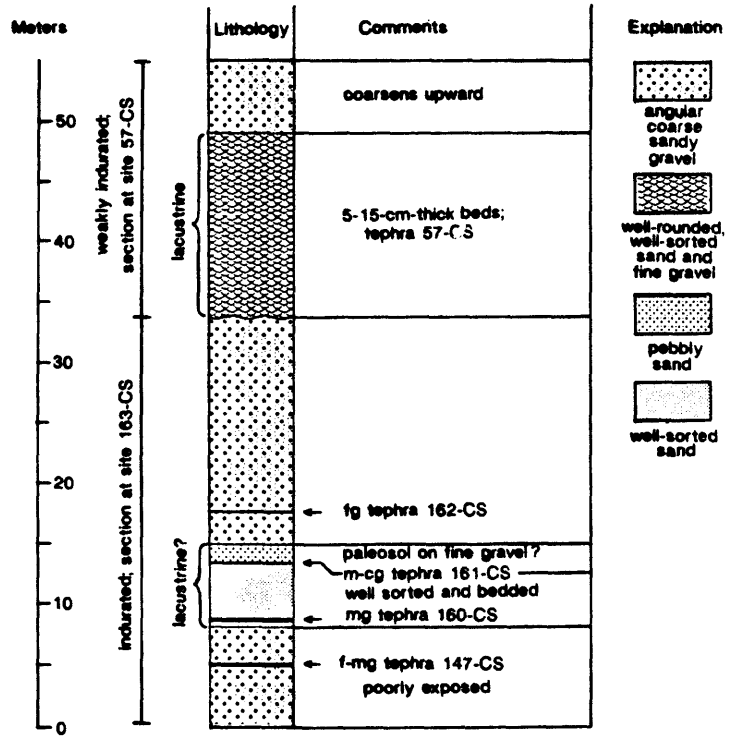

Figure 4. Composite stratigraphic section of beach and alluvial-fan deposits at sites 57-CS and 163-CS (fig. 2), measured using a Brunton compass.

Stratigraphy and sedimentology

At site 57-CS (fig. 2), hand-dug excavations revealed a stratum of loose, well-rounded sand and fine gravel about 15 m thick (fig. 4). This sandy unit lies in sharp contact above indurated, very gravelly, angular, cobble-sized fan gravel and is interbedded upward with moderately sorted, angular to subangular, granule- to cobble-sized fan gravel in a matrix of sand and silt. The sandy unit consists mainly of glass and pumice with grains of volcanic and sedimentary rocks like those in the fan gravel; the lithic grains are few at the base of the unit and increase upward. The sandy unit consists of alternating layers, 5-15 cm thick, of well-sorted, crossbedded, lenticular, medium to coarse sand and coarse sand to fine gravel. Pumice clasts up to 0.5 cm long are better rounded than the lithic grains. Crossbedding within the individual layers is flat to gently dipping and the layers have thin laminae of heavier lithic grains alternating with laminae of lighter pumice and glass; such laminations are characteristic of beach sands (Pettijohn and others, 1973).

Dating

The major-oxide composition of glass from near the base of the sandy unit (FLV-57-CS, table 1) is most like that of the Bishop ash, although it is also similar to the older ashes from Glass Mountain. Based on the size of pumice clasts and the thickness of the sandy unit, the unit was most likely deposited during and shortly following the Bishop eruption, which was much larger than eruptions from the Glass Mountain area. Pumice clasts are not as large as those in the deltaic deposit at McAfee Creek, but the sandy unit southeast of the playa was deposited in a lower-energy environment and lies 25 km farther from Long Valley.

Stratigraphic relations (fig. 4; discussed below) with probable ~1-Ma Glass Mountain tephra beds in underlying dissected fan deposits, which are in turn underlain by tephra beds of the tuff of Taylor Canyon and, provisionally, the Huckleberry Ridge Tuff

Ma) in lacustrine deposits, support the identification of the tephra at site 57-CS as the Bishop ash.

Interpretation

From the grain size, sorting, and roundness of the grains and the nature of bedding and stratification, we believe that the sandy unit represents deposition in shallow water at the shoreline of a lake (Reheis, in press a). The sharp lower contact of the sandy unit with fan gravel suggests either (1) an abrupt change in lake level at or just before the eruption of the Bishop Tuff, or (2) a motion on one of the strands of the Emigrant Peak fault zone east of the outcrop (fig. 2) at about the time of the ash eruption that dropped the former fan surface below lake level. In either case, the lake level must have dropped shortly after the eruption, because the sandy unit is buried by as much as 50 m of fan gravel.

Older deposits nearby

West and north of site 57-CS, the elevation of the pumiceous beach sand rises from about 1500 m to about 1560 m (Reheis, in press a) due to tectonic tilting. At site 163-CS, about 50 m of deposits are exposed below the beach sand (fig. 4), including 10 m of loose sandy fan gravel underlying the beach sand. Below this gravel the sediments are indurated, suggesting either an unconformity at the base of the loose gravel, or cementation due to submergence beneath the Bishop-age lake. The major-oxide chemistry of sample FLV-163-CS is similar to that of the Bishop and Glass Mountain ash beds (table 1), and the layer from which this tephra was sampled can be traced almost continuously from site 163-CS to site 57-CS.

The indurated sediments that lie below the pumiceous, loose sandy unit at site 163-CS contain four lenticular tephra beds (FLV-147-, 160-, 161- and 162-CS, table 1). Two of these beds (FLV-160- and 161-CS), finer-grained than the tephra in the sandy unit, bracket a fine- to medium-grained, well-sorted, pumiceous sandstone about 5 m thick (fig. 4). The major-oxide chemistry of the four tephra beds is similar to that of glass from the Bishop and Glass Mountain eruptions (table 1). We currently think that these beds are correlative with tephra of Glass Mountain (0.9-1.0 Ma; Izett, 1981; Sarna-Wojcicki and others, 1984; Metz and Mahood, 1985; Izett and others, 1988) because they underlie the loose sandy unit believed to be of Bishop age, and because they are in turn underlain by lacustrine deposits containing ~2-Ma tephra correlated to the tuff of Taylor Canyon and, provisionally, the Huckleberry Ridge Tuff (discussed below). Hence, the pumiceous sandstone in the indurated sediments may represent deposition by a lake at about 1 Ma.

The Sinter Mound

Half-buried under gently sloping late Pleistocene and Holocene fan gravel southwest of the playa (fig. 2) is a small (<0.5 km^2) apron-shaped outcrop of rock mapped as Tertiary sedimentary rocks by Robinson and others (1976) and as Quaternary/Tertiary tuffaceous sandstone and siltstone and freshwater limestone by Robinson and Crowder (1973). The outcrop extends from about 1425 to 1443 m in elevation, and appears to be cut on the southeast by a low fault scarp (Reheis, in press a); the height of this scarp is about 5 m. The fault may be active, for springs occur along it and a 1-m-high scarp offsets Holocene (?) deposits about 2 km southwest of the outcrop along the fault. However, the fault appears to have had relatively little cumulative vertical offset in Pleistocene time.

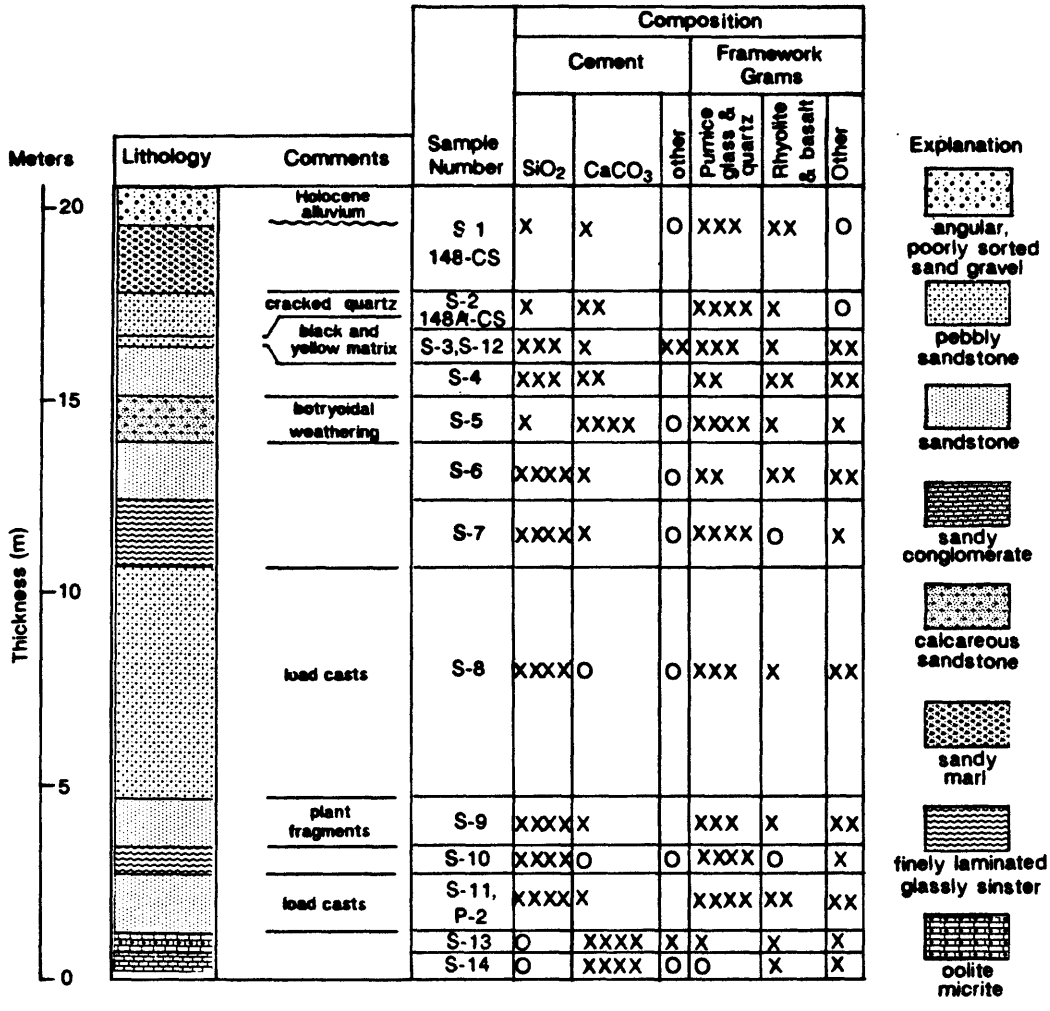

Figure 5. Stratigraphic section at sinter mound, measured by Abney level and tape (fig. 2). Relative abundances of cement and framework grains are visually estimated from hand samples, thin sections, and XRD data: 0, absent; X, minor; XX, common; XXX, abundant; XXXX, dominant. S-, rock sample; 148-CS, tephra sample; P-, paleomagnetic sample.

Stratigraphy and sedimentology

The outcrop consists mainly of interbedded sandstone, amorphous and opaline silica, and minor conglomerate (fig. 5). The beds are well sorted and stratified but thin (0.3-2 m) and very lenticular; individual beds cannot be traced across the outcrop. At the base of the outcrop, oolite micrite and weakly indurated marl are locally exposed. The rocks grade southwest along the fault into weakly to moderately indurated sandy travertine and calcareous sand around active springs.

Sandstone beds are fine- to medium-grained, thinly bedded, and pumiceous (Reheis, in press a). Their glass and pumice content increases upward at the expense of locally derived lithic grains of rhyolite, basalt, quartz, feldspar, and minor amounts of other minerals. The sand grains are subangular to subrounded and cemented by light-gray opaque silica and some carbonate. Plant fragments, including root casts, are observed in

some samples, and load casts are common in some beds. Near the top of the outcrop, the pumiceous sandstone is in part cemented by black and yellow microcrystalline minerals.

Silica deposits are finely laminated, but the laminations are highly irregular in detail, and consist of light-gray, amorphous to opaline silica that breaks conchoidally. The siliceous beds contain abundant fine- to medium-grained, subangular to subrounded, volcanic glass shards and pumice grains.

The uppermost part of the outcrop is silica- and carbonate-cemented, poorly sorted sandy conglomerate consisting of granule- to pebble-size subangular pumice clasts, large sand-size grains of cracked euhedral quartz, and smaller bubble-wall glass shards, admixed with subangular to subrounded rhyolite and basalt clasts derived from the Volcanic Hills to the north (fig. 2). Throughout most of the outcrop, the pumice grains have flattened vesicles. In the upper part, however, the pumice grains have open round vesicles partly filled with secondary carbonate.

Microscopic and XRD examination of secondary minerals

Thin sections and x-ray diffraction data (fig. 6) indicate that the dominant cementing agent throughout the section is silica, but carbonate is locally dominant, and minor amounts of other secondary minerals occur in some beds. A sharp-crested but broad peak centered at 22^{o} 2O is considered characteristic of opal-CT (Jones and Segnit, 1971) and occurs in most of the XRD traces (fig. 6). The less crystalline form, opal-A, is probably also present. Thin sections show some small areas of chalcedony. In the uppermost beds, some quartz grains have been dissolved, but this process appears to have been minor and could not have provided the amount of secondary silica present in the lower beds. In samples where opaline cement dominates, small amounts of carbonate appear to have precipitated in void spaces following cementation by opal, but in other samples, carbonate cement dominates and apparently preceded opal cementation. Small rosette-like crystals that are seen rarely in thin section may be alunite.

Tephra sample FLV-148-CS is from the uppermost pumiceous layer (fig. 5). Based on major-oxide composition of the glass, this sample appears to have been hydrothermally altered (table 2). Sample FLV-148A-CS, also from the upper part of the sinter mound, has a composition like that of the Bishop ash (table 1). If the altered sample had an initial composition like that of the average of five unaltered samples of probable Bishop ash from Fish Lake Valley, then the net total deficit of oxides leached from the altered sample is 5.86 percent by weight (table 2). The remaining 6 percent deficit from 100 percent represents the approximate amount of gas and water of hydration present in the glass, plus very small amounts of several oxides and anions that were not analyzed by the electron microprobe (F, P, S, Cl, Rb_2O, SrO, ZrO_2, and BaO; 0.5 percent or less). Note that all of the manganese has been leached from the altered sample, as well as significant amounts of silica, iron, sodium, and potassium. Conversely, magnesium and calcium are considerably enriched, probably from reaction of the glass with hot water that contained these elements.

Just below the uppermost layers, a black, opaque, botryoidal mineral is interlayered with opal. Based on its appearance and XRD character, it is probably a form of pyrolusite. A yellowish microcrystalline mineral is laterally associated with the pyrolusite along the outcrop, but has not yet been identified. The layer containing these black and yellow secondary minerals underlies the layer from which the leached sample of ash was collected (fig. 5).

At the base of the outcrop, calcareous marl and oolitic rocks are locally exposed (fig. 5). Thin sections and XRD analyses (fig. 6) of the oolitic rocks indicate that most of the oolites have cores of micrite, but some have cores of micrite-cemented sand-size grains of quartz, feldspar, glass, and (or) lithics. These cores were probably derived from the micritic marl, which contains many non-carbonate grains. The concentric layers of the

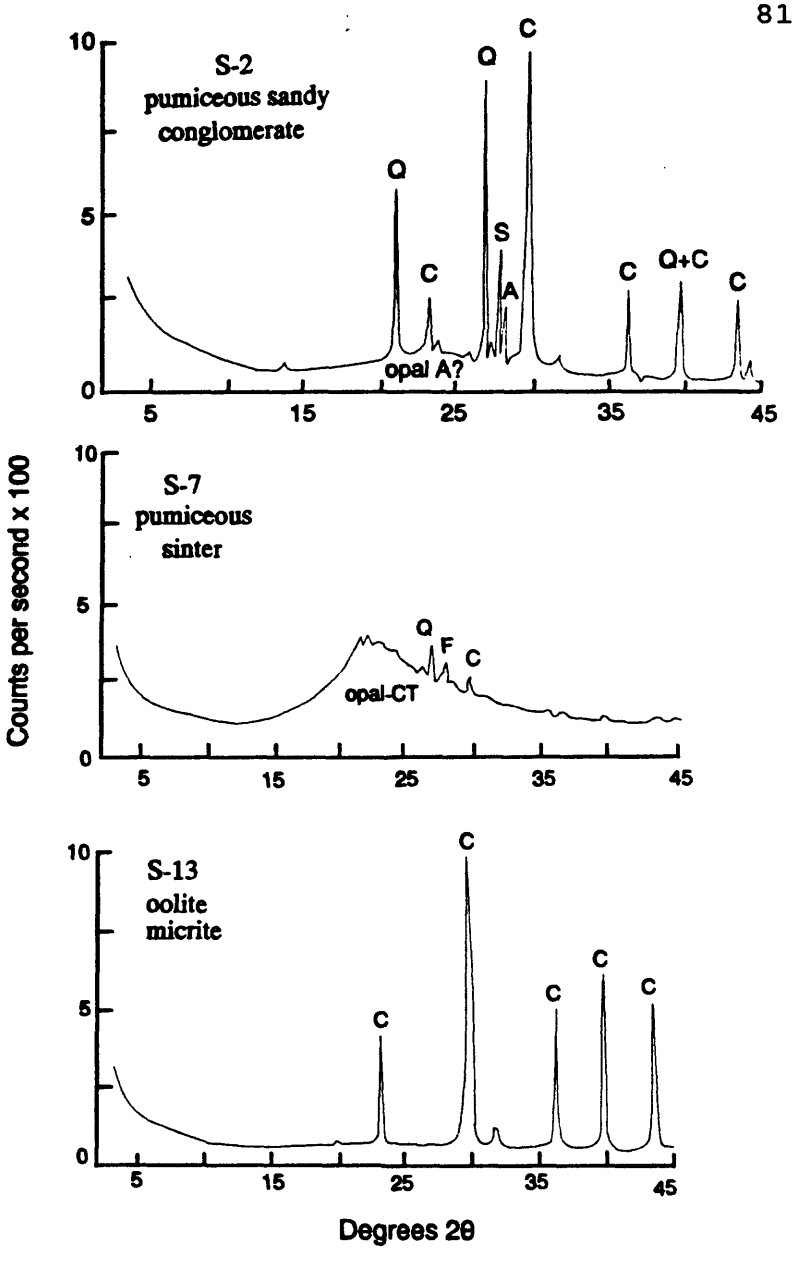

Figure 6. Representative XRD traces of rocks (powder mounts) from sinter mound (figs. 2 and 5). Opal identification follows Jones and Segnit (1971). Q, quartz; C, calcite; F, feldspar; S, sanidine; A, high-temperature albite.

ooids consist of alternating light and dark bands, mostly micrite but locally microsparite. Voids are commonly lined with micrite layers, but some contain a late-phase authigenic mineral that may be alunite.

Dating

Two samples were analyzed for major oxides of the volcanic glass (table 1). Sample FLV-148-CS is from the uppermost bed (fig. 5) where the pumice clasts are largest. The major-oxide composition of this sample matched no known widespread tephra layers in the western United States. As discussed above, the upper layers of the outcrop have been hydrothermally altered (table 2). Sample FLV-148A-CS is from layer S-2 of the outcrop (fig. 5). The major-oxide composition of this sample is a good match for that of the Bishop ash, but it is also close to that of the Glass Mountain D ash bed. The size of the pumice clasts (up to 2 cm in diameter) in the uppermost bed favors, but does not prove, a correlation to the Bishop ash.

In summary, we believe that the pumice and bubble-wall shards were derived from the Bishop eruption. It is possible that pumice from more than one eruption, especially from the chemically similar Glass Mountain tuffs, could be present in the mound. However, there are no unconformities or discontinuites in the stratigraphic section (fig. 5) as might be expected if the mound had been deposited over a span of 300,000 years (1.0-0.7 Ma).

Interpretation

The abundance of opal as discrete layers and as cement in this outcrop strongly suggests a hot-spring origin. The presence of opal layers in Fish Lake Valley is unique to this and nearby outcrops to the northeast, discussed below. Modern spring water in northeastern Fish Lake Valley is nearly saturated with dissolved silica, in contrast to springs in other parts of the valley (Macke and others, 1990). Several other associations and characteristics, discussed by White and others (1989), support a hot-spring origin for these rocks: (1) They form an apron-shaped outcrop that is conformable with the Quaternary land surface. (2) They are spatially associated with relatively young volcanic rocks and lie on a fault active in Quaternary time. (3) They crop out only 1.5 km southwest of a deep drill hole near a Quaternary fault subparallel to the one that bounds the outcrop; this drill hole intersected artesian hot water. (4) The opal layers contain highly irregular bedding laminations. The thin layers are similar to thin-bedded opaline sinter formed by primary discharge on broad aprons at Steamboat Springs, Nevada (White and others, 1964). Some textures reported to be common in hot-spring sinters, such as columnar structures perpendicular to bedding laminations (White and others, 1989) were not observed in the rocks in Fish Lake Valley.

We infer that the sinter mound was formed in shallow water at the edge of a lake, and that the majority of the mound was constructed just after the eruption of the Bishop Tuff, based on the following observations: (1) The mound contains numerous beds of well-sorted sandstone. The sandstone beds do not exhibit trough crossbedding or other structures indicative of fluvial deposition, and they are too well sorted and bedded to represent alluvial-fan deposition. (2) The majority of the grains in the sandstone beds and throughout the mound consist of pumice and bubble-wall shards. Near the top, there are some euhedral, cracked quartz grains, some of which are contained within large pumice grains and hence must have come from the same source as the pumice. (3) There are no unconformities or apparent breaks in depositional style or composition throughout the mound. (4) The siliceous deposits overlie lacustrine marl and oolitic rocks. Oolites must have formed in carbonate-enriched, shallow water, and have been reported from both ancient and modern sediments of lakes in the Great Basin (Russell, 1885; Gilbert, 1890). (5) The pumice grains in most of the mound contain flattened vesicles, but near the top of the mound, vesicles are spherical. This suggests a sort of grading in which the lighter, air-filled pumices floated whereas heavier pumices with flattened vesicles sank.

The elevation of the uppermost beds of the sinter mound probably represents the paleo-shoreline of the lake, because this bed contains large, air-filled pumice clasts intermixed with pebbles of rhyolite and basalt derived from the Volcanic Hills to the north. The shoreline elevation may be slightly higher now due to uplift along the small fault that bounds the outcrop, but major changes in elevation are unlikely. The elevation of the uppermost bed is presently 1,443 m; hence, the paleo-shoreline is inferred to have been at about 1,440 m.

Tertiary Sediments East and West of the Playa

Fine-grained Tertiary sediments crop out east and west of the playa in northeastern Fish Lake Valley (fig. 2). East of the playa, these sediments are conformable with, and

grade upward into, indurated gravel of late Tertiary-early Quaternary age (Reheis, in press a). Both outcrops were previously inferred to represent deposition in an alkaline lake on the west side of the Silver Peak Range (Robinson, 1964, and Robinson and others, 1976). The Tertiary rocks consist of green and grayish-green, weakly indurated claystones, tan, fine-grained sandstones, and tephra beds up to 50 cm thick. Southwest of the playa, lenses of siliceous sinter crop out that are similar to those in the sinter mound.

Two beds of tephra (table 1) were sampled in the southwestern area of Tertiary sediments. The lower bed, 15 cm thick (FLV-150-CS), overlies green claystones and consists of very well sorted, medium-sand-sized pumice grains. The lower bed is overlain by 1 m of well-sorted tan pumiceous sandstone grading upward into green pumiceous mudstone. The mudstone is in turn overlain by 50 cm of fine-sand-sized tephra (FLV-151-CS). This tephra is capped by 4.5 m of sediments like those between the tephra beds. Both tephras are similar to tephras of the tuff of Taylor Canyon, based on major-oxide chemistry of the glass, and hence are inferred to be about 2.1-2.2 Ma (Izett, 1981; Izett and others, 1988; Sarna-Wojcicki and others, 1984, and in press).

The Tertiary lacustrine beds on the east side of the playa are particularly well exposed at site 179-EP, just recently discovered. These beds contain multiple layers of fine-grained, white pumiceous tephra that have not yet been sampled or analyzed. Above these layers, near the top of the lacustrine beds, is a 0.5-m-thick layer of reworked, fine-grained, bluish-gray tephra (FLV-179-EP). Based on major-oxide chemistry (table 1), we provisionally correlate this layer with the Huckleberry Ridge ash bed, erupted from the area of Yellowstone National Park about 2.01 Ma (Christiansen, 1979; Izett, 1981).

The upper Tertiary sediments east and west of the modern playa indicate the presence of a lake in northeastern Fish Lake Valley at about 2 Ma. The extent of this lake is unknown, but based on the presence of claystones it must have been deeper in this area than the lake represented by shoreline deposits of the Bishop ash. Robinson (1964) inferred that it did not extend far westward into the Volcanic Hills, because these sediments lap at gentle dips onto more steeply dipping older tuffs in these hills. Similar sediments crop out as far north as The Gap (fig. 2), but apparently do not crop out north of The Gap in Columbus Salt Marsh (Robinson and others, 1976). The 2-Ma lake could not have extended as far east as site 8-13-CS (fig. 2), because tephra beds correlated to the tuff of Taylor Canyon (table 1) are there contained within alluvial-fan gravel (Reheis, in press a). Tertiary lacustrine sediments, if present, are buried beneath Quaternary sediment south of the playa. Gypsiferous green claystones occur at the southern end of Fish Lake Valley but are slightly older than those at the northern end; the southern claystones range in age from about 3.2 to more than 2.0 Ma (Reheis and others, this volume; ages based on tephrochronology by A. Sarna-Wojcicki). The upper Tertiary claystones are so weakly indurated that they probably could not be differentiated from Quaternary sediments in drill holes.

The Connection to Columbus Salt Marsh

A narrow valley about 8 km long connects the modern playa of Fish Lake Valley with Columbus Salt Marsh (fig. 2). The valley narrows to the north; the flat alluvial floor of the valley is less than 0.5 km wide at the north end. Gently sloping alluvial fans broken by small, low-standing outcrops of Tertiary and Paleozoic rocks (Robinson and others, 1976) extend up to bedrock valley walls at elevations of about 1,440 m, extending the width of the valley to as much as 1.3 km. Despite a continuous gentle gradient of about 3.8 m/km, there is no surface drainage in most years (Beaty, 1968) and no channel exists; however, there are numerous springs and wet marshes.

The valley is floored mainly by fine-grained marsh deposits of unknown thickness that grade upslope into Holocene fan deposits (Reheis, in press a). At the northern end of the valley are several active springs, three of which emerge from spring mounds constructed mostly of well sorted calcareous sand, probably eolian sand trapped by the vegetation around the springs. A few late Pleistocene fan deposits occur on the fan slopes, and they are composed of locally derived clasts.

Late Pleistocene shorelines and beach deposits of a lake in Columbus Salt Marsh stand at an elevation of about 1,380 m at the mouth of the valley, coincident with two active spring mounds. Beneath the loose sand of the mounds, and locally exposed in arroyos that cut the Holocene fan deposits blanketing the shoreline, are massive, well-cemented beds of sandy travertine (Reheis, in press a). The travertine has not been dated, but judging from its relations to the spring mounds, the shoreline, and the younger fan deposits, it was probably deposited by voluminous groundwater discharge from Fish Lake Valley into the pluvial lake in Columbus Salt Marsh in late Pleistocene time.

Interpretation

The narrow, gently sloping valley of The Gap presently serves as a shallow groundwater conduit and probably had the same role in late Pleistocene time. The buried travertine suggests that the late Pleistocene groundwater discharge was greater than that today. No distinct drainage channel exists, but it is possible that one is buried under Holocene marsh deposits.

An older (early Pleistocene?) channel that carried overflow from Pluvial Fish Lake at 1,440 m elevation into Columbus Salt Marsh is possible, but if so the evidence to document the channel has been obscured. No lag gravel of exotic composition is found on slopes below that elevation in the valley of The Gap, nor are there distinct benches cut at appropriate elevations (one low bench, possibly that mentioned by Free, 1914, is blanketed by Holocene deposits). A deep channel buried by Holocene and older deposits is unlikely, because Tertiary rocks crop out randomly on the valley floor (Reheis, in press a) and hence the alluvial fill is probably thin. However, the valley could have been a shallow sill connecting two lakes at the same shoreline elevation.

Well Logs

The sediments reported in the drilling logs are dominantly sandy or clayey gravel that reflect alluvial-fan sedimentation, but there are significant thicknesses of mudstone and sandy clay interbedded with the gravel at depth (fig. 7). Fifteen of the logs (including three wells drilled by the U.S.G.S.), mainly those near the playa and along the valley axis, describe beds as much as 35 m thick of green, blue, gray, or white clay or sandy clay at depths ranging from 20 to 230 m. Such colors are believed to be characteristic of lacustrine clays, as reported by Morrison (1964) of drillers' logs in the Lahontan basin, in contrast to yellow, yellowish-red, or brown colors that typify fine-grained valley-fill sediments interbedded with alluvial-fan gravel. Significantly, two of the water-well logs report "volcanic ash" beds as much as 5 m thick at depths ranging from 100 to 150 m. Three other water-well logs in the southern part of the valley report "gypsum" beds at about the same depth as a nearby well log that reported "volcanic ash". Because gypsum beds do not crop out anywhere around Fish Lake Valley, these "gypsum" beds are inferred to be volcanic ash beds. One of the U.S.G.S. logs (#1 in fig. 7; Pantea and others, 1981) reported shell fragments at 110 m depth in a 3-m interval within a thick sequence of grayish-yellow clay and sandy clay.

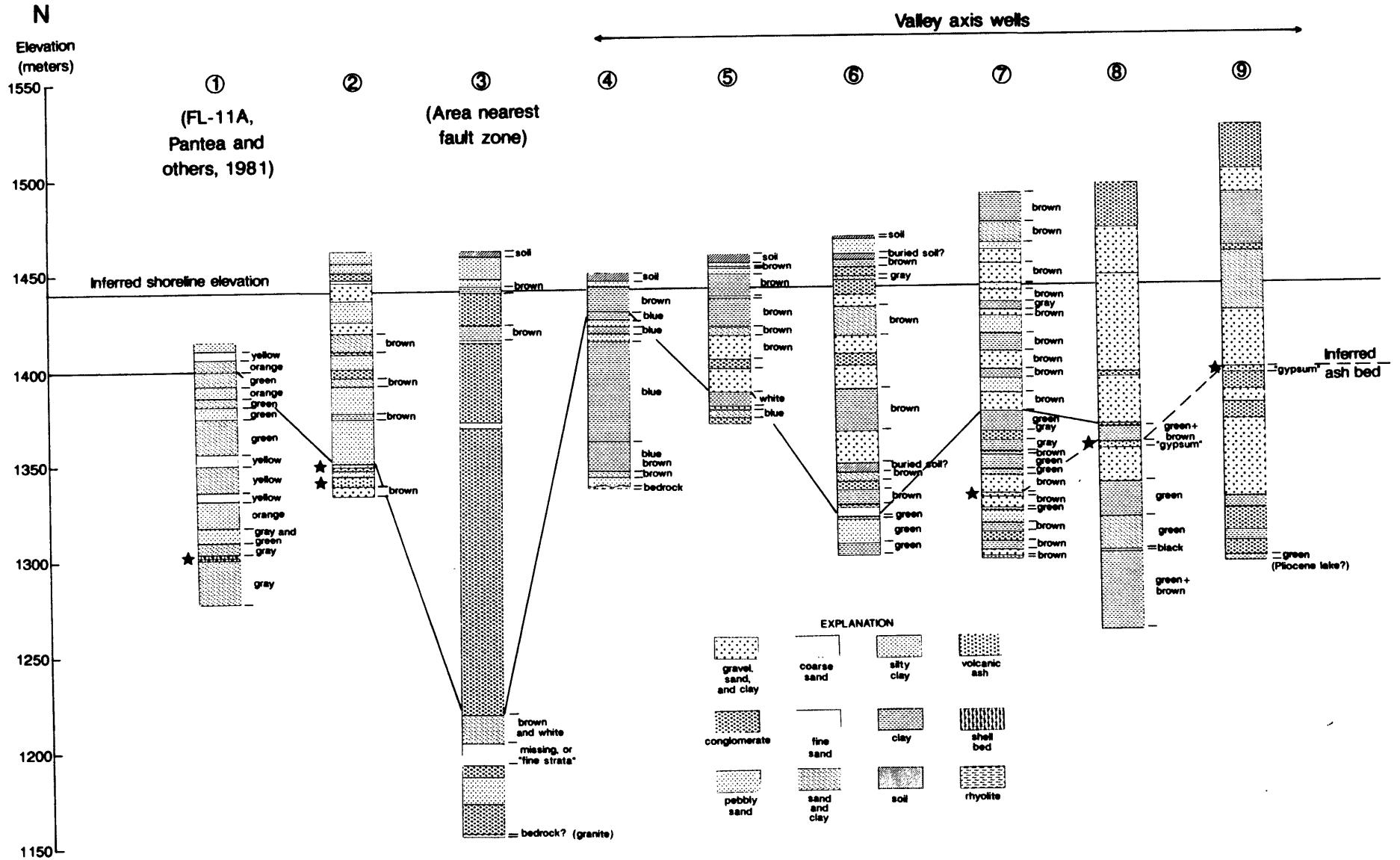

Figure 7. Representative well logs reporting lacustrine sediments and ash beds in Fish Lake Valley (fig. 2). Star, ash bed or "gypsum" bed; asterisk, bed containing shell fragments. Column to right gives sediment colors where reported (drillers often report colors only for clay beds).

Interpretation

The sequences of green, blue, gray, and white clay and sandy clay in the well logs at depth are inferred to represent intervals of lacustrine sedimentation. This inference is supported by the existence of a shell bed in one drill hole. Although drilling logs may be unreliable, the concurrence of fifteen logs made by several different drillers in the description of fine-grained sediments at depth and an abrupt change to yellow or brown sediments above is believed significant.

Three of the beds of "volcanic ash" and "gypsum" that is believed to be volcanic ash (figs. 2, 7) lie within, or are closely associated with, fine-grained sediments. In the northern well (#2, fig. 7), the two reported ash beds total about 7 m of a 13-m-thick sequence of sandy clay (no color described) that lies between beds of clayey and sandy gravel. The thickness of these ash beds suggests that their source was the eruption of the Bishop Tuff. If this correlation is correct, the thinness of the fine-grained sediments in this well may mean that the ash was deposited near the northern shoreline.

In two of the southern wells (#7 and #8, fig. 7), the 2-3-m-thick ash and "gypsum" beds lie in sequences of green and some brown clays interbedded with clayey gravel. Lacustrine sedimentation, represented by about 45 m of green and gray clay interbedded with gravel that overlie the ash and "gypsum" beds (fig. 8), must have continued episodically for some time after deposition of the ash and "gypsum" beds. Assuming that the ash in the southern wells is the Bishop ash, then the average rate of post-Bishop sedimentation indicated by these well logs is about 0.2 m/ka, and the length of post-Bishop lacustrine sedimentation in this area may have been roughly 200,000 years.

The "gypsum beds" reported in two wells south of Oasis (only one shown; #9, fig. 7) lie in thick sequences of clayey and sandy gravel at shallower depth than the ash and "gypsum" described in the two wells north of Oasis (figs. 2 and 7). None of the three well logs in this area describe green, blue, or white clay, except for one bed at the bottom of one hole, 100 m below the "gypsum" (#9, fig. 7). If these "gypsum beds" are tephra from the Bishop Tuff eruption, their occurrence in these holes suggests that the lake did not extend south of Oasis at Bishop time.

DISCUSSION AND REGIONAL IMPLICATIONS

Identification of the Bishop and Older Ash Beds

Identification of the thick, coarse-grained ash bed in Pleistocene fluvial and lacustrine deposits of Fish Lake Valley as the Bishop ash bed would date the shoreline deposits, and thus one stand of the pluvial lake in this basin, at about 0.74 Ma. Currently, the most reliable isotopic age of the Bishop Tuff is 0.738 Ma (mean age from conventional K-Ar analyses on sanidine; Izett and others, 1988, p. 23). Although our identification of this layer in Fish Lake Valley would be supported by additional analyses of the glass for trace and minor elements and by determination of magnetic polarity, its identity as the Bishop is presently indicated by sedimentologic (grain size and thickness), stratigraphic (underlain in sequence in northeastern Fish Lake Valley by fine-grained, thin beds of probable Glass Mountain tephra, fig. 4, and by ash beds of the tuff of Taylor Canyon), and chemical data (table 1), as well as by the notion that the most probable and obvious choice is likely to be the right one, as discussed below.

The eruption of the Bishop tephra from Long Valley caldera, a few tens of kilometers west of Fish Lake Valley, was one of the most explosive and largest in Pleistocene time, producing an estimated 500 km^3 of tephra (Bailey and others, 1976). Although the Bishop ash bed is present to the west and southwest of Long Valley (Sarna-Wojcicki and others, 1987), most identified sites are to the east, extending as far as south-

central Nebraska (Izett and others, 1970, 1988). Consequently, the principal direction of transport was eastward, in the direction of prevailing winds.

Considering that Fish Lake Valley is only about 70-80 km due east and directly downwind of Long Valley, it is reasonable to expect that the coarsest, thickest, and most pervasive Pleistocene tephra layer there, and one with glass chemistry characteristic of the Long Valley-Mono Glass Mountain source area as well, will be the Bishop ash bed.

Tephra layers having chemical compositions similar to those of the Bishop ash bed have been erupted from the Mono-Glass Mountain source area at the east margin of Long Valley caldera. Glass Mountain is an older vent complex that was active between about 2.2 and 0.8 Ma (Metz and Mahood, 1985). Only the youngest tephra erupted from this source, such as the Glass Mountain G (about 1.0 Ma) and D (about 0.9 Ma) ash beds, can be confused with the Bishop on the basis of electron-probe shard compositions. Glass shards of the Glass Mountain G and D ash beds have the same shapes and indices of refraction as the Bishop ash bed. Furthermore, Glass Mountain G and D and the Bishop ash beds have similar mineralogy. Consequently, these ash beds cannot be distinguished from the Bishop ash bed by petrographic criteria or electron-microprobe analyses alone (Izett and others, 1988, p. 30-31).

The Glass Mountain tephra layers were produced by considerably smaller eruptions than that of the Bishop ash bed. For example, at localities at the southern end of the volcanic tableland formed by the Bishop Tuff (table 1, 7-9), about 50 km southeast of Long Valley caldera, the airfall Bishop ash bed contains coarse pumice clasts up to several centimeters in diameter, but the underlying Glass Mountain D and G ash beds consist mostly of silt- and sand-sized clasts.

Older tephra erupted from the Glass Mountain source area, such as the ~2-Ma tuff of Taylor Canyon (Krauskopf and Bateman, 1977), in addition to being thinner bedded and finer grained than the Bishop, is chemically distinguishable from the younger tephra of Glass Mountain and the Bishop ash bed (table 1). In particular, Fe, Mn, and Ca differ significantly between the 0.74-1.0-Ma tephra layers and the 2-Ma Tuff of Taylor Canyon (Izett, 1981).

Although glass of the Bishop ash bed cannot be confidently distinguished by the electron microprobe from that of the younger Glass Mountain tephra layers, these units can be distinguished by the more sensitive technique of instrumental neutron activation analysis of the glass (Sarna-Wojcicki and others, 1984), and we are currently conducting this type of analysis. In addition to chemical criteria, the Bishop ash bed can be distinguished from the Glass Mountain D and G ash beds by magnetic polarity. The former was deposited shortly before the end of the Brunhes Normal Polarity Chron, whereas the latter two were deposited during the Matuyama Reversed Polarity Chron. Sarna-Wojcicki and others (1984) suspected that the Glass Mountain G ash bed was deposited prior to the Jaramillo Normal Subchron, and the Glass Mountain D ash bed after. Paleomagnetic analysis is being performed on samples from the sandstones of the sinter mound in Fish Lake Valley; the other two shoreline deposits in the valley are too coarse-grained for this type of analysis.

Several thin, fine-grained tephra layers (table 1) are present in late Tertiary deposits in northeastern Fish Lake Valley (fig. 2). East of the Emigrant Peak fault zone, these layers are within thick gravel deposits (FLV-8- to 13-CS); west of the modern playa, the layers are within lacustrine deposits (discussed above; FLV-150- and 151-CS). These tephra layers are chemically identical to tuffs of the compound tuff of Taylor Canyon (Krauskopf and Bateman, 1977). Previously, Izett (1981) reported conventional K-Ar ages of sanidine in pumice of the tuff of Taylor Canyon as 2.1 Ma. Conventional K-Ar analyses on obsidian chunks picked from several emplacement units of this tuff, and preliminary laser-fusion $^{40}Ar/^{39}Ar$ analyses on sanidines separated from this tuff, also indicate that it

ranges in age from about 2.0 to 2.1 Ma (J.K. Nakata, C.E. Meyer, and A.M. Sarna-Wojcicki, unpublished data), an age compatible with the older ages (to 2.2 Ma) obtained on the flow rocks of Glass Mountain by Metz and Mahood (1985).

Chronology, Size, and Connections of Pluvial Lake Rennie

The three thick, coarse-grained, shallow-water outcrops of tephra in northern Fish Lake Valley collectively demonstrate that a pluvial lake existed in this valley, most likely at the time of the eruption of the Bishop Tuff. This conclusion is supported by the well-log descriptions of deep-water lacustrine clays, thick shoreline beds of volcanic ash, and one bed of shell fragments. This lake, or one occupying approximately the same position (at least in the northeastern part of the valley), also existed in the late Pliocene based on lacustrine deposits east of the modern playa that contain ~2-Ma tephra. In addition, a bed of well-sorted sand below the Bishop ash and above a probable Glass Mountain tephra at site 163-CS (fig. 2) suggests the presence of a pluvial lake at about 1 Ma. Lacustrine sedimentation may have continued into the middle Pleistocene in deeper parts of the basin, but there is no evidence to support a late Pleistocene lake.

Details concerning the depth, the geographic extent, and the nature of the connection of Pluvial Lake Rennie with Columbus Salt Marsh are sparse, but some reasonable inferences can be made. Based on the elevation of the sinter mound, the shoreline elevation was at about 1,440 m. The lowest elevation of probable lacustrine sediments reported in the well logs is about 1,215 m (fig. 7). However, most of the valley floor has been significantly dropped relative to the White Mountains along the Fish Lake Valley fault zone in Quaternary time (Sawyer, 1990; Reheis and McKee, this volume). If the motion was mostly absorbed by uplift of the range, the lake may have been as much as 230 m deep. If the motion was mostly absorbed by dropping the valley floor, the lake may have been much shallower.

The geographic extent of the Bishop-aged Pluvial Lake Rennie can be approximated from the three shallow-water outcrops of probable Bishop ash and the well logs (fig. 2). The northwestern part of the lake is poorly constrained due to the lack of well logs in this area. However, the deltaic sediments at the mouth of McAfee Creek suggest that the shoreline, for an unknown distance north of the delta, was at or close to the range front. The lake probably did not extend north much past Chiatovich Creek, based on the thinness of fine-grained sediments containing volcanic ash in well log #2 (fig. 7). The lake extended about as far south as Oasis (fig. 2), based on the lack of lacustrine sediments in wells south of Oasis. This conclusion is supported by reconstructions of stream drainages and restoration of right slip along the southern part of the Fish Lake Valley fault zone (Reheis and McKee, this volume) that suggest that the depositional basin probably terminated to the south around Oasis at 0.74 Ma. For example, the course of Cottonwood Creek at the time of the Bishop eruption was southeasterly, parallel to the Fish Lake Valley fault zone and on the present drainage divide between Fish Lake Valley and Deep Springs Valley (fig. 2). Clearly, this topography could not have existed in its present form 740,000 years ago.

Given a pluvial lake in Fish Lake Valley at 1,440 m elevation, a connection must have existed to the north into Columbus Salt Marsh (fig. 2), which is at about 1,350 m elevation at its lowest point. Although a few north-dipping faults have been mapped on the north end of the Volcanic Hills and the Silver Peak Range (Dohrenwend, 1982; Robinson and others, 1976), Quaternary offset on these faults is probably not enough to account for the total elevation difference of the two basins. There are three permissible scenarios for such a connection: (1) Pluvial Lake Rennie was dammed on the northeast and drained northward primarily by groundwater discharge, as the valley does today. (2)

Pluvial Lake Rennie was dammed on the northeast and drained northward by a relatively high-energy overflow channel. (3) A contiguous lake at 1,440 m elevation was connected between Pluvial Lake Rennie and Columbus Salt Marsh via a sill in The Gap.

These scenarios are difficult to evaluate. Late Pleistocene and Holocene sediments have largely buried older deposits, if present, in The Gap and to the north. If a dam existed, it probably consisted largely of readily erodible ash-flow tuff (Robinson and others, 1976). Such a dam probably could not have maintained a lake at 1,440 m elevation for long, whether discharge occurred by groundwater or by overland flow. The 1,380-m late Pleistocene shoreline in Columbus Salt Marsh (Reheis, in press a) is not high enough to permit a lacustrine connection into Fish Lake Valley. Two remnants of older shorelines at about 1,410 m exist on the eastern and northwestern margins of Columbus Salt Marsh (J.O. Davis, written commun., 1990). This elevation is high enough to permit a lacustrine connection with the modern playa in Fish Lake Valley, but little more. If a lacustrine connection over a sill existed at Bishop Tuff time, then either or both (1) a previously undiscovered shoreline at 1,440 m elevation exists in Columbus Salt Marsh, or (2) the northern part of Pluvial Lake Rennie has been elevated by faulting or tilting about 30 m relative to Columbus Salt Marsh since 0.74 Ma.

Comparison to Other Pluvial Lake Records and the Marine Oxygen-Isotope Record

Three large pluvial lakes and lake systems were situated within 100 km of Pluvial Lake Rennie: Lake Lahontan to the north, the system of overflowing lakes to the south beginning with Owens Lake, passing through Searles Lake, and terminating in Lake Manley (Death Valley), and Lake Tecopa, about 200 km southeast of Fish Lake Valley (fig. 1). The middle and early Quaternary records from these lakes can be compared with that of Pluvial Lake Rennie. Lake Lahontan and the southern chain of lakes were fed by perennial rivers heading in the Sierra Nevada and presumably had a more secure water supply than did Lake Tecopa, fed only by streams heading in unglaciated terrain, or Pluvial Lake Rennie, in the rain shadow of both the Sierra Nevada and the White Mountains. Thus, Pluvial Lake Rennie might have a record of fluctuations more similar to that of Lake Tecopa than to those of Lake Lahontan or the upper lakes in the southern chain.

In the Lake Lahontan basin, the best record is from outcrops at Rye Patch Dam. Here, a thick deposit of the 0.63-Ma Rye Patch Dam Bed (Davis, 1978; Sarna-Wojcicki and others, in press), is overlain by lacustrine deposits (the Rye Patch Dam Alloformation, Morrison and Davis, 1984) containing the 0.62-Ma Lava Creek B ash bed (Izett, 1981). This lake apparently dried up shortly after 0.6 Ma at this location, for the lacustrine sediments are thin and are overlain by a thick sequence of terrestrial sediments and paleosols. An older, poorly dated lake cycle may be represented by sediments below the terrestrial Lovelock Alloformation, which underlies the Rye Patch Alloformation.

The record from the southern chain of lakes is derived from interpretation of cores at Searles Lake (fig. 1; Smith, 1984) dated by volcanic ash stratigraphy, paleomagnetism, and sedimentation rates. The Searles Lake record indicates fluctuating but relatively high lake level from 2.0 to 0.6 Ma, when the lake dried up for a lengthy period.

Sediments at Lake Tecopa are well exposed, even in the central part of the lake basin, due to draining of the lake in the middle Pleistocene and subsequent incision (Sheppard and Gude, 1968; Sarna-Wojcicki and others, 1984). Lake sediments with interbedded fine-grained alluvium indicate that the level of Lake Tecopa fluctuated in the late Pliocene and early Pleistocene. The lake level was relatively high at 2 Ma and at 0.6 Ma, because tephra beds of the Huckleberry Ridge Tuff, the tuff of Taylor Canyon, and the Lava Creek Tuff occur in lacustrine sediments (Sarna-Wojcicki and others, 1984, 1987). The lake drained sometime after 0.6 Ma.

Because the Bishop ash bed is stratigraphically just above the Brunhes-Matuyama Chron boundary, and because this boundary is used as an important time marker in calibrating the oxygen isotope stratigraphy in the marine record (Shackleton and Opdyke, 1973; Imbrie and others, 1984), the ash bed and associated pluvial-lake shoreline deposits in Fish Lake Valley can be correlated to the marine oxygen-isotope record. At Lake Tecopa, stratigraphic evidence indicates that the Bishop ash was erupted during a minor interstadial, oxygen-isotope stage 19, that occurred between two major stadials, stages 18 and 20 (Sarna-Wojcicki and others, in press). Alluvium that includes reworked Bishop ash prograded over pluvial lake beds of the preceding stadial, stage 20. However, a continuous sequence of lake beds containing the Bishop ash bed is found at the center of the basin. Thus, although the size of Lake Tecopa decreased during stage 19, the lake did not dry out. The same chronology applies to Pluvial Lake Rennie, where the exposed stratigraphy suggests a wide nearshore deposit overlain and preserved by alluvial fans that prograded basinward as the pluvial lake shrank. In addition, volcanic ash beds reported in well logs in the axis of Fish Lake Valley, presumably the deepest part of the pluvial lake, are apparently underlain and overlain by lacustrine deposits.

The late Pliocene to middle Pleistocene record of Pluvial Lake Rennie, though spottily preserved, appears reasonably parallel to the records of Lake Lahontan, Searles Lake, and Lake Tecopa. Pluvial Lake Rennie existed at about 2.0 Ma, as shown by the lacustrine clays and tephra beds near the modern playa (fig. 2). It probably also existed at about 1.0 Ma, based on the well sorted sands overlying probable Glass Mountain tephra (fig. 4). Pluvial Lake Rennie had a high stand at 0.74 Ma as reflected by the shallow-water deposits of probable Bishop ash, and may have retained water for some time after that, if the ash in the wells north of Oasis is the Bishop. Pluvial Fish Lake experienced many large fluctuations in water level, based on the gravelly deposits interbedded with lacustrine clays that are reported in wells.

The late middle to late Pleistocene record of Pluvial Lake Rennie diverges sharply from those of Lake Lahontan and Searles Lake, but is similar to that of Lake Tecopa. Pluvial Lake Rennie apparently did not exist during this time, whereas Lake Lahontan and Searles Lake fluctuated from low to high water levels. These relations suggest that the late middle to late Pleistocene drying of Pluvial Lake Rennie has a tectonic cause rather than regional climatic cause, analogous to the demise of Lake Tecopa sometime after 0.6 Ma. If regional climatic change were responsible, such as an overall drying trend or a shift north or south in storm tracks, then the record of Pluvial Lake Rennie should be parallel either to both Lake Lahontan and Searles Lake, or to one of these lakes. It seems more likely that the drying of Pluvial Lake Rennie was due to the increase in the rain-shadow effect on Fish Lake Valley caused by a significant increase in elevation of the White Mountains, and perhaps in part the Sierra Nevada, relative to the intervening valleys in post-Bishop time.

ACKNOWLEDGEMENTS

Many people contributed helpful advice and discussion in the interpretation of the deposits and their analyses, including A. Gillespie (University of Washington), P. Phillips (Humboldt State University), and G.A. Izett, N. Fishman, and W. Simonds (U.S. Geological Survey). We are grateful for the enthusiastic assistance in the field of D. Rennie and T. Rennie (University of Nevada at Reno), L. Von Wald (Humboldt State University), and the members of the 1989 Humboldt State University field camp.

REFERENCES

Bailey, R.A., Dalrymple, G.B., and Lanphere, M.A., 1976, Volcanism, structure, and geochronology of Long Valley Caldera, Mono County, California: Journal of Geophysical Research, v. 81, p. 725-744.

Beaty, C.B., 1968, Sequential study of desert flooding in the White Mountains of California and Nevada: U.S. Army Natick Laboratories, Technical Report 68-31-ES, 96 p.

Christiansen, R.L, 1979, Cooling units and composite sheets in relation to caldera structure in ash-flow tuffs: Chapin, C.E., and Elston, W.E., eds., Geological Society of America Special Paper 180, p. 29-42.

Davis, J.O., 1978, Tephrochronology of the Lake Lahontan area, Nevada and California: Nevada Archaeological Research Paper 7, 137 p.

dePolo, C.M., 1989, Seismotectonics of the White Mountains fault system, east-central California and west-central Nevada: Reno, University of Nevada, M.S. thesis.

Dohrenwend, J.C., 1982, Preliminary surficial geologic map of the Excelsior Mountains area, west-central Nevada: U.S. Geological Survey Miscellaneous Field Studies Map MF-1372, scale 1:62,500.

Elliott-Fisk, D.L., 1987, Glacial geomorphology of the White Mountains, California and Nevada: Establishment of a glacial chronology: Physical Geography, v. 8, p. 299-323.

Fisher, R.V., 1964, Maximum size, median diameter, and sorting of tephra: Journal of Geophysical Research, v. 69, p. 341-355.

Free, E.E., 1914, The topographic features of the desert basins of the United States with reference to the possible occurrence of potash: U.S. Department of Agriculture, Bulletin 54, 65 p.

Gilbert, G.K., 1890, Lake Bonneville: U.S. Geological Survey Monograph 1, 275 p.

Hubbs, C.L., and Miller, R.R., 1948, The Great Basin. II. The zoological evidence: University of Utah Bulletin, v. 38, no. 20, p. 17-166.

Huber, N.K., 1981, Amount and timing of late Cenozoic uplift and tilt of the Sierra Nevada, California--Evidence from the upper San Joaquin River basin: U.S. Geological Survey Professional Paper 1197, 28 p.

Huber, N.K., and Rinehart, C.D., 1967, Cenozoic volcanic rocks of the Devils Postpile quadrangle, eastern Sierra Nevada, California: U.S. Geological Survey Professional Paper 554-D, 21 p.

Imbrie, J., and 8 others, 1984, the orbital theory of Pleistocene climate; Support from a revised chronology of the marine ^{18}O record, *in* Berger, A.L. and others, eds., Milankovich and climate, Part I: Dordrecht, D. Reidel Publishing Co., p. 269-305.

Izett, G.A., 1981, Volcanic ash beds; recorders of upper Cenozoic silicic pyroclastic volcanism in the Western United States: Journal of Geophysical Research, v. 86, no. B11, p. 10,200-10,222.

Izett, G.A., Obradovich, J.D., and Mehnert, H.H., 1988, The Bishop ash bed (middle Pleistocene) and some older (Pliocene and Pleistocene) chemically and mineralogically similar ash beds in California, Nevada, and Utah: U.S. Geological Survey Bulletin 1675, 37 p.

Izett, G.A., Wilcox, R.E., Powers, H.A., and Desborough, G.A., 1970, The Bishop ash bed, a Pleistocene marker bed in the western United States: Quaternary Research, v. 1, p. 121-132.

Jones, J.B., and Segnit, E.R., 1971, The nature of opal, nomenclature and constituent phases: Journal of the Geological Society of Australia, v. 18, p. 57-68.

Krauskopf, K.B., and Bateman, P.C., 1977, Geologic map of the Glass Mountain quadrangle, Mono County, California, and Mineral County, Nevada: U.S. Geological Survey Geologic Quadrangle Map GQ-1099, scale 1:62,500.

LaMarche, V.C., Jr., 1965, Distribution of Pleistocene glaciers in the White Mountains of California and Nevada: U.S. Geological Survey Professional Paper 525-C, p. C144-C146.

Macke, D.L., Schumann, R.R., and Otton, J.K, 1990, Uranium distribution and geology in the Fish Lake surficial uranium deposit, Esmeralda County, Nevada: U.S. Geological Survey Bulletin 1910, 22 p.

Meinzer, O.E., 1922, Map of the Pleistocene lakes of the Basin-and-Range Province and its significance: Geological Society of America Bulletin, v. 33, p. 541-552.

Metz, J.M., and Mahood, G.A., 1985, Precursors to the Bishop Tuff eruption: Glass Mountain, Long Valley, California: Journal of Geophysical Research, v. 90, no. B13, p. 11,121-11,126.

Mifflin, M.D., and Wheat, M.M., 1979, Pluvial lakes and estimated pluvial climates of Nevada: Nevada Bureau of Mines and Geology Bulletin 94, 57 p.

Morrison, R.B., 1964, Lake Lahontan: Geology of southern Carson Desert, Nevada: U.S. Geological Survey Professional Paper 401, 156 p.

Morrison, R.B., 1965, Quaternary geology of the Great Basin, in The Quaternary of the United States: Princeton University Press, p. 265-285.

Morrison, R.B., and Davis, J.O., 1984, Quaternary stratigraphy and archeology of the Lake Lahontan area: a re-assessment: Western Geological Excursions, v. 1, Geological Society of America 1984 Annual Meeting, p. 252-281.

National Climatic Data Center, 1986, Climatological data, annual summary, California: Department of Commerce, Asheville, N.C.

Pantea, M.P., Asher-Bolinder, Sigrid, and Vine, J.D., 1981, Lithology and lithium content of sediments in basins surrounding Clayton Valley, Esmeralda and Nye Counties, Nevada: U.S. Geological Survey Open-file Report 81-962, 23 p.

Pettijohn, F.J., Potter, P.E., and Siever, Raymond, 1973, Sand and Sandstone: Springer-Verlag, New York, 618 p.

Reheis, M.C., in press a, Geologic map of late Cenozoic deposits and faults in the western part of the Rhyolite Ridge 15' quadrangle, Esmeralda County, Nevada: U.S. Geological Survey Miscellaneous Investigations Map I-2183, scale 1:24,000.

Reheis, M.C., in press b, Geologic map of late Cenozoic deposits and faults in parts of the Soldier Pass and Magruder Mountain 15' quadrangles, Inyo and Mono Counties, California, and Esmeralda County, Nevada: U.S. Geological Survey Miscellaneous Investigations Map I-2268, scale 1:24,000.

Reheis, M.C., and McKee, E.H., 1991, Late Cenozoic history of slip on the Fish Lake Valley fault zone and surrounding areas of Nevada and California: U.S. Geological Survey Open-file Report 91-290, this volume, and Guidebook, Pacific Cell, Friends of the Pleistocene.

Reheis, M.C., Sarna-Wojcicki, A.M., Burbank, D.M., and Meyer, C.E., 1991, The late Cenozoic section at Willow Wash, east-central California: A tephrochronologic rosetta stone: U.S. Geological Survey Open-file Report 91-290, this volume, and Guidebook, Pacific Cell, Friends of the Pleistocene.

Robinson, P.T., 1964, The Cenozoic stratigraphy and structure of the central part of the Silver Peak Range, Esmeralda County, Nevada: Berkeley, University of California, Ph.D. thesis, 107 p.

Robinson, P.T., and Crowder, D.F., 1973, Geologic map of the Davis Mountain quadrangle, Esmeralda and Mineral Counties, Nevada, and Mono County, California: U.S. Geological Survey Geologic Quadrangle Map GQ-1078, scale 1:62,500.

Robinson, P.T., Stewart, J.H., Moiola, R.J., and Albers, J.P., 1976, Geologic map of the Rhyolite Ridge quadrangle, Esmeralda County, Nevada: U.S. Geological Survey Geologic Quadrangle Map GQ-1325, scale 1:62,500.

Rush, F.E., and Katzer, T.L., 1973, Water-resources appraisal of Fish Lake Valley, Nevada and California: Nevada Division of Water Resources, Reconnaissance Series Report 58, 68 p.

Russell, I.C., 1885, Geological history of Lake Lahontan: U.S. Geological Survey Monograph 11, 288 p.

Sarna-Wojcicki, and nine others, 1984, Chemical analyses, correlations, and ages of upper Pliocene and Pleistocene ash layers of east-central and southern California: U.S. Geological Survey Professional Paper 1293, 40 p.

Sarna-Wojcicki, A.M., Lajoie, K.R., Meyer, C.E., Adam, D.P., and Rieck, H.J., in press, Tephrochronologic correlation of upper Neogene sediments along the Pacific margin, conterminous United States, in Morrison, R.B., ed., Quaternary non-glacial history--Conterminous U.S.: Geological Society of America, Decade of North American Geology, v. K-2.

Sarna-Wojcicki, A.M., Morrison, S.D., Meyer, C.E., and Hillhouse, J.W., 1987, Correlation of upper Cenozoic tephra layers between sediments of the western United States and eastern Pacific Ocean, and comparison with biostratigraphic and magetostratigraphic age data: Geological Society of America Bulletin, v. 98, p. 207-223.

Sawyer, T.L., 1990, Quaternary geology and neotectonic activity along the Fish Lake Valley fault zone, Nevada and California: Reno, University of Nevada, M.S. thesis, 379 p.

Shackleton, N.J., and Opdyke, N.D., 1973, Oxygen isotope and paleomagnetic stratigraphy of equatorial Pacific core V28-238: Oxygen isotope temperatures and ice volume on a 10^5 and 10^6 year scale: Quaternary Research, v. 3, p. 39-55.

Sharp, R.P., 1968, Sherwin Till-Bishop Tuff geological relationships, Sierra Nevada, California: Geological Society of America Bulletin, v. 79, p. 351-364.

Sheppard, R.A., and Gude, A.J. III, 1968, Distribution and genesis of authigenic silicate minerals in tuffs of Pleistocene Lake Tecopa, Inyo County, California: U.S. Geological Survey Professional Paper 597, 37 p.

Smith, G.I., 1984, Paleohydrologic regimes in the southwestern Great Basin, 0-3.2 my ago, compared with other long records of "global" climate: Quaternary Research, v. 22, p. 1-17.

Snyder, C.T., Hardman, G., and Zdenek, F.F., 1964, Pleistocene lakes in the Great Basin: U.S. Geological Survey Miscellaneous Investigations Map I-416, scale 1:1,000,000.

Spaulding, W.G., 1980, The presettlement vegetation of the California desert: Bureau of Land Management, Riverside, California, Contract Report #CA-060-CT8-65, 97 p.

White, D.E., Thompson, G.A., and Sandbery, C.H., 1964, Rocks, structure, and geologic history of Steamboat Springs thermal area, Washoe County, Nevada: U.S. Geological Survey Professional Paper 458-B, 63 p.

White, N.C., Wood, D.G., and Lee, M.C., 1989, Epithermal sinters of Paleozoic age in north Queensland, Australia: Geology, v. 17, p. 718-722.